Republic of Iraq
Ministry of Higher Education
And Scientific Research
Babylon University
College of Engineering
Department of Electrical Engineering

Design and Simulation of an Optical Communication System Using WDM and SDM Techniques for Few-Made-Fiber

A thesis
Submitted to the department of Electrical Engineering, College of Engineering, University of Babylon, in partial Fulfillment of the requirements for the degree of master of Science in Engineering / Electrical Engineering / Communications

By:
Malak Kadhim Sadiq Omran
Supervised by:
Prof. Dr. Ibrahim Abdullah Murdas

2025 A.D. 1446 A.H

بِسْمِ اللَّهِ الرَّحْمَنِ الرَّحِيمِ

((يَا أَيُّهَا الَّذِينَ آمَنُوا إِذَا قِيلَ لَكُمْ تَفَسَّحُوا فِي الْمَجَالِسِ فَافْسَحُوا يَفْسَحِ
اللَّهُ لَكُمْ ۖ وَإِذَا قِيلَ انشُزُوا فَانشُزُوا يَرْفَعِ اللَّهُ الَّذِينَ آمَنُوا مِنكُمْ
وَالَّذِينَ أُوتُوا الْعِلْمَ دَرَجَاتٍ ۚ وَاللَّهُ بِمَا تَعْمَلُونَ خَبِيرٌ))

صدق الله العلي العظيم

سورة المجادلة ﴿الآية 11﴾

Supervisor's Certification

I certify that this thesis entitled "**Design and Simulation of an Optical Communication System Using WDM and SDM Techniques for Few-Made-Fiber**" was prepared by **Malak Kadhim Sadiq** under my supervision as part of the prerequisites for the degree of master in science of Electrical Engineering / Communication, at the department of Electrical Engineering, College of Engineering, University of Babylon.

Signature:

Name: ***Prof. Dr. Ibrahim Abdullah Murdas***

(Supervisor)

Date: / ***/2025***

In view of the above recommendation I am forward this thesis for discussion by the Examination Committee.

Head of Electrical Department

Signature:

Name: ***Prof. Dr. Ahmed Qasim Jumaah***

Date: / ***/2025***

Examining Committee Certificate

We Certify that we have read this thesis entitled

"**Design and Simulation of an Optical Communication System Using WDM and SDM Techniques for Few-Made-Fiber**"

And as an examining cee examined the student **Malak Kadhim Sadiq** in its content and that in our opinion it meets a standard of thesis for the degree of master in Engineering/Electrical Engineering.

Signature:

Name: Prof. Dr. Sinan M. Elias
(Chairman)
Date: / /2025

Signature:

Name: Prof. Dr. Ahmed Abdulkadim Hamad
(Member)
Date: / /2025

Signature:

Name: Asst. Prof. Mohammed Taih Gatte
(Member)
Date: / /2025

Signature:

Name: Prof. Dr. Ibrahim Abdullah Murdas
(Supervisor)
Date: / /2025

Approval of Head of Department

Signature:

Name: Prof. Dr. Ahmed Qasim Jumaah

Date: / /2025

Approval of the Dean of College

Signature:

Name: Prof. Dr. Laith Ali Abdul Rahaim

Date: / /2025

Acknowledgments

First and before all, I praise ALLAH, the almighty for providing me this opportunity and granting me the capability to proceed this work, despite the numerous challenges encountered along the way. Thanks be to God for the insight that inspired me, and praise be to him for the blessings he has bestowed upon me, and praise be to him for the blessings he has bestowed upon me, and to him is the credit for achieving what I aspire to in this research.

I want to express my most heartfelt, sincere, and grateful thanks to my supervisor, ***Prof. Dr. Ibraheem Abdullah Murdas****. Couldn't have asked for a better guide throughout this daunting process, making it a truly enjoyable experience through his constant help, support, and patience, calling from God success and brilliance in the scientific career.*

I would like to express my sincere gratitude to my parents for their unwavering spiritual support throughout my life, as well as to my sisters and brothers who have consistently believed in me along the way. In addition, I want to sincerely thank my friends for their constant support and concern during this project.

Malak Kadhim
2025

Dedications

Although it was difficult, I successfully accomplished it.

To the one who was and still is my support at every moment, to the one whose prayers were the secret of my success and prosperity, to the one who stayed up all night to support me, to the most beautiful person in my life, my beloved mother, the secret of my happiness, I dedicate this achievement to you, the source of my strength in my life.

To my first love, my dear father, you were the support that helped me overcome all difficulties. Thank you for your love and support throughout my journey. I dedicate this achievement to you, which is the result of your sacrifices and patience Thank you for everything you have done for me.

To my dear brothers, my support in life, to those who were always by my side and encouraged me in the most difficult moments, I dedicate to you the fruits of my labor, thank you for your love, support, and motivation, and for all the advice you have given me, you are the source of my strength and happiness.

To my beautiful sisters, lifelong companions, and partners in my joys and sorrows, to those who have always been my source of support in every step, I dedicate to you the fruits of our shared efforts and our challenging days. Thank you for always being by my side, for every moment, and for every encouragement. You are the greatest gift that God has given me.

And a very special dedication to my little sister, the strongest person I have ever known in my life, to the one who gave me the strength and determination and inspired me to complete this achievement, Zainab, my love, my child, and the most beautiful light in my life. I pray to God to keep you for me.

Abstract

The optical fiber communication system is considered the core of telecommunications systems that support the Internet. Digital communications have experienced tremendous advancement over the past thirty years due to the spread of social media platforms and websites and the significant expansion of the internet, along with commercial, financial, and military applications. Consequently, the need has arisen to provide efficient, multi-signal digital communication systems to transmit the required data rapidly, securely, proficiently, and with the lowest error rate. There are several methods to increase transmission capacity, such as combining multiple signals with optical carriers on one optical fiber by means of different frequencies, modulation using different levels of amplitude, and using two subcarriers and polarization. However, an additional dimension that can be leveraged using fiber optics to enhance information capacity is space.

This research work presents simulation models for Space Division Multiplexing (SDM) transmission systems that employ Few-Mode Fiber (FMF). This system also implements Wavelength Division Multiplexing (WDM) techniques to improve data transfer rates. To meet the ultra-high capacity demands of SDM, Few Mode Fiber (FMF) has been proposed as the optimal technology for ultra-high bit rate systems that enable long-haul transmission.

In this thesis, a WDM/SDM system is designed, simulated, and analyzed using OptiSystem software. Four modes are used to obtain ultra-high data rates. The proposed system is tested using four different cases: variable data rate, variable distance, variable power, and variable space channel. The system performance was evaluated and analyzed using different parameters:

the bit error rate analyzer, the worth of quality factor, and the amplitude of the eye diagrams opening.

Using a variable bit rate, 10 km distance, 5 mW power, and 0.8 nm channel spacing, the best Q-factor was 59.1721 at a bit rate of 109 bps. At a variable distance, 5 mW power, and 0.8 nm channel spacing, the best Q-factor was 29.975 at 10 km. At a variable power, 10 km distance, and 0.8 nm channel spacing, the best Q-factor was 30.0548 at 7 mW. At a variable channel spacing, 5 mW power, and 10 km distance, the best Q-factor was 30.0864 at 2 nm.

SDM techniques have been proven to be valuable & important as they allow a much greater degree of system flexibility, scalability, and capacity as well which assist with the better handling of multiple communication channels and the effective use of the available resources.

Tables of Contents

List of Tables

List of Figures

List of Abbreviation

Abbreviation	Definition
APD	Avalanche Photodiodes
BER	Bit Error Rate
CDM	Code Division Multiplexing
CW	Continuous-Wave
CWDM	Coarse Wavelength Division Multiplexing
DCF	Dispersion Compensation Fiber
DEMUX	Demultiplexer
DMGD	Differential Mode Group Delay
DWDM	Dense Wavelength Division Multiplexing
EDFA	Erbium-Doped Fiber Amplifier
EMI	Electromagnetic Interference
EML	Electro-absorption Modulated Laser
FDM	Frequency Division Multiplexing
FMF	Few Mode Fiber
FWM	Four-Wave Mixing
GVD	Group-velocity Dispersion
ISI	Inter-Symbol Interference
LD	Laser Diode
LED	Light-Emitting Diode
LP	Linearly Polarized
MDM	Mode-division multiplexing

MI-MMF	Measured-Index Multimode Fiber
MIMO	Multiple-Input-Multiple-Output
MMF	Multi-Mode Fiber
MUX	Multiplexer
MZMs	Mach-Zehnder modulators
NRZ	Non-Return-Zero
NLSE	Nonlinear Schrödinger Equation
OFDM	Orthogonal Frequency Division Multiplexing
OOK	On-Off Keying
PRBS	Pseudo-Random Bit Sequence
PDM	Polarization Division Multiplexing
PON	Passive Optical Networks
QAM	Quadrature Amplitude Modulation
RZ	Return-Zero
SE	Spectral Efficiency
SDM	Space Division Multiplexing
SMFs	Single-Mode Fibers
SPM	Self-Phase Modulation
TDM	Time Division Multiplexing
WDM	Wavelength Division Multiplexing
XPM	Cross Phase Modulation

List of Symbols

Symbol	Definition
$(.)^*$	Conjugate
$\sum$	Summation
∇	One-dimensional domain
$\int$	Integration
∂	Partial derivative symbol
$\boldsymbol{i}$	Imaginary Unit, $i^2 = -1$
α	Fiber losses coefficient
A_{eff}	Fiber effective area
a	Radius of the core of step-index fibers
ω	Pulsation (angular frequency)
β	propagation constant
β_1	Fiber group velocity inverse
β_2	Fiber group velocity dispersion
B	Magnetic flux densities
b	Normalized propagation constant
c	Speed of light in vacuum
D	Electric flux densities
E	Electric field
E_y	Transverse electric field of LP modes
E_{out} , E_{in}	Domains at the input and output of the modulators
ϵ_0	vacuum permittivity
h	Planck constant
H	Magnetic field
λ	Wavelength in vacuum
I_p	photocurrent
J	Current density vector
J_p	Bessel function of the first kind of order p

k_0	Propagation constant of light in vacuum.
k_r	Radial component of the propagation constant $(k^2\, n_1^2 - \beta^2)^{1/2}$.
ρf	Charge density
γ	non-linear coefficient
μ_0	vacuum permeability
R	response of a photodiode
P	electric polarizations
P_{in}	incoming photoelectric power
M	Magnetic polarizations
M	Total number of spatial modes supported by the multimode fiber
m	Integer number
n_1	Refractive index of the core of step-index fibers
n_2	Refractive index of the cladding of step-index fibers
n_{eff}	Effective index of one core in a multicore fiber
η	quantum efficiency
p	Azimuthal mode number
Q	Q- factor
q	electron charge
r	Radial position in cylindrical coordinate
t	Time
T	defined time frame
V	Normalized frequency ($\frac{2\pi a}{\lambda}\sqrt{n_1^2 - n_2^2}$)
$\mathbf{V}_1$, V_2	Voltages applied to the arms
$V_{\boldsymbol{\pi}}$	MZ extinction tension
v	photons frequency
$\boldsymbol{v}_g$	group velocity

Chapter One

Introduction

1.1 Introduction

In optical fiber telecommunications, information is sent using light pulses through optical fiber cables. Optical fibers are hair-thin with a diameter and are made from transparent substances like glass or plastic. The light pulses carry digital information over long distances with minimal loss of signal, making optical fibers the preferred medium for high-speed data transmission in telecommunications networks. Almost every phone call, text message, downloaded movie, and web application we use is converted into a beam of light that travels through the extensive network of optical fibers spanning billions of kilometers worldwide [1].

There has been a sharp increase in network traffic in the last couple of decades due to recently developed technologies, and software that have drastically changed contemporary social standards and the way we use data. The emergence of machine-to-machine applications that delegate tasks to other machines, together with the term coined as IoT 'Internet of Things' have created incredible levels of demand that they have yet to see as possibilities[1].

In response to the growing demands for higher bit rates, research in optical fiber communications has introduced several innovative solutions, leading to the development of high-bit-rate optical transmission systems [2]. To meet the ever-expanding requirements in optical networks, both the bit rate and the spectral efficiency (SE), defined as the total bit rate divided by the channel spacing between wavelengths have significantly increased. Space division multiplexing (SDM) is considered to be a solution that can be very effective in increasing the capacity of the fibers [3].

By using specially dimensions mounted multimode fibers, new records of higher single fiber capacity have recently been achieved, to exceeding 100 Tbps, which is a great advancement compared to the previous record of single mode fibers [4]. SDM has emerged as a cutting edge technology to handle the continuous traffic growth and to anticipate future Internet bandwidth requirements. Among the various SDM technologies, the utilization of Few-Mode Fiber (FMF) transmission has been the subject of extensive study [5]. Given that conventional Multimode fiber (MMF) is ill-suited for long-haul SDM transmission due to its significant numerous spatial modes and Differential Mode Group Delay (DMGD), few mode fiber has been designed to possess only a small number of spatial modes along with a comparatively reduced DMGD [6]. Figure (1.1) illustrates the development of transmission capacity within optical fibers, as demonstrated by modern laboratory transmission experiments conducted throughout the years [7].

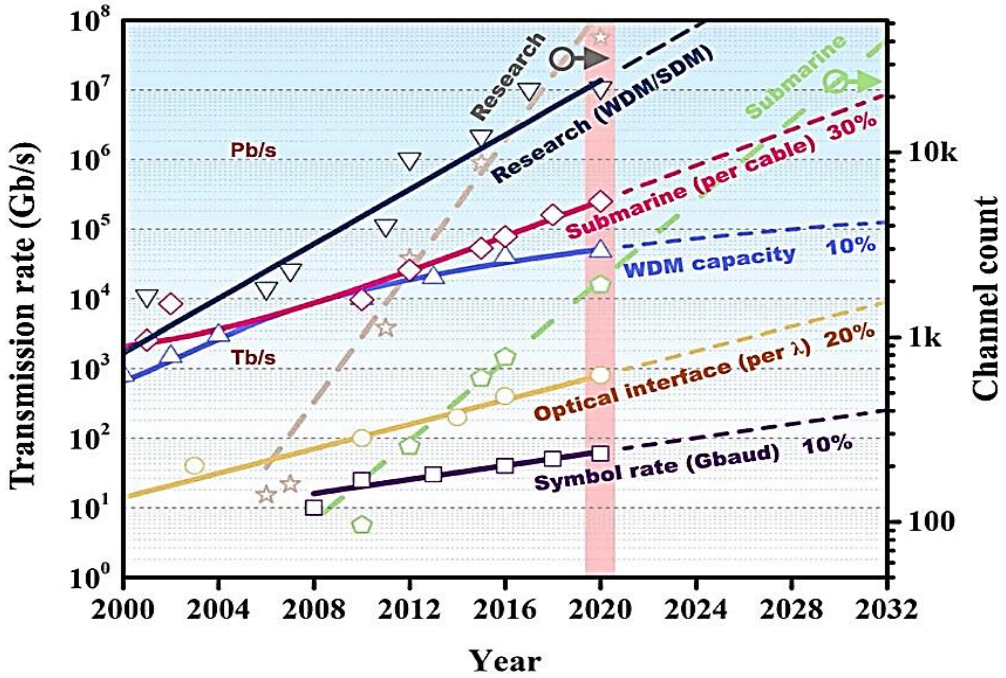

Fig. (1.1): Development of transmission capacity within optical fibers [7].

1.2 Optical Fiber Communication

Information is sent from a distinct location to another using a fiber optic communication system, which uses optic fibers as a transmission medium and light as a signal. It comprises an optical fiber, a transmitter with a laser or light-emitting diode (LED), and a receiver. Information is transformed from electrical to optical on the transmitting side, and the resulting light signal is then fired into the optical fiber. Usually, a photodetector at the receiving end transforms the optical signal back into an electrical signal. The system's transmitter employs devices semiconductor like LEDs or lasers, while the receiver typically features a PIN photodetector that converts light into electrical energy. Fiber optic cables with a silica base are commonly used as the medium or carrier in optical fiber communication systems. Propagation distances may range from a few meters within local networks (such as homes and businesses) to extensive thousands of kilometers in transoceanic connections supported by innovative optical amplification methods like using EDFA, especially in DWDM. To meet the request for increased data transmission rates for long-distance networks and communications, optical fiber technology is still developing quickly [8]. The three basic parts of a model fiber optic communication system are depicted in Figure (1.2): the optical fiber, the transmitter circuit with the light source, and the receiver circuit with the photodetector[9].

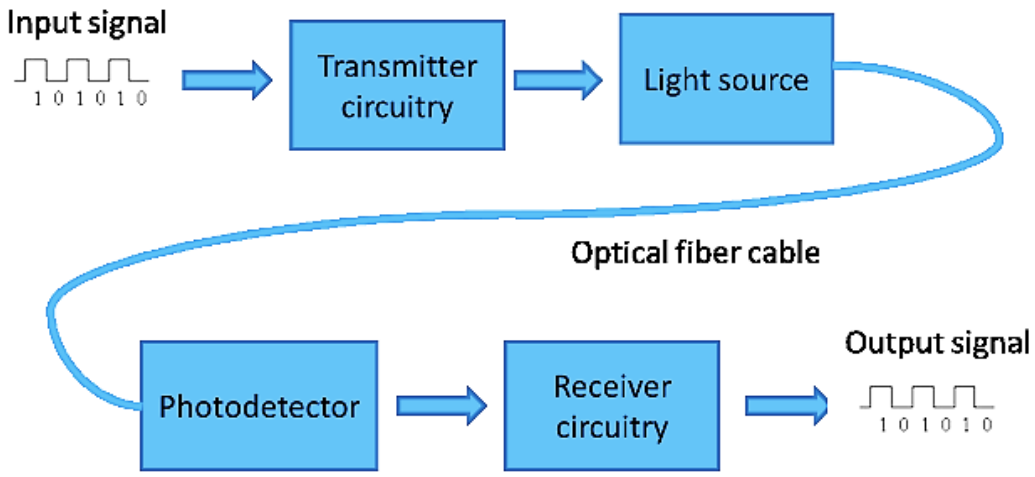

Fig.(1.2): illustrates the arrangement of components in a model optical fiber communication system[9].

1.2.1 Fiber Optical Communications Advantages

In fiber optical communication, the light source frequency surpasses that of typical electrical signals, resulting in lower attenuation compared to coaxial cables and microwave systems, offering numerous advantages. These benefits include:

- *High data capacity and wide bandwidth, allowing greater data transmission per fiber compared to copper wires.*
- *Low attenuation and long-distance transmission,* enabling efficient signal delivery over extended ranges.
- *Compact size and lightweight,* making fibers ideal for tight spaces and aerospace or marine applications.
- *Strong immunity to electromagnetic interference (EMI),* ensuring reliable operation in harsh environments like power grids, chemical plants, and oil fields.
- *Enhanced security,* as optical signals are harder to intercept than electrical ones.

1.3 Techniques for Extremely High Capacity Optical Transmission:

Ultra-high-capacity optical transmission techniques are sophisticated methods and technologies that are applied to optical fiber networks to attain extraordinarily high data transfer speeds. These strategies are critical to meeting the increasing need for high-speed data transfer in modern telecommunications networks. multiplex techniques in optical communication systems are show in Figure 1.3 [10].

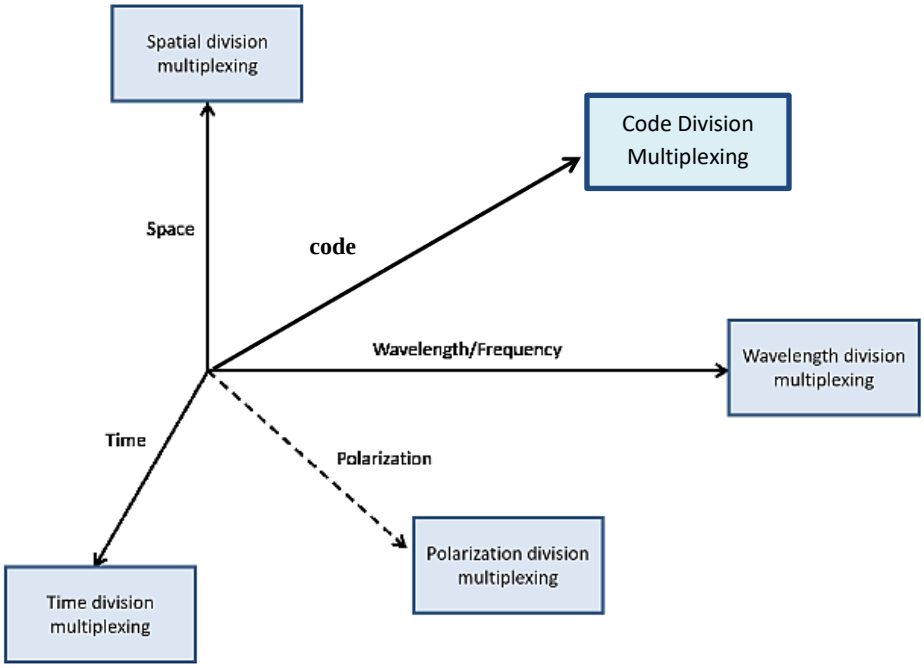

Fig.(1.3): multiplex techniques in optical communication systems [10].

1. **Wavelength Division Multiplexing (WDM):**

Wavelength Division Multiplexing (WDM) is a technique that uses various laser light wavelengths (colors) to carry distinct signals in order to multiplex multiple optical carrier signals on a single optical cable. Compared to conventional single-wavelength systems, this enables a considerable increase in the fiber's data capacity. Dense Wavelength Division Multiplexing (DWDM) and Coarse Wavelength Division Multiplexing (CWDM) are the two basic forms of WDM [11].

2. **Code Division Multiplexing (CDM)**:

Code Division Multiplexing (CDM) utilizes distinct codes to differentiate between original signals. In optical fiber communication systems employing Optical Code Division Multiplexing, each user is assigned a unique address code from a collection of orthogonal codes. Consequently, the optical transmitter encodes the information by employing this address code, whereas the optical receiver decodes the identical address code, enabling the amalgamation of the intended signal set [12].

3. **Time Division Multiplexing (TDM)**:

Time Division Multiplexing (TDM) is a method that's commonly employed. The communication bandwidth is divided into intervals of time by it. Each channel occupies a specific time interval, allowing transmission in a defined sequence. TDM is a well-established multiplexing method that is frequently utilized in optical and communication systems [13].

4. **Polarization Division Multiplexing (PDM):**

Polarization Division Multiplexing (PDM) is a physical multilayer transmission method that enables the transmission of two independent channels at the same carrier frequency by using two waves in orthogonal polarization states. Two optical channels of orthogonal polarization states are transmitted together and transmitted over an optical fiber link in polarization multiplexed communication systems [14].

5. **Frequency Division Multiplexing (FDM)**

Frequency Division Multiplexing (FDM) constitutes a methodology wherein the accessible frequency spectrum is partitioned into several non-overlapping subchannels, with each subchannel being assigned to a distinct signal. This is frequently used in cable television and radio broadcasts, when several TV channels and radio stations use separate frequencies [15].

6. **Space Division Multiplexing (SDM)**

Single-Mode Fiber (SMF) has served as the backbone of modern optical communication systems due to its low attenuation and mature infrastructure. However, as the demand for higher data transmission rates continues to rise, SMF systems are approaching their fundamental performance limits. One of the primary constraints is the Shannon capacity limit, which defines the theoretical maximum data rate of a communication channel based on its bandwidth and signal-to-noise ratio (SNR). Despite the use of advanced modulation formats, forward error correction (FEC), and dense wavelength division multiplexing (DWDM), current SMF systems are nearing this capacity boundary. Moreover, spectral efficiency (SE) improvements are increasingly difficult to realize. While SE can be enhanced by employing higher-order modulation schemes and tighter channel spacing, this leads to greater susceptibility to inter-channel interference and amplifier bandwidth limitations, particularly within the constrained C and L bands. A more fundamental limitation of SMF is its ability to support only a single spatial mode, thereby restricting the system to a single transmission path per fiber [9].

To address these challenges, Space Division Multiplexing (SDM) has emerged as a promising solution. Space Division Multiplexing (SDM) is evolution of optical transmission technology with high-capacity which allows bypassing the limits inherent to single mode optical fibers. This is accomplished through the introduction of extra spatial dimension into the optical fiber medium, which thus increases the complexity of digital signal processing systems [16]. Unlike current devices that use single mode fibers (SMFs), space division multiplexing (SDM) can be implemented with multimode fibers (MMFs) featuring a sufficiently broad core diameter for multi-mode propagation. Also, SDM can be implemented using multi-core

fibers (MCFs) which have several cores in one cladding. While Space Division Multiplexing (SDM) presents a promising avenue for scaling the capacity of optical communication systems beyond the limits of Single-Mode Fiber (SMF), it introduces several technical and practical challenges. One of the primary issues is inter-channel crosstalk, which arises due to the coupling between spatial modes in Few-Mode Fibers (FMFs) or between cores in Multi-Core Fibers (MCFs). This crosstalk leads to signal degradation and necessitates the use of complex multiple-input multiple-output (MIMO) digital signal processing to recover the transmitted signals, especially in mode-division multiplexed systems. Mode coupling is a critical challenge in SDM systems, particularly those using Few-Mode Fibers (FMF). To counteract these impairments, Digital Signal Processing (DSP) techniques based on Multiple-Input Multiple-Output (MIMO) algorithms are employed at the receiver [16, 17]. The Table 1.1 shows a comparison of the advantages and disadvantages of the different SDM.

Table [1-1]: Comparison of variant SDM systems [65].

SDM Technique	Mode of Operation	Advantages	Challenges
FMF	Transmits few spatial modes in a single core	- Increased capacity - Compatible with MIMO processing	- Mode coupling - Modal dispersion - Complex receiver DSP
MCF	Uses multiple cores in a single cladding	- High isolation between cores - Easier signal separation	- Core crosstalk - Fabrication complexity - Alignment challenges
MMF	Carries many spatial modes through one large core	- High spatial capacity - Mature fiber technology	- High mode-dependent loss and dispersion - Difficult to scale
Coupled-Core MCF	Uses coupled cores for supermode transmission	- Enables superchannel formation - Better spectral efficiency	- Strong inter-core crosstalk - Complex MIMO needed

1.4 Literature Review

D. J. Richardsonet al in 2013 highlighted the advancement of space division multiplexing (SDM) as an approach to increase the data transmission limits for optical communication networks. SDM enables the utilization of different spatial interfaces within a single optical fiber, including multiple cores or modes, allowing concurrent transmission of multiple data streams. This advancement mitigates the challenges posed by single-mode fiber systems which are nearing their capacity limits [17].

R. Ryf et al in (2013) showcased the transmission of 32-Wavelength Division Multiplexing (WDM) signals for a distance of 177 kilometers in a few-mode fiber (FMF) achieving a spectral efficiency of 32 bits/s/Hz, utilizing 12 spatially and polarization-divided modes. It introduced a practical WDM-SDM setup with real-time signal processing, providing valuable insights into the technical feasibility of mode-division multiplexing for long-haul systems. However, it was limited in terms of scalability, system cost evaluation, and energy efficiency, and required complex MIMO-DSP algorithms for signal recovery [18].

P. J. Winzer in (2014) discusses the use of space-division multiplexing (SDM) as a means to drastically enhance the data capabilities of the optical fiber networks, with a focus on metro and core networks. With the ever-increasing data traffic on a global scale, there is a need for a change in the optical communication technology in use. Spatial multiplexing provides a way to increase the capacity of fibers by using several spatial channels like different cores of the fiber or modes [19].

R. Ryf et al in (2015) introduced a new advance in the field of optical fiber technologies. The researchers achieved an important milestone by

demonstrating the transmission of 10 data streams simultaneously over a 125-kilometer stretch of multimode fiber. This achievement illustrates the significant potential for increasing optical network capacity through the application of mode-division multiplexing (MDM) [20].

LI, Borui, et al in (2016) Introduced a new concept of a bidirectional symmetric WDM-SDM optical access network and experimentally demonstrated it, which advanced the data transmission in the optical networks. Within a 20 km radius, 48 users were connected which illustrated the multi-user simultaneous access potential of the network with high access rates of 1 Gb/s. The study highlights multi-core fibers for network performance augmentation and concludes symmetric WDM-SDM networks enhance the user experience and the overall network efficiency [21].

Y. Tian et al in (2017) presented a new approach called Wavelength-Interleaved (WI) to mitigate boundary modal crosstalk in Division-Mode Multiplexing (MDM) systems. This technique improves the transmission design of weakly-coupled few mode and multi-mode fibers. WI schemes also reduce inter-spatial-channel crosstalk in short-range applications. A notable result presented in the paper claims to have achieved a record 10 G-per-channel MDM-WDM transmission over two mode FMF fibers for 120 km [22].

Y. Tian et al in (2017) posited a novel WI scheme to enhance signal fidelity in weakly coupled FMF transmission systems. The research proposers were able to show a 2x3x10 Gbps IM-DD MDM-WDM over 120 kilometers on two-mode FMF which showcased the capability of high-speed data transmission through the 2 mode FMF. The system was implemented without MIMO processing which simplified the system further making practical deployment more feasible and cost-effective. This research works

toward creating more affordable and effective fiber optic communication systems by solving modal crosstalk and achieving long-distance transmission [23].

J. Li et al. in (2018) demonstrated ultra-low noise mode division multiplexing (MDM) using eight WDM (wavelength division multiplexing) channels over a 100 km long Few Mode Optical Fiber (FM-OF) transmission for the first time. It shows how to reduce mode-dependent gain to below 0.7 dB because of backward depolarized pumping at certain wavelengths by stating that two backward depolarized pumps are launched at certain wavelengths. The paper also indicates that a Few-Mode second-order Raman Amplifier (FMRA) reduces the Improvement Spontaneous Emission (ISE) noise floor by 1.8 dB yielding an effective noise figure of roughly -3dB [24].

M. N. Ismael et al. in (2019) focused on the performance of hybrid wireless communication systems with free-space optics (FSO) combined with few-mode fiber (FMF), investigating the influence of different meteorological conditions utilizing a linear Bessel filter. Centers on correction of atmospheric turbulence and modal dispersion for optical communications systems. In the study, the system was equipped with 12-channel Spatial Division Multiplexing (SDM) FSO links to bolster system bandwidth. Simulation results show a remarkable enhancement of bandwidth with a data rate of 120 Gbps over a distance of 8500m from the FSO during clear weather as well as during heavy haze [25].

N. M. Mathew et al in (2020) demonstrate how two spatial channels are used to carry out MIMO with reduced few-mode transmission over a one-kilometer two-mode graded index fiber operating at 10 Gb/s. An air-clad photonic lantern is used to multiplex and demultiplex these channels. The power in the two degenerate LP11 modes is electrically combined and

treated as one channel. The quality factor (Q values) for LP01 and LP11 channels recorded as 5.4 and 4.7, correspondingly. In addition, the study demonstrates that the reduction in the quality of the signal due to modal noise can be improved by using various laser sources for various spatial channels, provided there is adequate separation in wavelengths. For a 10 GHz receiver bandwidth, a 0.2 nm separation is shown to raise the Q factor when compared to employing one laser source [26].

M. Kumari et al in (2021) present a next-generation hybrid bidirectional system based on 4×10Gbps MDM, TWDM-PON/FSO, analyzed under various atmospheric conditions. Results show that performance deteriorates with increasing atmospheric conditions, but enhances beneath weak-to-strong turbulence levels, routing errors, and GL. The system's long transmission distance under clear air climate is 1000 meters for FSO and 155 km for fiber links, while under dust-fog conditions, it reduces to 600 m and 145 km. Upstream channels outperform downstream channels, causing disturbances. The system can enhance fiber-FSO links utilization and transition to next-generation access networks under various weather conditions [27].

Y. Liang et al in (2022) present an all-fiber-based mode converter that was developed and constructed by utilizing a fused tapering technique to mat a single-mode fiber (SMF) with a self-made 5-mode fiber (5MF). The 5MF has a weakly coupled structure and a highly effective mode area with an attenuation of 0.277 dB/km. High-efficiency mode conversions between the fundamental mode of the SMFs and the five modes in the 5MF were achieved. The five conversion processes had 0.952, 0.930, 0.990, 0.923, and 0.998 coupling efficiencies at 1550 nm. The five converters were cascaded in order to construct a 5-mode-division multiplexer with the converters placed in descending order. For high-capacity mode division multiplexing

communication systems, the 5MF integrated with mode converters and multiplexers offers a practical and efficient solution [28].

J. Cui et al in (2023) present an all-fiber low-interference orthogonal combine the reception scheme for degrade linearly-polarized modes, enhancing signal integrity during transmission. The design involves the fabrication of a pair of 4-LP-mode mode multiplexers/demultiplexers using cascaded mode-selective couplers and orthogonal combiners, achieving low back-to-back modal crosstalk and insertion loss. The paper successfully demonstrated a constant real-time 4 modes × 4 λ × 10 Gbit/s mode division multiplexing (MDM) wavelength division multiplexing (WDM) setup transmission across a 20 km distance utilizing few-mode fiber. The proposed scheme's scalability indicates potential for supporting more modes in future implementations [29].

M. Kumari et al. (2024) presented a study that demonstrates the integration of Wavelength Division Multiplexing (WDM) and Mode Division Multiplexing (MDM) to achieve a total transmission capacity of 160 Gbps. This was realized by utilizing 16 wavelength channels, each operating at 10 Gbps, over two spatial modes in a few-mode fiber (FMF) and employing coherent detection and MIMO signal processing to mitigate intermodal crosstalk. However, the work is limited by using only two modes, testing over short distances, and not addressing nonlinear effects or DSP complexity [72].

Table [1-2]: Comparison with previous works.

Criteria	[18]	[20]	[21]	[24]	[25]	[27]
Multiplexing	WDM + SDM	10-mode SDM	WDM + SDM	MDM-WDM	SDM-FSO/FTTH hybrid	MDM-WDM hybrid
Fiber Type	FMF	MMF	MCF	FMF + Raman amplifier	Free space + SMF	FMF + FSO
Distance	177 km	125 km	Short-reach access	100 km	Variable (weather-based)	40 km
Bit Rate	9.6 Tb/s	Not specified	Not specified	Ultra-low noise at high rate	Variable	40/40 Gbps
Q-Factor	Not reported	Not specified	Not specified	High SNR Not specified	Not reported	Reported
BER	Not reported	Not specified	Not specified	Low BER with Raman	Weather-dependent	Reported under fading
Spectral Efficiency	32 bit/s/Hz	Not specified	Not specified	Not specified	Not main focus	Modeled
Main Strength	Real-world spectral efficiency demo	High-mode count over long span	Access network proof-of-concept	Raman amp with ultra-low noise	Novel FSO/FTTH hybrid with SDM	Integrated MDM-TDM-FSO system
Main Limitation	High DSP complexity	Limited scalability	Limited to access scale	Expensive Raman implementation	Environmental sensitivity	Complexity in hybrid fading model

1.5 Problem Statement

1) One of the key challenges in optical communication systems is increasing the data transmission rate while addressing both linear and nonlinear losses that arise at high bit rates, particularly over extended transmission distances.
2) Implementing a hybrid WDM/SDM system to accommodate more users and enhance data transmission.

1.6 Aim of the thesis

1) Design and simulation of multiple dependencies on the space division multiplexing (SDM) method to enhance data exchange speed.
2) Design and simulation of a hybrid WDM-SDM system to enhance user capacity and improve data transfer rates.
3) Simulation of the system under varying operational conditions, including bit rate, transmission distance, input power, and channel spacing.

1.7 Thesis Organization & Contents

The chapters of this thesis are arranged as follows:

Chapter 1 is an introduction to the topics of the thesis, a review of the literature, problem formulation, the aim of the thesis, and thesis organization & contents are given. Chapter 2 provides an overview of the transmitter and receiver optical, fiber channel, wavelength division multiplexing (WDM), and space division multiplexing (SDM) technologies. The suggested proposed optical space division multiplexing (SDM) system design schemes are described in detail in Chapter 3. Results and discussion of simulation

tests are provided in Chapter 4. Chapter 5 contains conclusions and future works.

Chapter Two

Theory

2.1 Introduction

This chapter contains the theoretical part of the optical communication system and also contains the theoretical part of multiplexer methods.

2.2 Optical Transmitter

At the initial of the optical transmitter, the bit sequence is transformed into an electrical signal that modulates the optical carrier generated by the laser source.

2.2.1 Laser and LED Structures

To convey data across optical fibers, an optical transmitter transforms electrical impulses into optical signals. It is made up of a modulator and a light source, which is often a light-emitting diode (LED) or laser. The choice of light source depends on the application requirements such as data rate, distance, and cost [30].

A laser diode utilizes semiconductor material to produce laser radiation by inducing the process of stimulated emission that occurs within the energy bands (specifically the conduction and valence bands) of semiconductors. The process necessitates population inversion to generate the desired stimulated emission.

An LED is a semiconductor device that converts electrical energy into optical energy through spontaneous emission. The emitted light is incoherent, with a broad spectral bandwidth ranging from 30 to 60 nm and a relatively large emission divergence angle from 120° to 180°[31].

LEDs may be used as light sources in both graded index fiber and multi-mode step index fiber (MMF). Table 2.1 provides an overview of typical

characteristics of semiconductor sources that are employed in optical fiber communication [32].

Table (2-1): The usual defining factors of semiconductor diodes that are employed in optical fiber communication [32].

Parameters	LEDs	Single mode laser diode	Laser diode
Spectral width.	20 ~ 100 nm	< 0.2 nm	1 ~ 5 nm
Cost.	Low	Very high	High
Coupling Efficiency.	Low	High	Moderate
Modulation bandwidth.	< 300 MHz	Up to 6 GHz	Up to 10 GHz
Adapted fiber.	MMF	SMF.	MMF and SMF
Rise time.	2 ~ 250 ns	0.05 ~ 1 ns	0.1 ~ 1 ns
Application.	Medium distance Medium speed	Ultra-long distance Ultra-high speed	Long distance High speed

2.2.2 The Modulation

In optical communication systems, modulation refers to the process of encoding information onto a carrier light wave for transmission over an optical fiber. Optical modulators are typically characterized by their electro-optic bandwidth, extinction ratio, and insertion loss. Through modulation, the optical transmitter transforms electrical signals into optical signals. Modulation involves altering specific characteristics of the light wave, such as intensity, phase, frequency, or polarization, in response to the input electrical signal. Various optical modulation techniques are used, including direct modulation of the laser and external modulation using devices such as Mach-Zehnder modulators to alter the continuous wave output [33, 34]. Among these components are Intensity Modulation (IM), Phase Modulation

(PM), Frequency Modulation (FM), Amplitude Modulation (AM), Mach-Zehnder modulators (MZMs), and electro-absorption modulators. The most widely used modulation technique in fiber-optic communication systems is on-off keying (OOK) [9]. Using direct intensity modulation of a laser, while straightforward, introduces an unwanted fluctuation in the lasing frequency, known as frequency chirp. This chirp refers to a momentary change in frequency during pulse transmission and is closely related to the laser's operating mode. It primarily arises due to carrier-induced changes in the refractive index. As a result, frequency chirp leads to pulse spreading and ultimately limits the effective transmission distance of the system [2]. The effect of low frequency of electrical absorption rate frequencies, which relies on the modification of the absorption coefficient of a semiconductor material, allows them to be monolithically integrated with lasers to create a small and inexpensive component known as an electro-absorption modulated laser (EML). Another common device for long-distance high-speed optical communications that exhibits extremely low frequency chirping is the MZM external modulation component, which features a wide electrical optical bandwidth (up to 40 GHz), high extinction ratio (≥ 20 dB), and a modest insertion losses (≤ 4 dB). Furthermore, MZM have a recognized weak wavelength dependence. When compared to direct modulation, external modulation has a number of benefits. For example, modulation rates can be increased, and the optical source may be employed at a relatively low cost without compromising functionality [34]. As illustrated in Figure 2.1, two widely adopted modulation schemes are currently used in optical communication systems: direct modulation and indirect modulation [9].

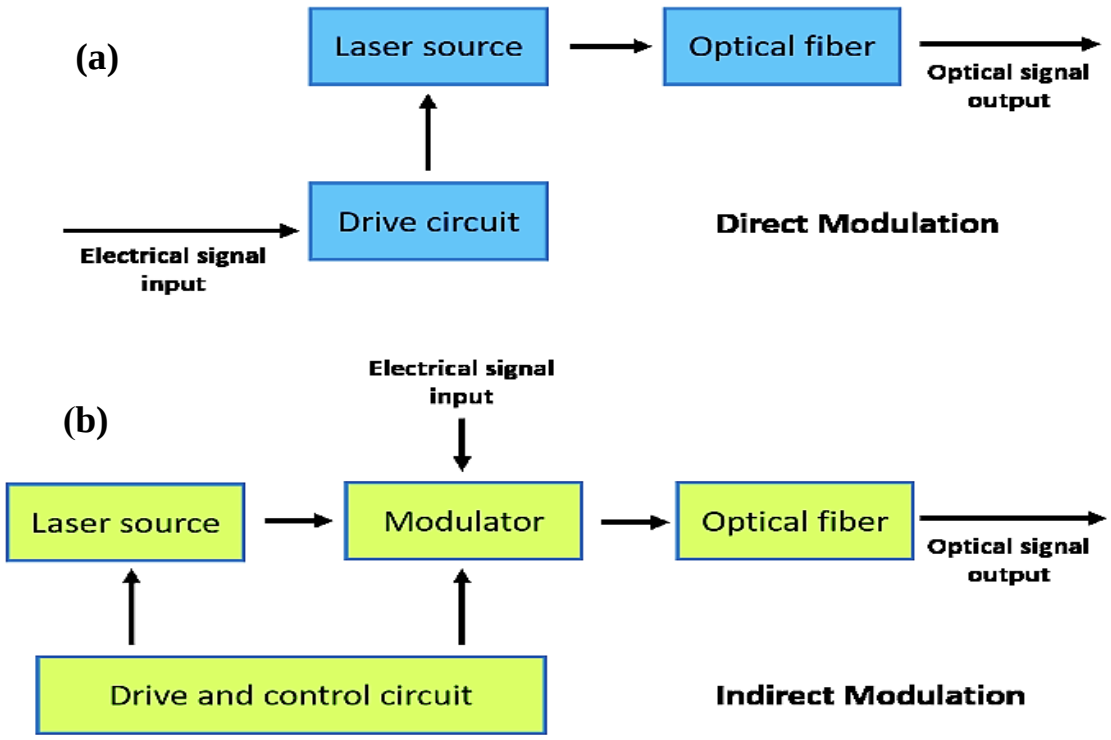

Fig. (2.1): The two primary methods of optical modulation: (a) direct modulation and (b) indirect modulation. [9].

2.2.2.1 The Mach-Zehnder Modulator (MZM)

A Mach-Zehnder Modulator is an interferometer made up of duo arms of Lithium Niobate crystal and two 3 dB couplers ,as seen in figure (2.2). Modulation is achieved through the application of a voltage to the arms, which alters the refractive index and thus controls the phase of the light traveling by them, resulting in interference at the MZM's output, both detrimental and constructive. The optical signal experiences amplitude variations as a result of this interference [35]. The operational behavior of an MZM is described by its input-output relationship:

$$E_{out} \propto E_{in} \cos\left(\pi \frac{V_1 - V_2}{2V_\pi}\right) \quad (2.1)$$

Where E_{out} and E_{in} represent the optical fields at the output and input of the modulator, respectively. V_1 and V_2 denote the voltages applied to the two

arms of the Mach-Zehnder Modulator (MZM),while Vπ refers to the modulator's half-wave voltage, i.e., the driving voltage required to induce a phase shift corresponding to a transition from constructive to destructive interference. MZMs can be utilized for both analog modulation schemes, such as Orthogonal Frequency Division Multiplexing (OFDM), and digital modulation formats like On/Off Keying (OOK), Quadrature Amplitude Modulation (QAM), and Binary Phase Shift Keying (BPSK), provided that the driving electrical voltages are sufficiently high [35].

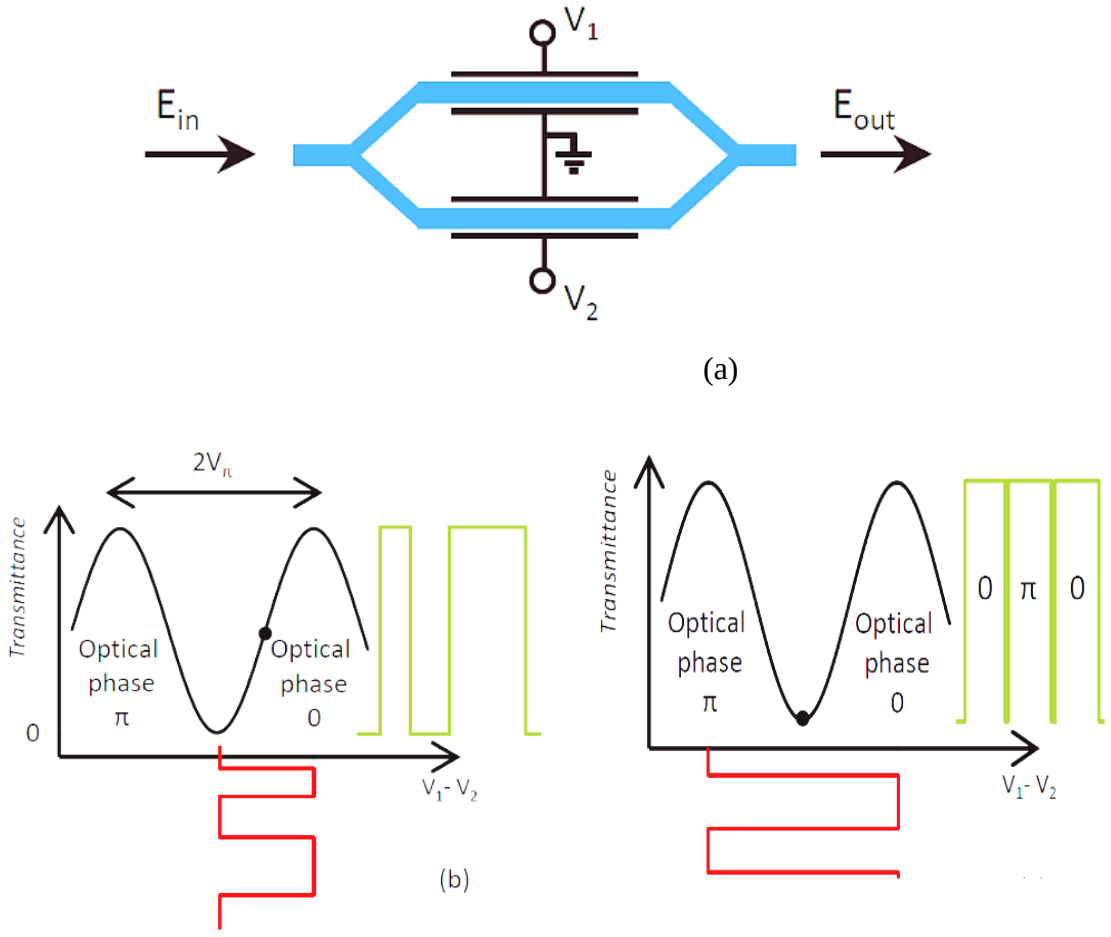

Fig.(2.2) : Mach-Zehnder modulator (MZM): (a) Mach-Zehnder modulator schematic, (b) MZM biased Power transmittance at the quadrature, and (c) MZM biased Power transmittance at the trough point [35].

2.3 Fiber Channel

The Schrödinger equation proves to be a highly effective instrument employed for the purpose of simulating wave propagation in different scenarios, such as the transmission of light in optical fibers [36]. where Pulse propagation in single mode fibers is commonly described by a generalized nonlinear Schrödinger equation (NLSE) that characterizes the change in the electric field amplitude envelope of an optical pulse as it moves through the fiber [37, 38]. The Nonlinear Schrödinger Equation (NLSE) is able to explain the phenomena of dispersion and nonlinear effects that take place as light travels through an optical fiber. The most well-known use of the NLSE, the explanation of supercontinuum production, wherein both linear and nonlinear dispersion phenomena combine to produce remarkable widening of the light spectrum, frequently occurring within brief propagation distances [39]. Nevertheless, it is crucial to comprehend that when it comes to practical utilization in fiber optic communication systems, engineers commonly depend on established numerical techniques instead of solving the Schrödinger equation directly, because complexity, numerical methods, and computing can be costly.

In the Nonlinear Schrödinger Equation (NLSE), the primary variable of evolution is space, specifically, the longitudinal position along the fiber. The derivation of the NLSE from Maxwell's equations involves several assumptions, which are typically valid in modern fiber-optic communication systems [40].

The transmission of optical fields in fibers, similar to all electromagnetic phenomena, is controlled by Maxwell's equations. These equations are represented by [41] :

$$\nabla \times \mathbf{E} = -\frac{\partial \mathbf{B}}{\partial t}\,, \tag{2.2}$$

$$\nabla \times \mathbf{H} = \mathbf{J} + \frac{\partial \mathbf{D}}{\partial t}, \quad (2.3)$$

$$\nabla \cdot \mathbf{D} = \rho f, \quad (2.4)$$

$$\nabla \cdot \mathbf{B} = 0, \quad (2.5)$$

In the electromagnetic fields, the letters H and E refer to the magnetic and electric fields, while B and D stand the respective magnetic and electric flux densities. The sources of the electromagnetic field are the charge density ρf and the vector representation of current density J. The constitutive equations establish a relationship between the flux densities B and D, which emerge in reaction to the magnetic and electric fields propagating within the medium [41]:

$$\mathbf{D} = \epsilon_0 \mathbf{E} + \mathbf{P} \quad (2.6)$$

$$\mathbf{B} = \mu_0 \mathbf{H} \quad (2.7)$$

Here, P stand for the induced electric polarizations, μ_0 for vacuum permeability, and ϵ_0 for vacuum permittivity.

Optical fibers are non-magnetic media, as indicated by the relation M = 0. Additionally, because they are a medium devoid of free charges, J = 0 and ρf = 0 will inevitably occur [40].

Nonlinear phenomena in optical fibers are commonly investigated through the utilization of brief optical pulses, as the dispersive characteristics are more pronounced under such conditions. The analysis of optical pulse propagation within fibers involves the application of Maxwell's equations. Within the context of the tardily changing envelope approximation, the solution to these equations gives rise to the NSE.

The transmission of a light pulse through an optical fiber over a distance z can be described using the propagation equation NLSE[42].

$$\frac{\partial A}{\partial z} + \beta_1 \frac{\partial A}{\partial t} + \frac{i\,\beta_2}{2}\frac{\partial^2 A}{\partial t^2} + \frac{\alpha}{2}\boldsymbol{A} = i\,\gamma|A|^2\,\boldsymbol{A}. \tag{2.8}$$

where $\boldsymbol{\alpha}$ is fiber losses coefficient, β_1 is Group delay, β_2 is fiber group velocity dispersion, γ is a nonlinear coefficient parameter that may be defined as:

$$\gamma = \frac{n_2\omega_0}{cA_{eff}} \tag{2.9}$$

where the effective core area, denoted as parameter $\boldsymbol{A}_{eff}$, refers to the region in an fiber optical where light is confined. It is defined as such:

$$\boldsymbol{A}_{\text{eff}} = \frac{\int_{-\infty}^{+\infty} |F(x,y)|^2 dxdy}{\int_{-\infty}^{+\infty} |F(x,y)|^4 dxdy} \tag{2.10}$$

where the modal distribution of the mode moving through the optical fiber is represented by $F(x,y)$. The fiber properties, such as core size and core-cladding index difference, determine the effective area. When silica glass is used, $\boldsymbol{A}_{\text{eff}}$ typically ranges from 20 to 100 μm^2, where n_2 is approximately 2.6 × 10^{-20} m^2/ W. As a result, the matching value of γ falls between 1 and 100 W^{-1}/ km^{-1}.

The propagation of a pulse within the fiber of optical is delineated by equation (2.8). It is commonly known as the nonlinear Schrödinger equation (NLS). Where $\boldsymbol{A}$ is the pulse envelope's gradually changing amplitude, and this equation accounts for the impacts of fiber losses denoted by α, chromatic dispersion represented by β_1 and β_2, as well as nonlinearity ($\gamma > 0$) on the pulses that propagating inside the optical fibers. In short, the propagation of the pulse envelope occurs at the group velocity vg, which is defined as the Group delay (inverse group velocity) of the parameter β_1, whereas the impact

of group-velocity dispersion (GVD) is determined by the parameter β_2. The GVD parameter may exhibit positivity or negativity contingent upon whether the wavelength λ falls below or exceeds the zero-dispersion wavelength λ_D characteristic of the fiber. where, based on the sign of the coefficient β2, sign β2 = ±1. A positive or normal dispersion regime is implied by a positive value, whereas an anomalous or negative dispersion regime is indicated by a negative value. In standard silica fibers, β2 ∼ 50ps2/Km in the visible region but becomes close to −20ps2/Km near wavelengths ∼ 1.5μm, the change in sign occurring in the vicinity of 1.3μm [43].

The main boundary condition is the initial pulse shape at the input of the fiber:

$$A\ (z = 0, t) = A_0\ (t) \tag{2.11}$$

Where A(z,t) is the slowly-varying envelope of the optical field, and $A_0(t)$ is the input optical pulse.

Equation (2.8) governs the pulse propagation within a fiber of optical. The term β_1 represents the reciprocal of the group velocity $1/v_g$, indicating the speed at which the pulse is propagating, within a newly defined time frame T aligned with the group velocity.

$$T = t - \frac{z}{v_g} = t - \beta_1\, z \tag{2.12}$$

Eq. (2.8) be:

$$\frac{\partial A}{\partial z} - i\ \frac{\beta_2}{2}\frac{\partial^2 A}{\partial T^2} + \frac{\alpha}{2}\boldsymbol{A} = i\,\gamma|A|^2\,\boldsymbol{A} \tag{2.13}$$

Where A is the slowly varying envelope, α is the fiber loss, $\beta 2$ the GVD. Equation (2.12) is usually known as the Nonlinear Schrödinger (NLS) Equation. This equation is responsible for dictating the progression of the

envelope and elucidating its characteristics in relation to the distance traveled by the field distribution within the optical fiber [44].

2.4 Nonlinear generalized Schrodinger Equation for Multimode Fibers

For multiple modes $A_p(z,t)$ the boundary conditions extend similarly:

$$A_p(z=0, t) = A_{0,p}(t) \qquad \text{for all modes p}$$

Where $A_{0,p}(t)$ defines the input signal for each spatial or polarization mode.

The design of an optical link take into account the non-linear effects that arise in the fiber when the injected input powers are sufficiently high or the transmission distance is sufficiently long. In our work, we will solely focus on linear effects in MDM systems. Knowing that the effective core areas of multi-mode fibers are larger than those of SMFs, the non-linear parameter γ given in (2.9) which is inversely proportional to A_{eff} will be smaller for MMFs and one would expect an enhanced tolerance to non-linearity. The authors theoretically studied inter-modal cross phase modulation and inter-modal four-wave-mixing in MDM systems. They found that rapidly varying birefringence in the fiber reduces the number of inter-modal non-linear terms in the NLS propagation equation which can be written for the p-th mode as [2]:

$$\frac{\partial A_p}{\partial z} = -\frac{\alpha}{2}\boldsymbol{A}_p - i\,\beta_{1p}\frac{\partial A_p}{\partial t} - \frac{i\,\beta_{2p}}{2}\frac{\partial^2 A}{\partial t^2} + i\,\frac{\gamma}{3}\sum_{1,m,n} f_{plmn}\,[(a_1^T\, a_m)\, a_n^{*} + 2\,(a_n^t\, a_m)\, a_l\,] + i\sum_m q_{mp}\, a_m \qquad (2.14)$$

Where $A_p = [A_pX, A_pY\,]^T$ is the electrical field vector of the p-th mode, $\boldsymbol{\alpha}$ is fiber losses coefficient, β_1 is Group delay, β_2 is fiber group velocity dispersion, and f_{plmn} and q_{mp} are the non-linear and linear couplings among spatial modes. However, further investigations of non-linear effects in multi-

mode and multi-core fibers are required in order to establish the capacity limit for SDM schemes as well as their NLT operation point.

The propagation of the slowly varying pulse envelope $A_p(z,T)$ propagating in mode p in an optical fiber supporting N total number of modes can be generally described as [44]:

$$\frac{\partial A_p}{\partial z} = -\frac{\alpha}{2}\boldsymbol{A}_{\mathrm{p}} + i(\beta_{0p} - \beta_{0r})A_p - \left(\beta_{1\mathrm{p}} - \frac{1}{v_{gr}}\right)\frac{\partial A_p}{\partial T} - i\,\frac{\beta_{2\mathrm{p}}}{2}\frac{\partial^2 A_p}{\partial T^2}$$

$$+ i\sum_{l=1}^{N}\sum_{m=1}^{N}\sum_{n=1}^{N}\gamma_{plmn}\,\mathrm{A}_l\,\mathrm{A}_{\mathrm{m}}\,\mathrm{A}_{\mathrm{n}}^{*} \qquad (2.15)$$

where $A_p(z,T)$ slowly varying amplitude envelope of the p-th mode, z propagation distance, T is Time in a co-moving frame, the symbol α represents the attenuation coefficient, which may vary depending on the mode. v_{gr} and β_{0r} denote the reference values for group velocity and propagation constant, correspondingly. $\beta_{0p} = \beta_p(\omega_0)$, $\beta_{1p} = \partial\beta_p/\partial\omega|_{\omega 0}$, and $\beta_{2p} = \partial^2\beta_p/\partial\omega^2|_{\omega 0}$ represent the propagation constant IGV, and GVD of the p$^{\mathrm{th}}$ mode, respectively. The nonlinear part in the multi-mode NLSE is defined by γ_{plmn}, which is the nonlinear coefficient as earlier defined in Equation (2.9) as follows:

$$\gamma_{plmn} = \frac{n_2\omega_0}{c\boldsymbol{A}_{eff}^{(plmn)}} \qquad (2.16)$$

Nonetheless, the following overlap defines the effective region in this instance

$$A_{eff}^{(plmn)} = \frac{\left(\iint|F_p|^2dxdy\ \iint|F_l|^2dxdy\ \iint|F_m|^2dxdy\iint|F_n|^2dxdy\right)^{1/2}}{\iint F_p^{*}\,F_l^{*}\,F_m^{*}\,F_n\,dxdy} \qquad (2.17)$$

where the field distributions of the (p,l,m,n)$^{\mathrm{th}}$ modes are denoted, respectively, by F($plmn$). Equation (2.13) may be rewritten as Equation

(2.8) when the multimode fiber's single fiber mode is activated, and Equation (2.10) can be used to express the effective area.

2.5 Optical Receiver

At the end of the fiber, the optical receiver converts an optical signal to an electric signal [8]. The various parts of the receiver depend on several factors, such as the system's data rate and modulation scheme. The block diagram of an optical receiver is shown in Figure 2.3. comprises a photodetector and a demodulator, which functions as the signal processor.

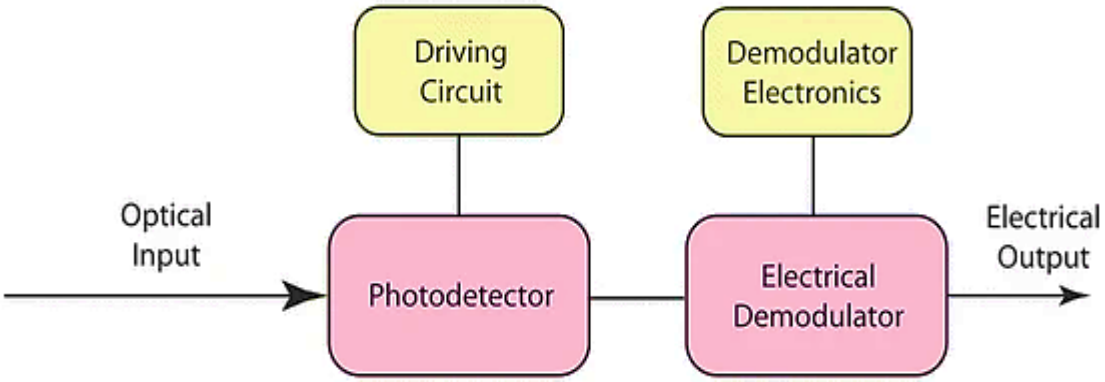

Fig.(2.3) : the block diagram of an Optical Receiver [45].

2.5.1 Photodiode PIN and APD

Optical receivers utilized in fiber optic communication systems typically employ semiconductor-based PIN photodiodes (PINs) or avalanche photodiodes (APDs) to convert the incoming signal. PIN photodiode is a desirable option for optical detecting applications due to its rapid speed, high responsivity, inexpensive, and mini size and weight. A notable distinction between a standard PN diode and a PIN diode lies in the incorporation of an intrinsic region (i) positioned amidst the p and n regions, thereby resulting in an enlarged depletion region. This intrinsic region, with a width of 5 to 50μm,

facilitates the absorption of a significant portion of photons, as illustrated in figure (2.4) [46].

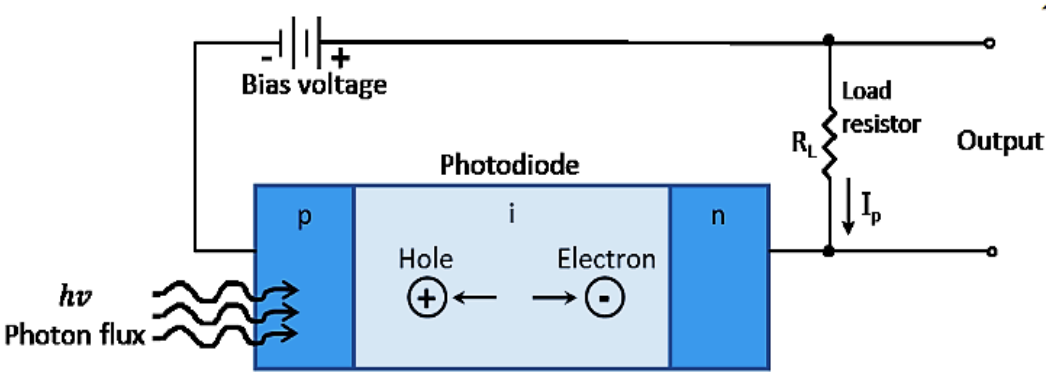

Fig.(2.4) : The photodiode PIN circuit layout with reverse bias applied [46].

An electron-hole pair may form if the input photon's energy hν surpasses the bandgap energy E_g and is absorbed by the depletion zone. The photo generated electron-hole pair is swept across the junction by the reverse bias provided to the *pn* junction, and the photocarriers create a current flow in the external circuit. This resulting current flow is referred to as the photocurrent I_p. The photocurrent I_p, also known as the photodetector current I_{det}, varies linearly in response to variations in the incident optical power. This process transforms the optical signal into a current, which then creates a voltage across a resistor. The number of electron-hole pairs created for every incoming absorbed photon of energy hv is known as the quantum efficiency, or η, and can be expressed as:

$$\eta = \frac{I_p/q}{P_{in}/h\nu} \tag{2.18}$$

The photocurrent I_p represents the current produced by a photodetector when exposed to a constant optical power Pin .

The response of a photodiode is known as the relationship between the output photocurrent and the incoming photoelectric power, and can be expressed as follows.

$$R = \frac{I_p}{P_{in}} \approx \frac{\eta q}{h\nu} \approx \frac{\eta \lambda}{1.24} \quad (2.19)$$

where Planck's constant h = 6.63×10^{-34} J·s, electron charge q = 1.6×10^{-19}C, while the frequency of incoming photons is symbolized by ν[9].

Avalanche photodiodes are comparable to other types of photodiodes that have an inherent gain because of their substantial biasing potential. When incident photons are swept over an area of the APD with a strong electrical field, they accelerate the process of electron-hole pair formation and acquire enough energy to eject more further electron-hole pair from atoms in the network. A secondary electron-hole pair is the pair of electrons produced by impact ionization. As the new secondary electron and hole pairs pass through the area of strong electric field, they accelerate and may smash with other atoms several times, leading to ionization. The avalanche effect of this mechanism tends to produce a fast rise of photo-carriers. To put it briefly, an APD is a very sensitive photodetector that multiplies photocurrent by using the avalanche phenomenon [47].

2.5.2 The Bit Error Rate (BER) And Eye Diagram

The Bit Error Rate (BER) is a critical parameter in evaluating the performance of digital communication systems, including optical communication systems. It measures the rate at which errors occur in the transmitted data over a communication channel. The quantity of bit errors divided by the total number of bits transmitted in a given time period is known as the bit error rate or BER [44]. Mathematically, it is expressed as:

$$BER = \frac{Number\ of\ Bit\ Errors}{Totel\ Number\ of\ Bits\ Transmitted} \quad (2.20)$$

High-grade optical fiber signals typically necessitate a bit error rate that is below 1×10^{-9}. The conversion of the optic signal to an electric signal is

performed by the photodetector. Subsequently, the electrical signal is sampled by the decision circuit to ascertain the corresponding bit value of either 1 or 0. The decision circuit compares the value of the sample with the threshold value I_D. If I > I_D , it determines the bit to be 1, and if I < I_D , it determines the bit to be 0.Nevertheless, when subjected to the impact of optical receiver noise, it is possible for a 0 bit to be mistakenly identified as a 1 bit if the current falls below I_D. Likewise, in cases where the current exceeds I_D, a 1 bit could be inaccurately perceived as a 0 bit [42]. As a result, the probability of error can be characterized as follows:

$$\text{BER} = \text{P}(1)P(0/1) + \text{P}(0)P(1/0) \tag{2.21}$$

where P(0) and P(1) represent the likelihood of receiving bit '0' and bit '1' , correspondingly. The notation P (0/1) denotes the probability of incorrectly identifying bit '1' as bit '0', whereas P(1/0) signifies to the probability of incorrectly identifying bit '0' as bit '1'. Given that the probabilities of encountering bit “1” and bit “0” are identical [42], the Bit Error Rate (BER) can be expressed as

$$\text{BER} = \frac{1}{2}[P(0/1) + P(1/0)] \tag{2.22}$$

This equation is only used when the transmission probabilities are equal; it is not applicable when the distribution is asymmetrical. Lastly, equation (2.23) demonstrates the relationship between BER and the Q factor.

$$\text{BER} = \frac{1}{2}\text{erfc}\left(\frac{Q}{\sqrt{2}}\right) \approx \frac{\exp(-Q^2/2)}{Q\sqrt{2\pi}} \tag{2.23}$$

where the Q factor is provided by

$$\text{Q} = \frac{I_1 - I_0}{Q_1 + Q_0} \tag{2.24}$$

Where $I_1$is mean optical power for bit "1", I_0 is mean optical power for bit "0", and Q_1, Q_2 is standard deviations of noise for "1" and "0" levels. Figure (2.5) illustrates how the Q factor affects BER. and the BER falls off as Q rises. BER < 10^{-12} when Q > 7, and BER ≈ 10^{-9} when Q = 6.

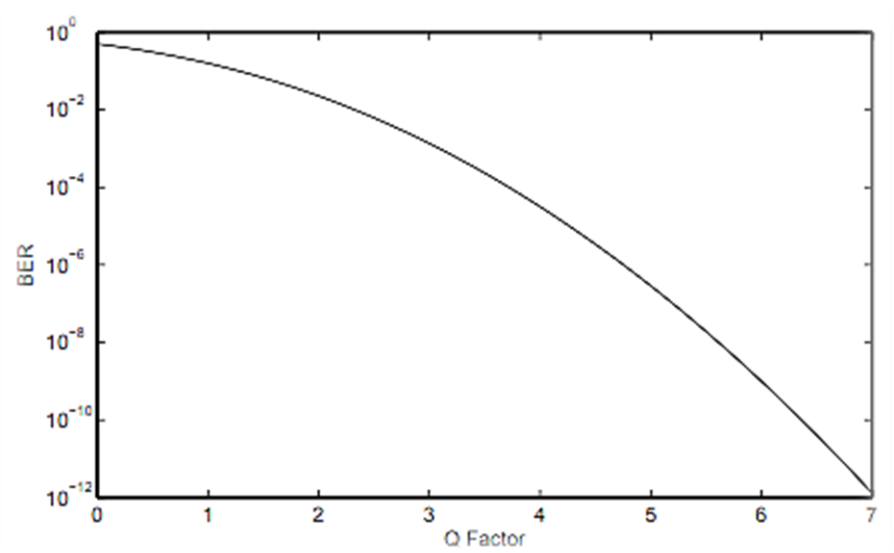

Fig.(2.5) : The correlation between Q factor and BER [32].

Typically, the oscilloscope is used to view the received signal's waveform and assess how noise and inter-symbol interference affect the system's performance. For this, the eye diagram is typically employed. Eye diagrams offer a visual representation to assess the quality of the signal that has been received. Typically, an eye diagram is produced by cumulatively showing the serial signal bits that were gathered via the afterglow technique. The figure that is superimposed has an eye-like form, which is why it is called the "eye diagram." There are essentially eight different bit patterns in a full eye diagram, ranging from "000" to "111." As seen in figure (2.6), an eye picture is created by adding the eight different bit patterns at random [48].

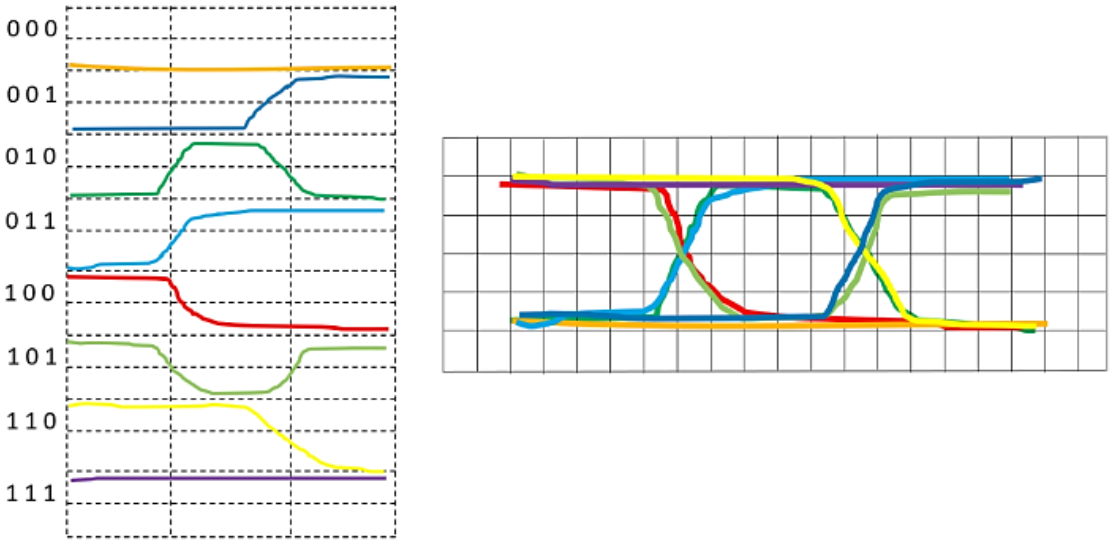

Fig.(2.6) : Formation Of An Eye Diagram [48].

There is no distortion in the waveform and each symbol will overlap in the ideal scenario where there is no inter-symbol crosstalk or noise. The oscilloscope displays a bright, distinct "eye" that is primarily open. Crosstalk between the signals causes distortions in the waveform and obscures the eye pattern's trace. Gradually, the "eye" commences to narrow. As a result, the "eye" opening's size indicates both the grade of distortion and the intensity of inter-symbol interference. This further highlights the capability of the eye diagram to assess the quality of an optical fiber communication system by illustrating the effects of noise and inter-symbol interference [48].

2.6 Multiplexing Methods

2.6.1 Wavelength Division Multiplexer (WDM)

Wavelength Division Multiplexer is a technological approach that involves the utilization of multiple transmitters and receivers in order to transmit and receive diverse optical carrier wavelengths [49, 50]. The WDM multiplexer and demultiplexer are composed of 2n selection lines . Enabled by powerful, broadband optical amplifiers, WDM involves sending separate streams data through various wavelengths known as “channels” that propagate

simultaneously over the same fiber, as seen in Figure (2.7) [2]. With the high available bandwidth of THz, WDM allowed the system capacity to be increased 100-fold and support traffic growth at an extremely low cost per bit[51]. According to ITU-T G.694.1 guidelines, one of the main benefits of WDM is that it does not cause linear interference between channels, even in dense WDM systems with wide channels at 50 GHz and 25 GHz. Before integrated into the transmitter and detected in the receiver, each channel can be filtered independently. Up to 220 channels can be broadcast on the 50GHz network using both C and L bands [52]. Utilizing WDM with multimode fiber offers the benefit of greater capacity compared to single-mode fiber [51].

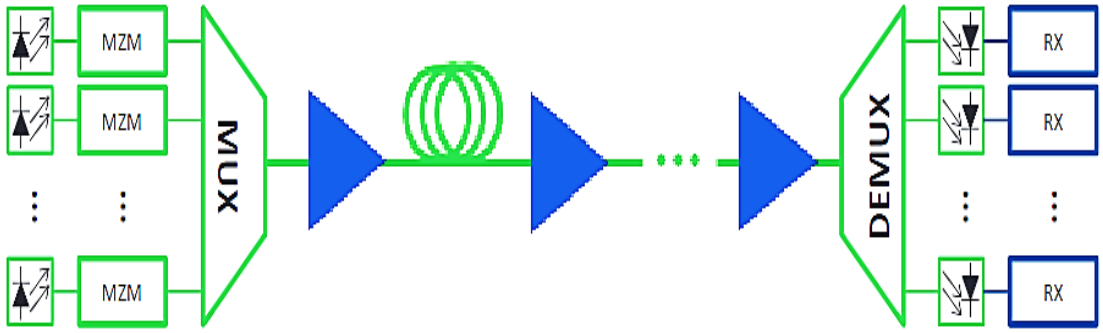

Fig. (2.7) : A transmission scheme using wavelength division multiplexing [2].

Nevertheless, non-linear inter-channel crosstalk brought on by Cross phase modulation (XPM) and Four wave mixing (FWM) might affect WDM systems. XPM, similar to Self-phase modulation (SPM), results from the optical Kerr effect causing intensity fluctuations in one wavelength λ1 to impact the phase of another wavelength λ2. On the other hand, FWM happens when two wavelengths λ1 and λ2 traveling in the same direction generate two additional components at wavelengths $\lambda 3 = 2\,\lambda 1 - \lambda 2$ and $\lambda 4 = 2\,\lambda 2 - \lambda 1$, which might coincide with other wavelengths carrying data, leading to interference and potential loss of information [40].

In WDM systems, the penalties caused by XPM can be mitigated by raising the channel secession. Effective strategies to counteract FWM include uneven channel spacing, specific dispersion maps with non-zero local dispersion, and zero total mean chromatic dispersion [53, 54]. However, when the number of channels increases, each one is impacted by several others, and the resulting penalties vary depending on a variety of factors, including the bitrate of the channel, the dispersion coefficients, the channel spacing, and the modulation styles utilized. In fact, the signals interact for a considerable amount of time at lower bit rates and-or lower chromatic dispersion, resulting in large non-linear phase changes. This interaction gets shorter as bit rates and-or chromatic dispersion increase. Nevertheless, with high bitrates, each channel's bandwidth is larger, and nonlinear effects akin to XPM and FWM will manifest within each channel [55]. The terms XPM and intra-channel FWM (IXPM and IFWM) are used to describe these phenomena. Research is currently underway to mitigate these nonlinearities using powerful digital signal processing capabilities and coherent detection. Among the most effective, albeit complicated, solutions are backpropagation and Volterra based methods that attempt to reverse the propagation equation (2.8) [56].

2.6.2 Space Division Multiplexing (SDM)

Space is now thought to be the final degree of freedom that may be utilized in an optical fiber to increase the transmission system's capacity [57]. The concept of using space-division multiplexing (SDM) to increase an optical fiber's capacity is almost as ancient as optical fiber communications. Since the 1970s, Space Division Multiplexing (SDM) has been proposed for signal transmission over multiple fiber cores, but precise control of crosstalk between cores has been a challenge. Recently, due to the predicted capacity limitations of single-mode fiber, SDM technology is being reconsidered as a promising solution for meeting future bandwidth demands, supported by

advancements in advances in the manufacturing of optical components [58]. SDM is a fascinating technique that can be applied to ultra-high-capacity, short-distance networks, such as those connecting data centers. To make greater use of the spatial capacity within the fiber, in-fiber space-division multiplexing (SDM) can be implemented using bundled single-mode fiber (SMF) [17], multimode fiber (MMF) [59], or multi core fiber (MCF) [60]. The type of fiber significantly affects modal dispersion and inter-modal crosstalk. The spatial modes in few-mode fiber (FMF) systems exhibit strong mode coupling and a large differential mode group delay (DMGD) [61]. A key advantage of SDM techniques is the ability to orthogonally establish transmission paths capable of carrying independent data streams within the same fiber while maintaining system component integration constraints. This approach reduces both the cost and power consumption of the overall system, including integration into the fiber itself [6, 62], the transponders [63], and the optical amplifiers [64].

The propagation of optical fields is controlled by Maxwell's equations, where the optical fiber is considered a circular wave. In the cylindrical coordinate system (r, ϕ, z), where the magnetic field (H) and electric field (E) electromagnetic waves should be considered is being indicated as [65]:

$$\mathbf{E}\,(r, \phi, z, t) = E(r, \phi)\ \exp[j(\omega t - \beta z)] \tag{2.25}$$

$$\mathbf{H}\,(r, \phi, z, t) = H(r, \phi)\ \exp[j(\omega t - \beta z)] \tag{2.26}$$

where the frequency is represented by ω, t is time, and β is propagation constant. The electric and magnetic fields are transverse distribution by $E(r, \phi)$ and $H(r, \phi)$, respectively. Guided modes can be used to image optical fields propagating through optical fibers, each mode having a propagation constant and field distribution. Effective indices (n_{eff}) are utilized to characterize fiber modes, with the propagation constant (β) of each mode can be given by [65]:

$$\beta = n_{eff} k_0 = n_{eff} * \frac{2\pi}{\lambda} \quad (2.27)$$

where n_{eff} is the effective index of each mode, in range $k_0 n_1 > \beta > k_0 n_2$ and k_0 is the propagation constant in free space, which is defined as[19]:

$$k_0 = \frac{\omega}{c} = \frac{2\pi}{\lambda} \quad (2.28)$$

where ω is the frequency, c is the speed of light, and λ is the wavelength.

The handled modes are shown in Figure (2.8) with respect to the propagation constant (β) and normalized-frequency (V).

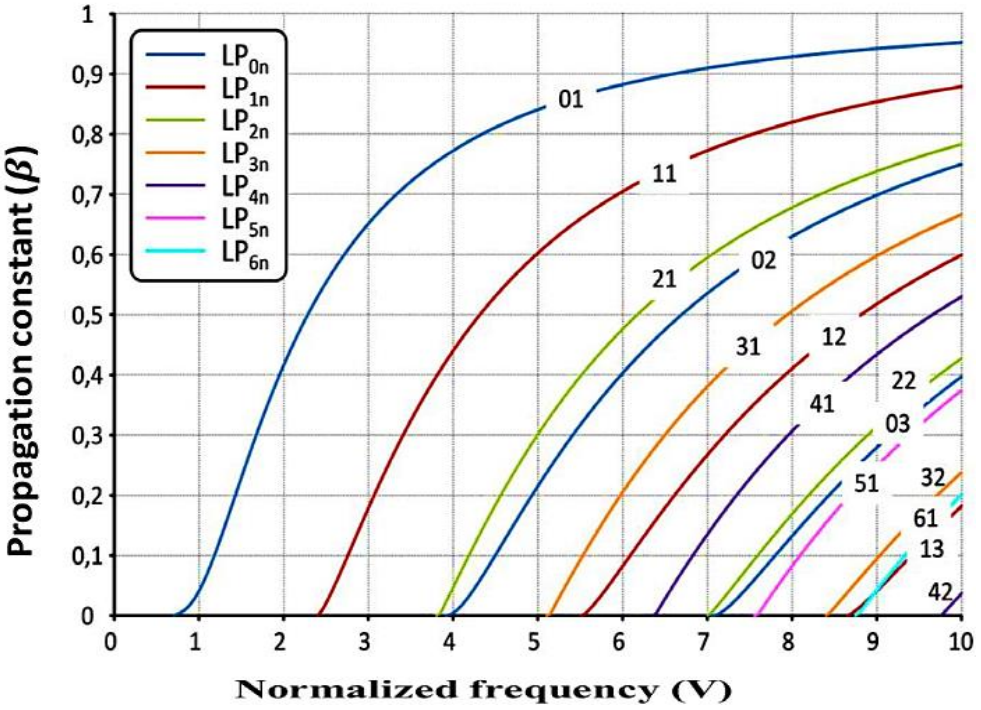

Fig. (2.8): The handled modes with respect to the propagation constant (β) and normalized-frequency (V) [66].

linearly polarized (LP) modes, which are called scalar modes, are usually used to represent fiber modes as an approximation of the vector modes. All LP modes are a linear combination of different true fiber modes, except for LP_{0m} that are just composed of HE_{1m} modes. Each mode exists in two orthogonal polarizations. Therefore, the modes LP_{0m} have a degeneracy of two. However, besides the two orthogonal polarizations that the mode LP_{11}

can have, two orthogonal field distributions can be obtained by a rotation of $\pi/2$, and the mode LP_{11} distributions are usually referred to as LP_{11a} and LP_{11b}, where a and b are the orientation of the mode. Thus there are four degenerate LP_{1m} modes (two orientations of the lobes, each with two possible polarizations). Similarly, the modes having an azimuthal number ν ≥ 2 have a degeneracy of four. The cutoff condition is used, when a given mode cease propagating if V becomes smaller than a specific number. For example, the propagation of the mode LP11 is not allowed in the fiber when V becomes smaller than 2.405. However, the mode LP01 that is called fundamental mode or HE11 mode, has no cutoff condition because it is always allowed, and every fiber supports this mode [65].

An important parameter that has been utilized to describe the guided modes in fibers of optical is the V, which is called the natural frequency and is given by [67]:

$$V = \frac{2\pi a}{\lambda} \sqrt{n_1^2 - n_2^2} \tag{2.29}$$

where a is the fiber core radius, and the refractive indices of the cladding and core are n_2 and n_1, correspondingly.

The normalized frequency is useful for determining the cutoff conditions, as well as other parameters such as the total number of allowed modes, hence, it provides an answer as to whether a given mode will propagate in the fiber or not. Therefore, the normalized frequency should be chosen first when designing a fiber with a given number of modes The normalized propagation constant b is used to characterize the mode guiding strength, and is defined as [65]:

$$b = \frac{\beta^2 - k_0^2 n_2^2}{k_0^2 (n_1^2 - n_2^2)} \tag{2.30}$$

where b is the normalized propagation constant, β is the propagation constant, and k_0 is the free space propagation constant.

In the step-index fiber, the refractive index $n1$ is evenly distributed equally between the core, which is surrounded by the cladding with $n2$. The propagation constant β for all modes is limited by (n_1 k_0, n_2 k_0) where k_0 indicates the propagation constant of light in a vacuum. A circular step-index optical fiber characterized by a rising cross-sectional area is schematically provided in Figure (2.9).

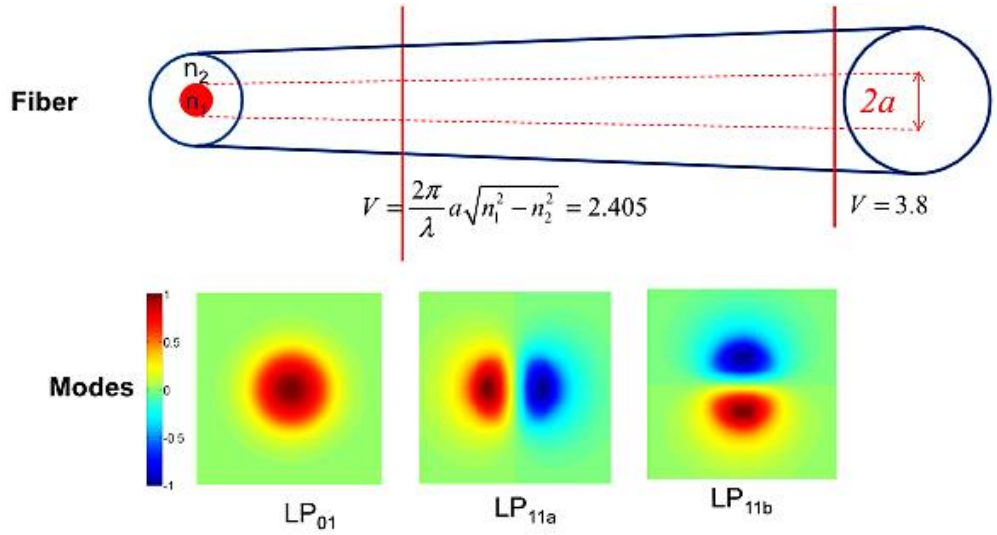

Fig. (2.9): Diagrammatic of a circular fiber display supported profile modes along the fiber and a step-index of cross-sectional area [68].

The LP modes for the core of weakly guiding fibers with higher mode capacity have the following transverse field structure [68]:

$$E_y(r, \theta) = E_y(a) \frac{J_p(k_r r)}{J_p(k_r a)} \cos(p\theta) \tag{2.31}$$

Where a represents the core radius, p is the azimuthal mode number (a non-negative integer), and $k_r = (k^2 n_1^2 - \beta^2)^{1/2}$. A non-negative integer q represents the number of zero crossings of the field in the radial direction, which introduces discrete values for the same value of p. The total number of modes supported by a step-index core fiber can be approximately given by [35]:

$$M \approx \frac{1}{2} V^2 \tag{2.32}$$

2.6.2.1 Modeling and impairments of FMF transmission system

The model system of FMF can be expressed below:

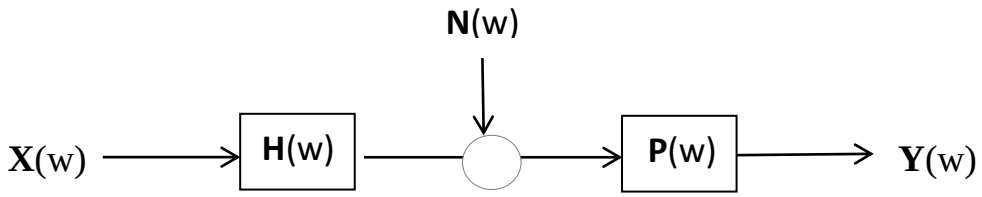

Y(w) will be expressed as the below equation:

$$\mathbf{Y}(w)= (\mathbf{H}(w)\cdot \mathbf{X}(w)+ \mathbf{N}(w))\cdot \mathbf{P}(w) \tag{2.33}$$

Where Y(w) corresponds to the output signals vector in the frequency-domain [$Y_1(w)$, $Y_2(w)$, … $Y_M(w)$]T, M is the number of modes, T is the interval of symbol, while the angular-frequency is *w*. Y*M(w) performs the output signal in the frequency domain on M mode. Also, X(w) represents the vector of M input signals in frequency-domain, and X*M(w) act as the input signal in frequency-domain in mode M. The frequency-domain illustration of propagation matrix is H(w). The H(w) that has M number of modes in FMF system is presented as follows:

$$\mathrm{H}(w) = \begin{bmatrix} H11(w) & H12(w) & \dots H1M(w) \\ H21(w) & H22(w) & \dots H2M(w) \\ HM1(w) & HM2(w) & \dots HMM(w) \end{bmatrix} \tag{2.34}$$

So N(w) represents the impulse response of the frequency domain, which describes mode-coupling losses for the j mode channel on the i mode channel.

The impulse response in the frequency domain is influenced by various system impairments, including Mode-Dependent Loss (MDL), Mode-Dependent Gain (MDG), Differential Group Delay (DGD), Chromatic Dispersion (CD), and other forms of loss. The frequency-domain representation of Amplified Spontaneous Emission (ASE) noise is denoted

as N(w), which originates from the optical amplifiers used in the transmission links. In long-haul transmission systems, where multiple amplifiers are employed along the transmission path, system performance is primarily limited by ASE noise. The passband filter in the frequency domain is denoted as P(ω), which can be used to limit the ASE noise added to the channel's power spectrum. The bandwidth of P(ω) must be slightly larger than the bandwidth of the modulated signal to avoid inter-symbol interference (ISI) caused by overly narrow filtering [63].

2.7 Different SDM technologies

As seen in figure (2.10), many SDM fibers have been developed to enable SDM transmission in optical systems.

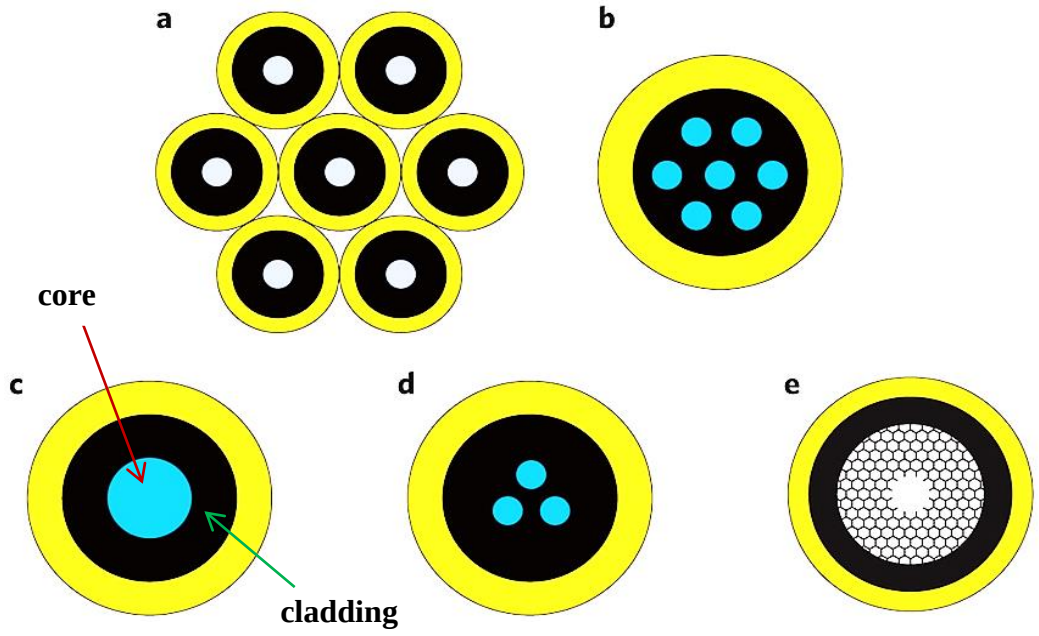

Fig. (2.10): Different approaches for realizing SDM: (a) Fiber bundle, (b) Multicore Fiber, (c) Multi-mode Fiber, (d) Coupled-core fibers, (e) Photonic Band Gap fibers [17].

a) The single-mode fibers: the fiber bundle consists of physically separate single-mode fibers that can achieve higher densities than current fiber cables through advanced design but cannot reduce system capacity costs, with costs increasing linearly as the number of the fibers in the bundle grows [69].

b) Multicore Fiber: the structure of a multicore fiber consists of separate single-mode cores within a single fiber, presenting challenges in controlling crosstalk. To reduce crosstalk, great attention should be used in designing the core distance and core profile. Ideally, there should be less crosstalk the greater the core distance. Nevertheless, the total diameter of multi-core fiber increases with an increase in the number of cores or core distance, and the fiber is brittle. As a result, the total number of cores in a multi-core fiber may be its limiting factor. Optical integration is another issue with multi-core fiber. In multi-core fiber Erbium-Doped Fiber Amplifier (EDFA), it is challenging to share the pump power for distinct cores as signals are conveyed through physically separate cores [70].

c) The multi-mode fiber: the use of multi-mode fibers (MMF) allows for transmission of multiple channels through various spatial modes, leading to inter-modal crosstalk due to signal sharing in the same physical space. Hundreds of spatial modes are supported by the commercial MMF available today, although there are extremely huge DMGD . With a limited number of spatial modes, FMF was developed in order to benefit from MMF in SDM. Modern FMF systems, for instance, are capable of supporting up to three spatial modes (LP01, LP11a, LP11b) at a time . As DSP technology advances, FMF systems are expected to accommodate more spatial modes, offering potential advantages in system cost and power efficiency through integrated optical components like FMF EDFA in space-division multiplexing (SDM) technology [71].

d) Coupled-core fibers: coupled-core fibers are known for their ability to achieve much greater spatial channel densities compared to isolated core MCF designs and have the same issue in optical integration.

e) Photonic Band Gap fibers: provides a special sort of fiber with low losses and a narrow band-gap. While experiments are carried out to explore the

feasibility of utilizing this kind of fiber for SDM transmission, SDM networks do not facilitate it.

Ultimately, due to its capacity scalability and potential for optical integration, Few-Mode Fiber (FMF) is considered one of the most promising SDM techniques for overcoming current capacity limitations in optical communication systems [17].

Chapter Three

Proposed Optical Space Division Multiplexing (SDM)

3.1 Introduction

In this chapter, the proposed system design of a space division multiplexing and wavelength division multiplexing system is explained. Where a four-channel across four-mode SDM system is designed using WDM technology. The proposed models of the study are discussed in detail.

3.2 Design of proposed system

The WDM-SDM system was proposed to enhance data transfer rate. A four-channel, 4-mode (LP_{01}, LP_{11}, LP_{21}, and LP_{02}) SDM system employing WDM technology was designed. The system's performance was evaluated under various conditions, including changes in bit rate, transmission distance, input power, and channel spacing. The global parameters used in the proposed system are listed in Table (3.1). Each component in the system architecture significantly influences the overall transmission network performance. The proposed systems were designed using the commercial software OptiSystem 18 from Optiwave, as illustrated in Figure (3-1).

Figure (3.1) illustrates the transmitter and receiver design of our model the transmitter section comprises an array of spatial continuous-wave (CW) laser sources connected to a modulator. The system operates at a channel frequency of 193 THz. The modulator includes a Pseudo-Random Bit Sequence (PRBS) coupled to a pulse generator for modulating the optical signals utilizing pulse forms such as Return-Zero (RZ) and Non-Return-Zero (NRZ). Subsequently, it interfaces with a Mach-Zehnder modulator (MZM) that acts as an intensity modulator. Measurement index multimode fiber is utilized with an optical link. At the receiver, spatial demultiplexing is employed to divide the

incoming frequencies. The signal is captured by a PIN photodiode and then filtered using a low-pass Gaussian filter. Furthermore, the signal is directed to a Bit Error Rate (BER) analyzer for graph generation, as well as an Oscilloscope Visualizer.

Table (3-1): The parameters of System simulation .

Parameter	***Value***	***Units***
Simulation Software	OptiSystem18 version	
Bit rate	1, 2, 3,and 3.5	Gb/s
Fiber type	graded index, FMF	
Attenuation factor,	0.2	dB/ km
Fiber Length	10 - 125	Km
Center Wavelength of operating system	1551.468	nm
Channel spacing for MUX And DEMUX	0.4, 0.8, 1.6, 2	nm
Power	1, 3 , 5 , 7	mW
Laser type	Spatial CW Laser	

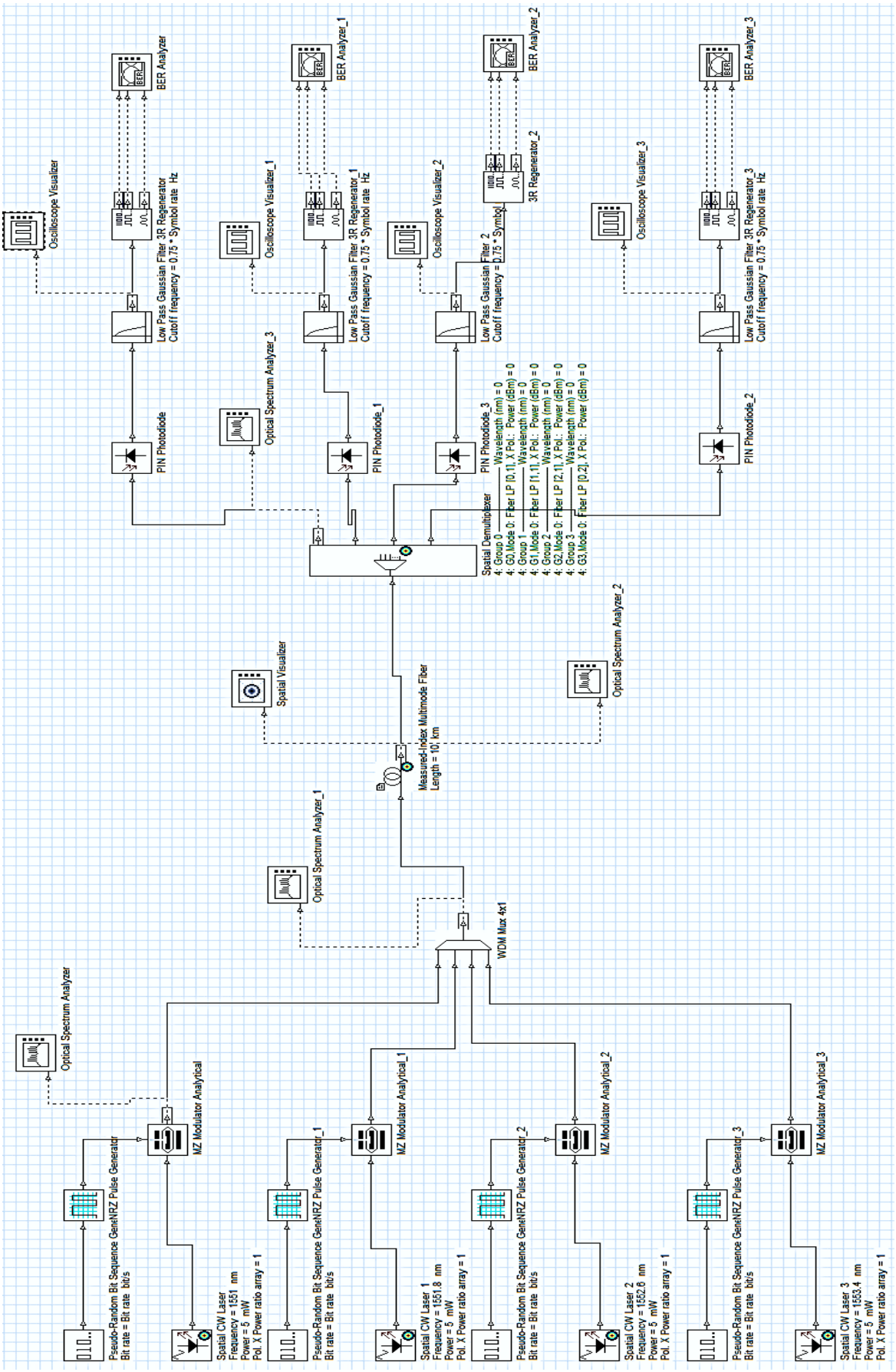

Fig.(3.1) : The Proposed System Design WDM/SDM in OptiSystem Software.

3.3 The Transmitter Part:

Figure (3.2) illustrates the 4-mode (LP_{01}, LP_{11}, LP_{21}, and LP_{02}) system's simulated transmitter portion. Four signals with different emission frequencies are produced to be transmitted by a WDM multiplexer. The transmission structure 4-WDM 4-mode system consists of a spatial CW laser source, PRBS and NRZ, and an MZM, 4-WDM channels transmitter. Below is a description of each component :

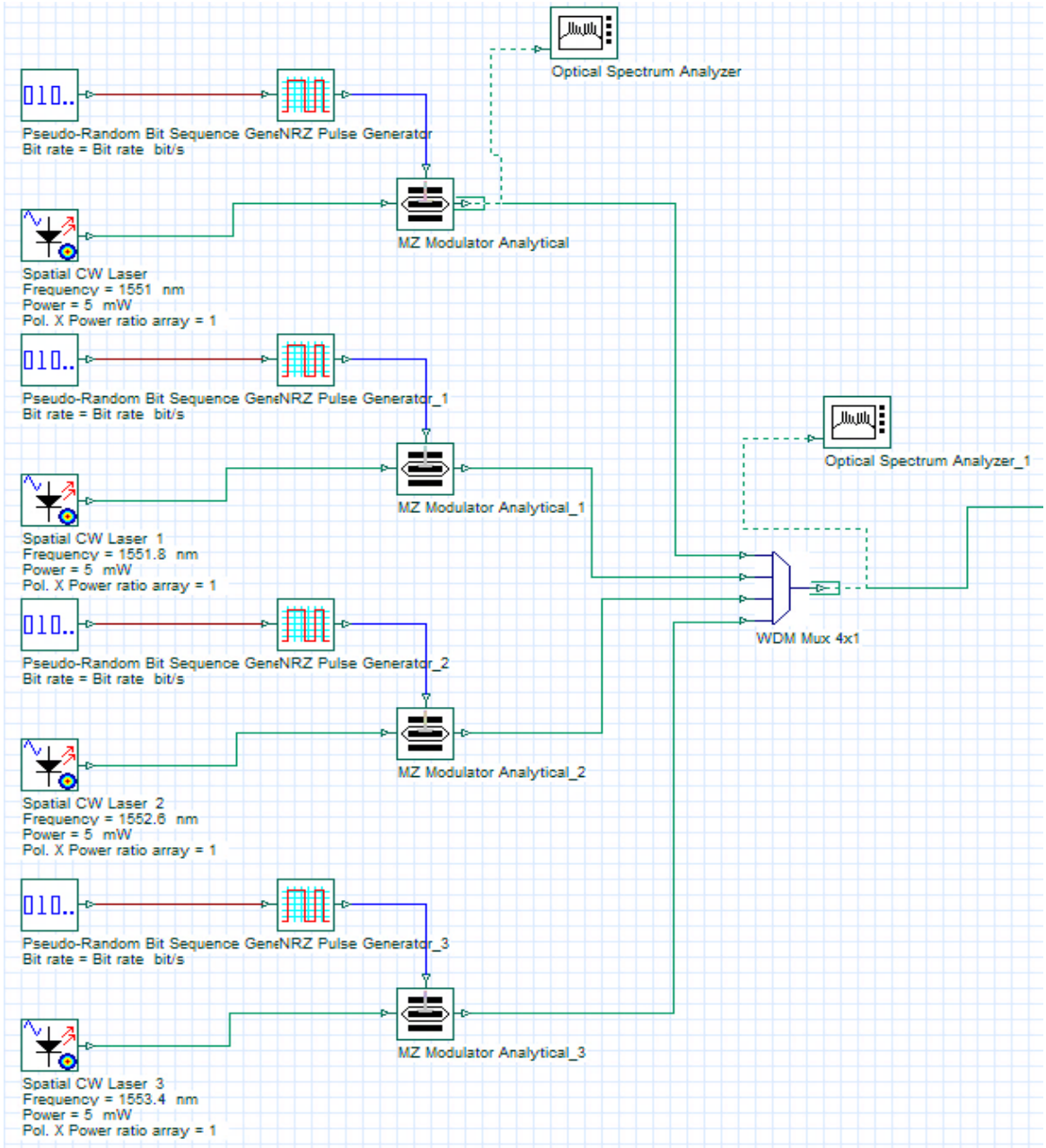

Fig.(3.2) : The transmitter part .

3.3.1 Spatial Continuous Wave (CW) Laser :

This module of the device is a continuous wave (CW) laser which incorporates transverse mode profiles in the optical output. The CW laser and multimode generator were used in the construction of this developed subsystem. A continuous wave optical signal is produced by a CW laser. The CW laser is a distributed feedback laser that generates a continuous wave optical signal. At the same time, the multimode generator integrator incorporates transverse mode profiles into the input signal. In addition, it enables the single-mode signals to be converted into multimode signals. The structure of the Spatial CW Laser is illustrated in Figure (3.3). Additionally, Table (3-2) displays the components of the simulated Spatial CW-laser module.

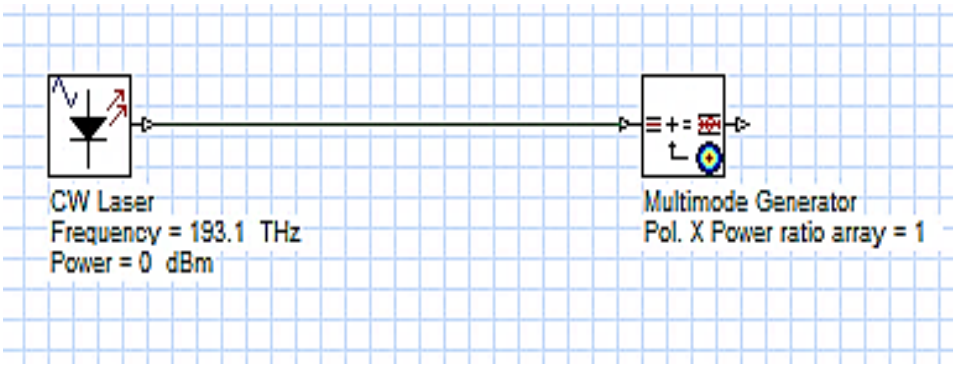

Fig.(3.3) : Spatial CW Laser subsystem.

Table(3-2): Spatial CW laser parameters.

Parameter	***Value***	***Units***
Wavelength	1551: 0.8 :1553.4	nm
Power	1, 3, 5, 7	mW
Line width	10	MHz
Initial phase	0	deg.
Pol. X Power ratio array	1	
Pol. X m,n index array	01,11,21,02	

3.3.2 Pseudo Random Binary Sequence (PRBS)

A Pseudo Random Binary Sequence (PRBS), also referred to as a pseudorandom bit sequence or pseudorandom code, is generated according to specific modes of operation. The primary purpose of the PRBS is to produce a sequence of bits that closely resembles the statistical properties of truly random data. In optical communication system simulations, PRBS is commonly used to emulate real-world data traffic. The components of the simulated PRBS module used in this study are listed in Table (3-3).

Table (3-3): Pseudo Random Binary Sequence (PRBS) Parameters.

Parameter	***Value***	***Units***
Bit rate	1, 2, 3, 3.5	Gb/s
Operation mode	Order	
Sequence length	1024	bit
Mark probability	0.5	

3.3.3 Mach-Zehnder modulator (MZM)

A MZM is a device utilized in optical communication systems. And also the MZM uses an interference principle as its basis as its foundation for the intensity modulation. An MZM essentially splits an incoming light beam into two paths and then recombines them. By precisely controlling the phase difference between these two paths, the MZM can modulate the intensity of the output light wave. The components of the simulated Mach-Zehnder Modulator (MZM) module are shown in table (3-4).

Table (3-4): Mach-Zehnder Modulator (MZM) Parameters.

Parameter	***Value***	***Units***
Extinction rate	30.	dB.
Bias point	Quadrature Point (0.5π)	
factor of symmetry	−1	

3.3.4 WDM multiplexer

This component is used to multiplex four incoming optical signals generated by the spatial CW laser modules through wavelength division multiplexing (WDM). The Bessel filter is used to reduce intersymbol interference (ISI) due to its linear phase response and constant group delay characteristics, making it particularly beneficial in optical communication systems. The parameters of the WDM multiplexer are presented in Table (3-5).

Table (3.5): WDM multiplexer Parameters.

Parameter	Value	Units
Channel spacing	0.4, 0.8, 1.6, 2	nm
Bandwidth	20	GHz
Loss of Insertion	0	d B
Type of filter	Bessel	
Depth.	100.	d B
Order of filter	2	
Wavelength for channel 1	1551	nm
Wavelength for channel 2	1551.8	nm
Wavelength for channel 3	1552.6	nm
Wavelength for channel 4	1553.4	nm

3.4 The Multimode Fiber Channel Section

This part illustrates the transmission of four spatial modes into multi-mode fiber (MMF). The supported modes are (LP01, LP11, LP21, and LP02). The module of Measured-index Multimode fiber is employed to simulate model signal transmission in few-mode fiber by accounting for the attenuation & varying group velocity characteristics in the modes of the fiber. The simulated optical channel part of the 4-mode system is shown in Figure (3.4).

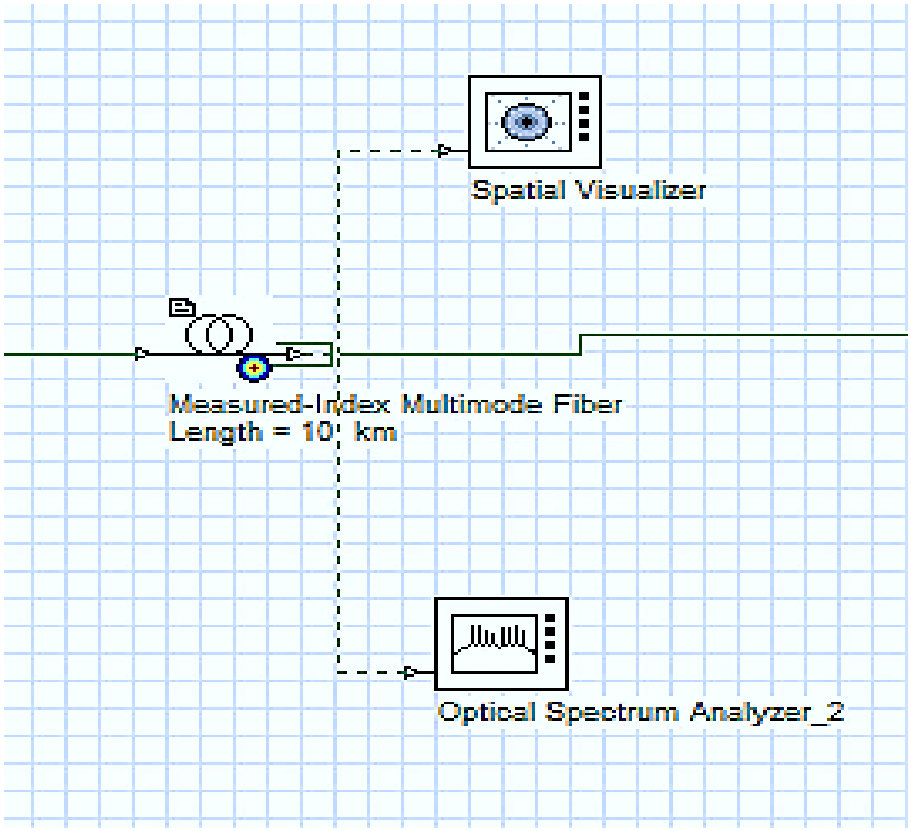

Fig.(3.4): optical channel part.

3.4.1 The Measured-index Multimode fiber

Measured-Index Multimode Fiber (MI-MMF) is a specialized type of multimode fiber where the actual refractive index profile of the manufactured fiber is measured and characterized. It simulates the propagation constants and transverse field profiles for every mode that the

fiber supports. Measured-index multimode fiber offers a unique approach to MMF design by tailoring the fiber characteristics based on actual measurements. Even though MI-MMF isn't as widely used as regular multimode fiber, it's very useful when you need tight control over how signals behave inside the fiber, especially to reduce signal distortion and improve overall performance. The following Table (3-6) displays the parameters of the measured-index multimode fiber.

Table(3-6) : The Measured-Index Multimode Fiber Parameters.

Parameter	***Value***	***Units***
Length	10 - 125	Km
Attenuation	0.2	dB/Km
Solver wavelength	1550	nm
Refractive Index	1.4	
Dispersion	-100	Ps / nm / Km
Slope of dispersion	0.5	Ps / nm^2 / k
LP(m,n)	LP01,LP11,LP21,LP02	
Min. signal power	-100	dBm
Mode solver	LP	
Fiber bandwidth cut-off	3	dB
Core radius	25	um

3.5 The Receiver Section

The simulated receiver part of the 4-mode system is shown in Figure (3.5), where the received mode signals pass through the spatial demultiplexer component. The receiver structure consists of a spatial demultiplexer, a PIN photodiode, a low-pass Gaussian filter, a 3R regenerator, a Bit Error Rate (BER) analyzer, and an oscilloscope. A description of each component is provided below.

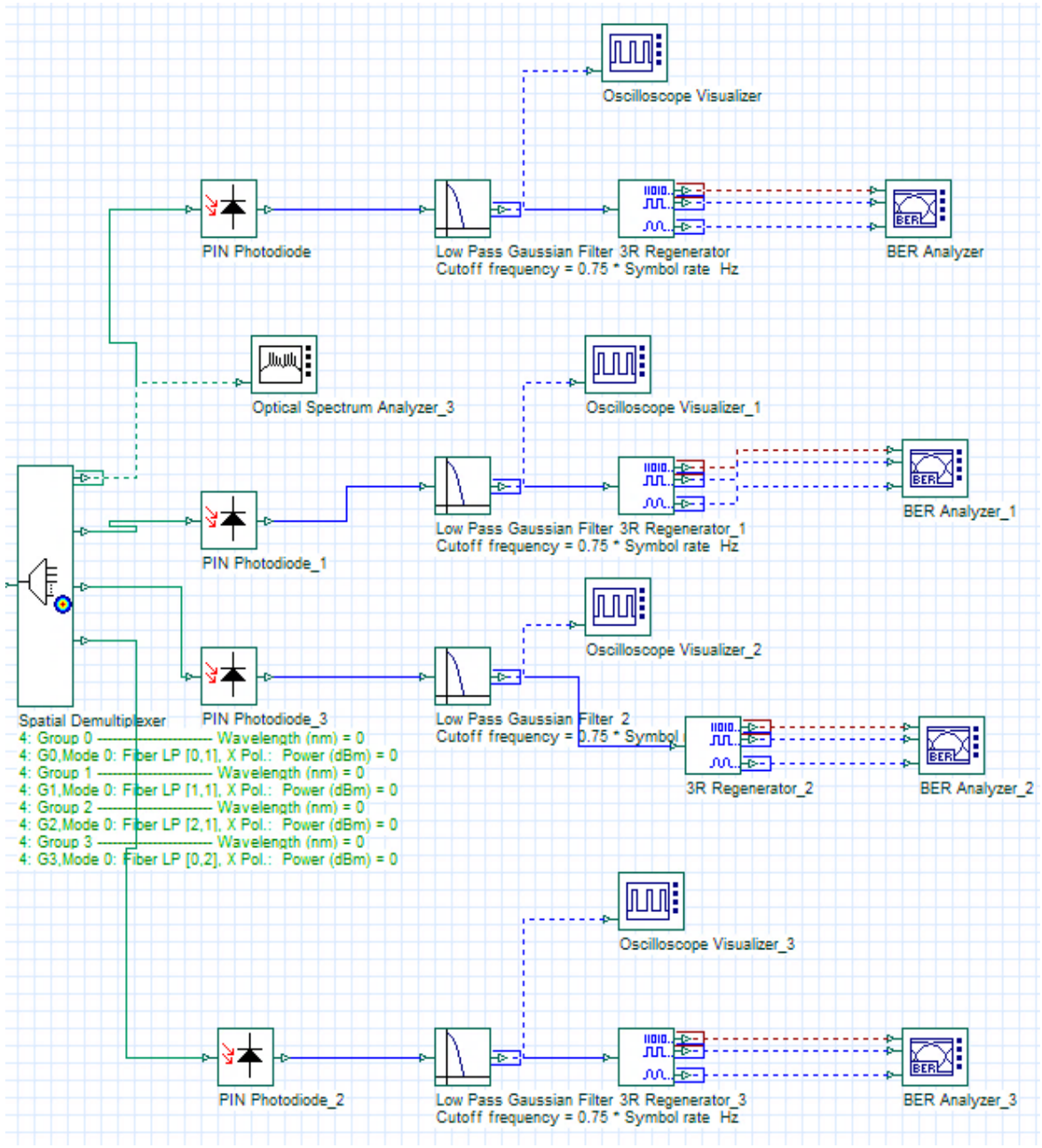

Fig.(3.5) : The Receiver Part.

3.5.1 Spatial Demultiplexer

A spatial demultiplexer is a device used in optical communication systems to separate multiple optical signals that are transmitted over a single optical fiber into individual spatial channels. This process is crucial in systems employing spatial multiplexing, as it enables efficient and high-capacity data transmission. The Spatial Demultiplexer component first demultiplexes several WDM spatial signal channels and then isolates each spatial mode associated with a particular channel. In this system, the input signal is divided into four separate signals, where the number 4 represents the number of output ports, corresponding to the number of spatial modes used. After demultiplexing, an optical filter is applied to each output to eliminate unwanted spectral components, improve signal quality, and reduce crosstalk. The mathematical model that describes the spatial demultiplexing process is based on mode and is given by Equation (3.1).

$$E(x,y,z,t)= \sum_{m=1}^{M} A_m\,(z,t)\psi_m\,(x,y)e^{i(\beta_m z-\omega t)} \qquad (3.1)$$

Where $A_m(z,t)$ is amplitude of mode m, $\psi_m(x,y)$ is transverse field distribution of mode m, β_m is propagation constant of mode m, ω is optical carrier frequency, M is total number of spatial modes [2]. The parameters of the Spatial Demultiplexer are shown in Table (3-7).

3.5.2 The PIN photodiode

A PIN photodiode is a type of photodetector used in optical communication systems to convert optical signals into an electrical signal. Its layered structure, high sensitivity, fast response time, and low noise characteristics make it a valuable component for converting optical signals into electrical signals. The following Table (3-8) displays the parameters of the PIN photodiode.

Table (3-7): Spatial Demultiplexer Parameters.

parameters	Value	Units
Number of wavelengths	4	
Bandwidth	20	GHz
Loss of Insertion	0	d B
Type of filter	Bessel.	
Depth	100.	d B
Order of filter	2.	
Number of spatial modes	4	
Wavelength for channel 1	1551	nm
Wavelength for channel 2	1551.8	nm
Wavelength for channel 3	1552.6	nm
Wavelength for channel 4	1553.4	nm

Table (3-8): The PIN photodiode Parameters.

Parameter	***Value***	***Units***
Responsivity	1	A / W
Dark current	10	n A
Modulation bandwidth	2	GHz
Center frequency	193.1	THz

3.5.3 The Low Pass Gaussian Filter

A low-pass Gaussian filter is a type of signal-processing filter that is used to eliminate high-frequency elements from a signal, allowing low-frequency components to pass through. It is characterized by a Gaussian-shaped frequency response, which results in a smooth and gentle attenuation of high frequencies. The following table (3-9) displays the parameters of the low-pass Gaussian Filter.

Table (3-9) : The low pass Gaussian Filter Parameters.

Parameter	***Value***	***Units***
Cutoff frequency	0.75 * Symbol Rate.	H z
Loss of Insertion	0	d B
Depth	100	d B

3.5.4 The 3R Regenerator

The 3R Regenerator is a component used to restore degraded optical signals by performing three key functions: boosting the optical signal power, restoring the original pulse shape to reduce distortion (such as that caused by dispersion), and aligning the signal with a clock to correct timing jitter. This regeneration process is especially useful in long-distance fiber-optic communication systems, where transmitted signals tend to degrade due to various impairments, including attenuation (signal weakening), dispersion (pulse broadening), timing jitter (bit misalignment), and noise. By executing these three functions the 3R Regenerator helps maintain signal integrity and ensures reliable high-speed data transmission across extended distances.

Finally, The Bit Error Rate is the parameter that was used in our system to compare the input and output signals in order to assess the quality of the signal and the degree to which noise and dispersion have affected the communication system. It measures the rate at which errors occur in the transmitted data over a communication channel. The evaluation of the receiver's functionality can be assessed by examining the eye diagram following the completion of a simulated design process.

Chapter Four

Results and Discussion

4.1 Introduction

This chapter presents a comprehensive performance evaluation and analysis of the proposed space division multiplexing (SDM) systems. All simulation results are thoroughly presented and discussed to assess the designs proposed in this work.

4.2 Results and Discussion

The optical spectrum analyzer is used for the spectrum view. Where the figure (4.1) displays the spectrum before the WDM multiplexer for each channel. Figure (4.2) displays the spectrum after WDM multiplexing. And after Spatial demultiplexing the four channel , the figure (4.3) shows Optical Spectrum of each channel.

Optical spectrum analyzer (OSNR) is the ratio of the optical signal power to the noise power per unit bandwidth (usually per 0.1 nm), typically expressed in dB. The compute OSNR as:

$$OSNR_{dB} = P_{signal} - P_{noise}$$

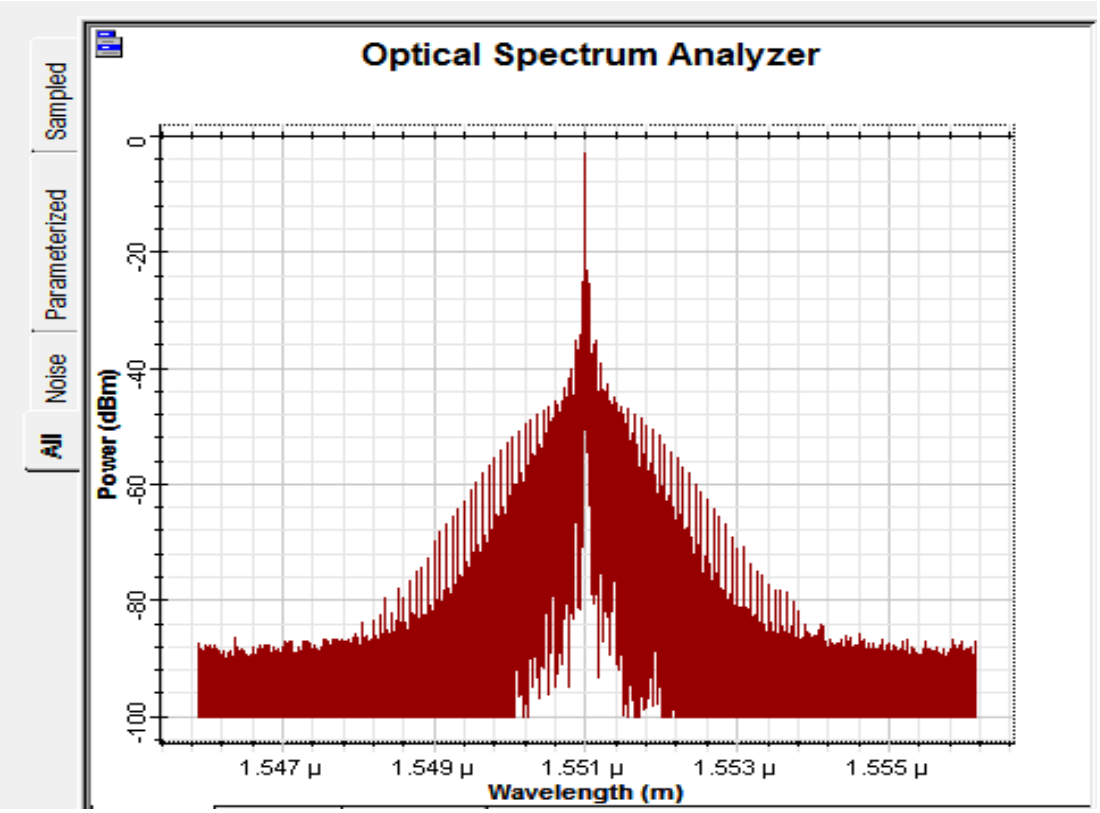

Fig.(4.1): Spectrum signal that precedes the Wavelength Division Multiplexer.

$OSNR_{dB}$ = 96.60dB in Figure 4.1.

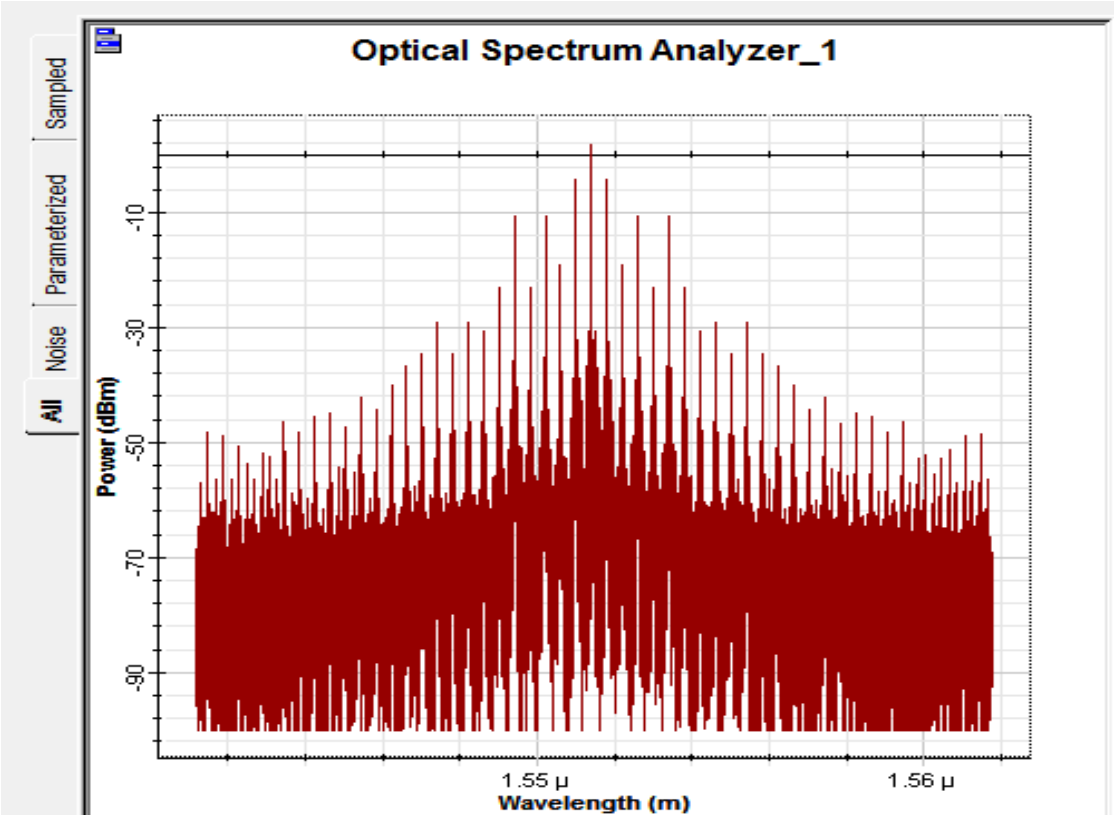

Fig.(4.2): Spectral signal subsequent to the wavelength division multiplexing.

OSNR $_{dB}$ = 101.89 dB in Figure 4.2.

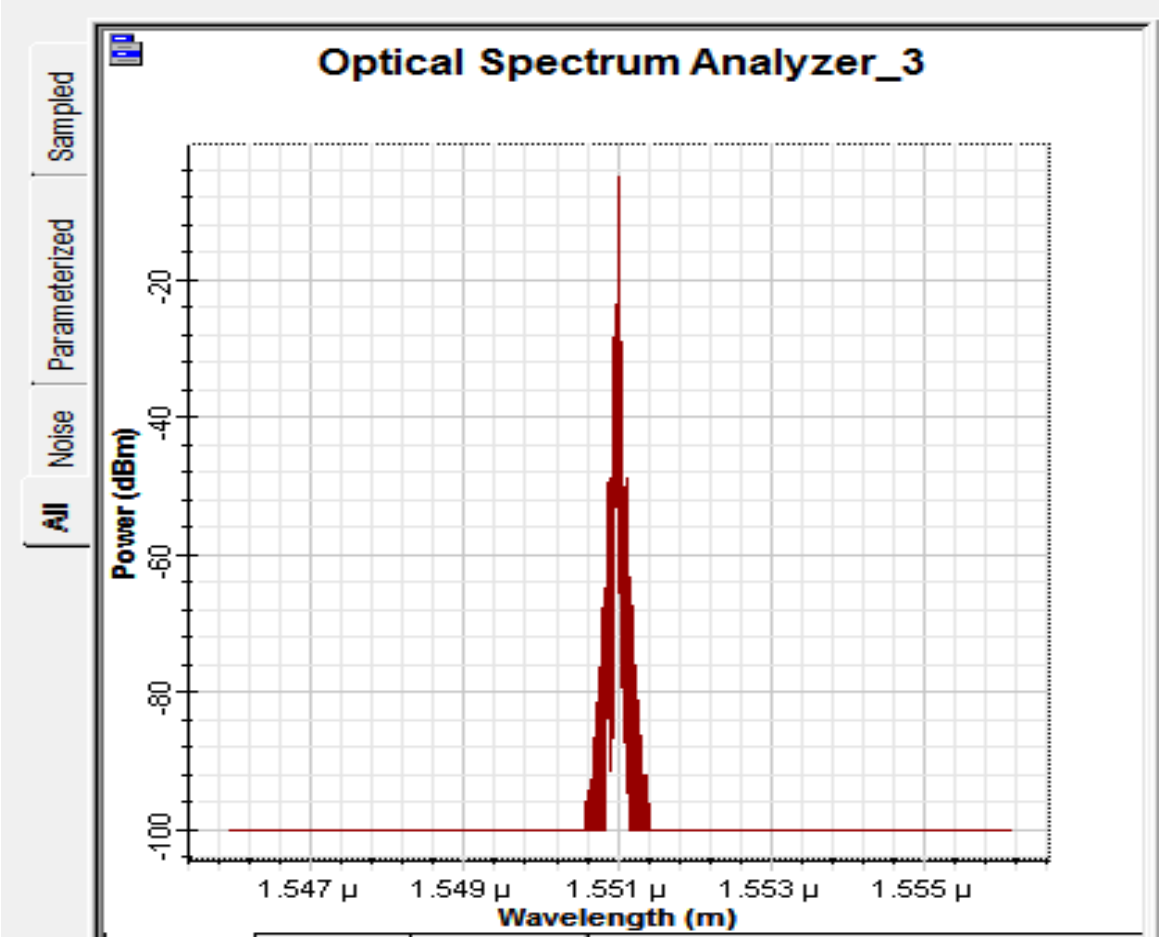

Fig(4.3): The spectral signal subsequent to the spatial demultiplexer.

OSNR $_{dB}$ = 94.38 dB in Figure 4.3.

The deformation of the optical signal from Figure 3 to Figure 1 is primarily due to Chromatic dispersion, leading to spectral broadening. Nonlinear effects cause signal distortion. ASE noise, degrading OSNR after amplification. This is a typical behavior in long-distance WDM/SDM optical communication systems and highlights the importance of using dispersion compensation, and optical filtering to maintain signal integrity.

4.2.1 Proposed System Description

The WDM/SDM system is implemented using the OptiSystem simulation software with Non-Return-to-Zero (NRZ) line coding. The analysis is conducted under four distinct scenarios, as outlined in the accompanying Table 4.1. The system performance is evaluated under different bit rates while keeping the transmission distance, power, and channel spacing constant. The effect of increasing transmission distance on system performance is analyzed, with bit rate, power, and channel spacing held constant. The impact of different transmission power levels is assessed while other parameters remain constant. And the effect of varying the channel spacing on the system's performance while other parameters remain constant.

Table [4.1]: Simulation of four cases for WDM/SDM System Evaluation.

Varied Parameter	Values of Varied Parameter	Fixed Parameters
Bit Rate	1×10^9, 2×10^9, 3×10^9, 3.5×10^9 b/s.	Distance = 10 km, Power = 5 mW, Channel Spacing = 0.8 nm
Distance	10, 50, 75, 100, 125 km	Bit Rate = 1×10^9 b/s, Power = 5 mW, Channel Spacing = 0.8 nm
Power	1, 3, 5, 7 mW	Distance = 10 km, Bit Rate = 1×10^9 b/s, Channel Spacing = 0.8 nm
Channel Spacing	0.4, 0.8, 1.6, 2.0 nm	Distance = 10 km, Power = 5 mW, Bit Rate = 1×10^9 b/s

4.2.2 Results of system design under bit rate variation

In this case, receiver performance analysis can be seen in running the bit error rate simulation and eye diagram. Where The results are obtained for the same distance of 10km and power 5mW and space channel 0.8nm with the data rate is varied as 10^9 b/s, $2*10^9$ b/s, $3*10^9$ b/s and $3.5*10^9$ b/s respectively. Where the results may be seen in Figures (4.4), (4.5), (4.6), (4.7) these describe below:

Figure (4.4) displays the Q-factor and eye diagram at data rate 10^9 in LP01 LP11 LP21 LP02 modes.

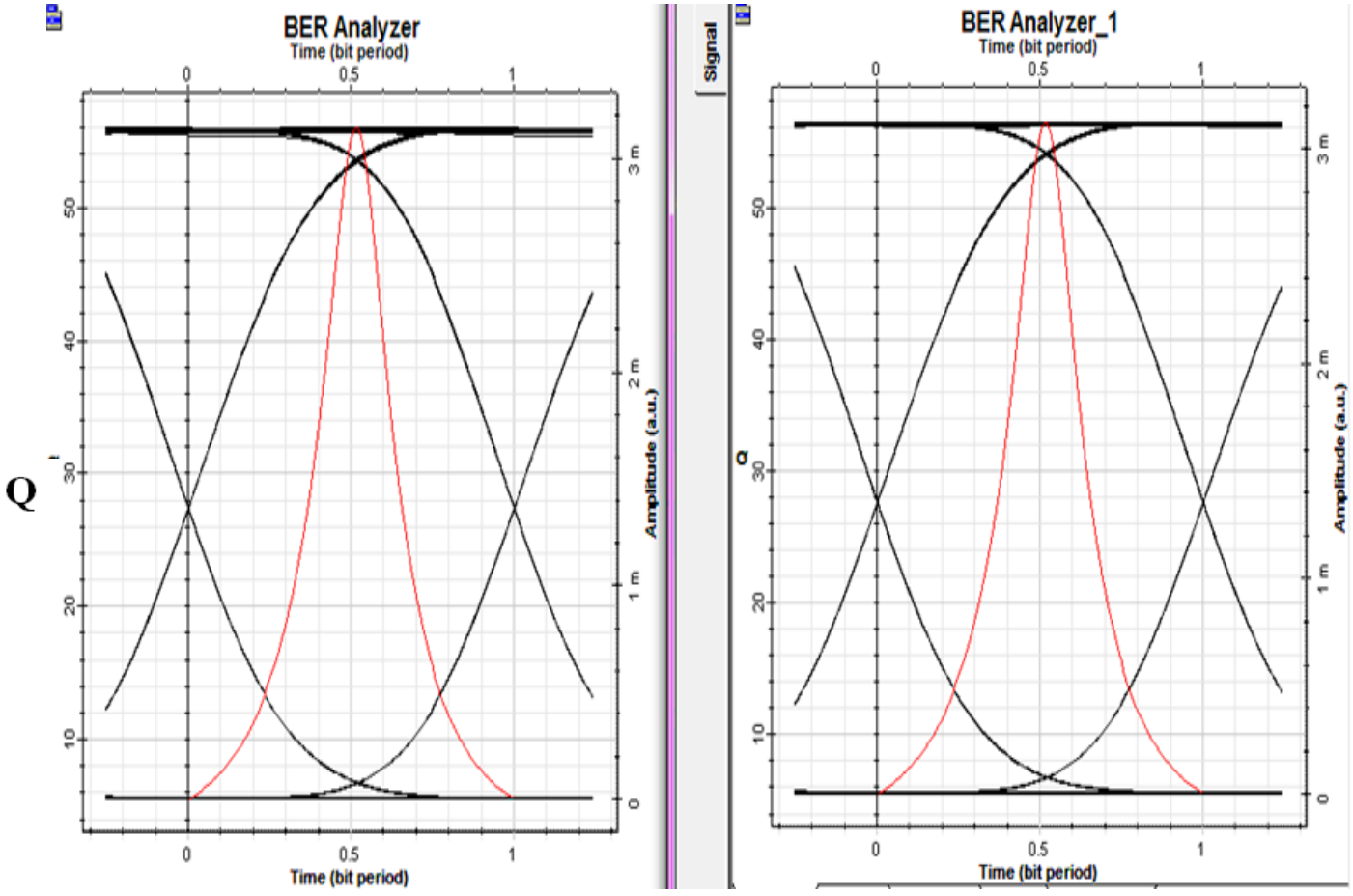

(a) LP01 (b)LP11

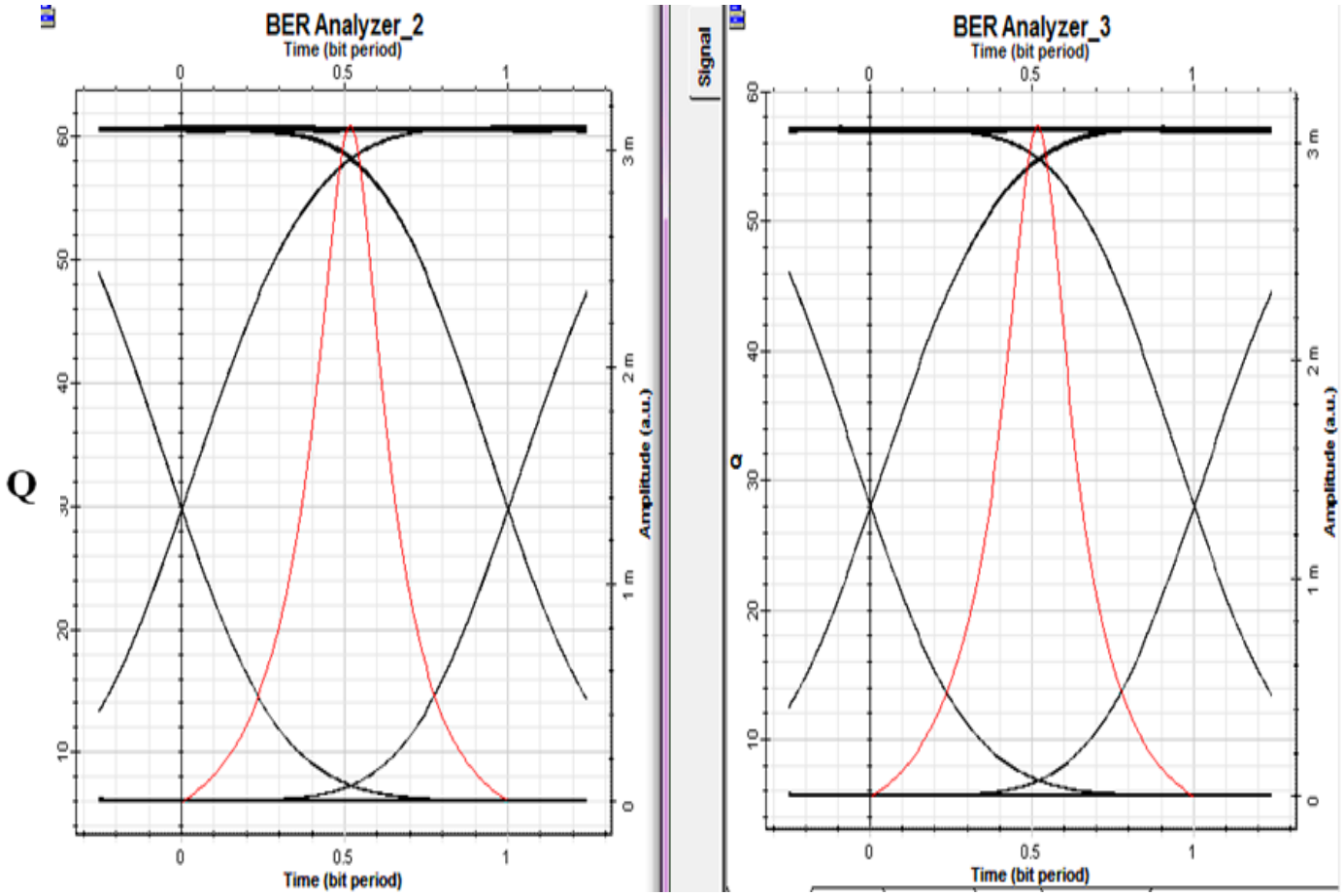

(c) LP21 **(d)** LP02

Fig.(4.4): The eye diagram and Quality factor for (a) LP01, (b) LP11, (c) LP21, and (d) LP02 modes with 10^9 bit rate at 10km, 5mW, and 0.8nm channel spacing.

Figure (4.5) displays the eye diagram and Q-factor at data rate $2*10^9$ in LP01, LP11, LP21, and LP02 modes. This eye diagram demonstrates signal integrity. The wide vertical opening indicates a high signal-to-noise ratio (SNR) and a clear distinction between '1' and '0' levels. The wide horizontal opening shows minimal inter-symbol interference (ISI). The tall, distinct red Q-factor curve signifies a high Q-factor, directly correlating to a low Bit Error Rate (BER).

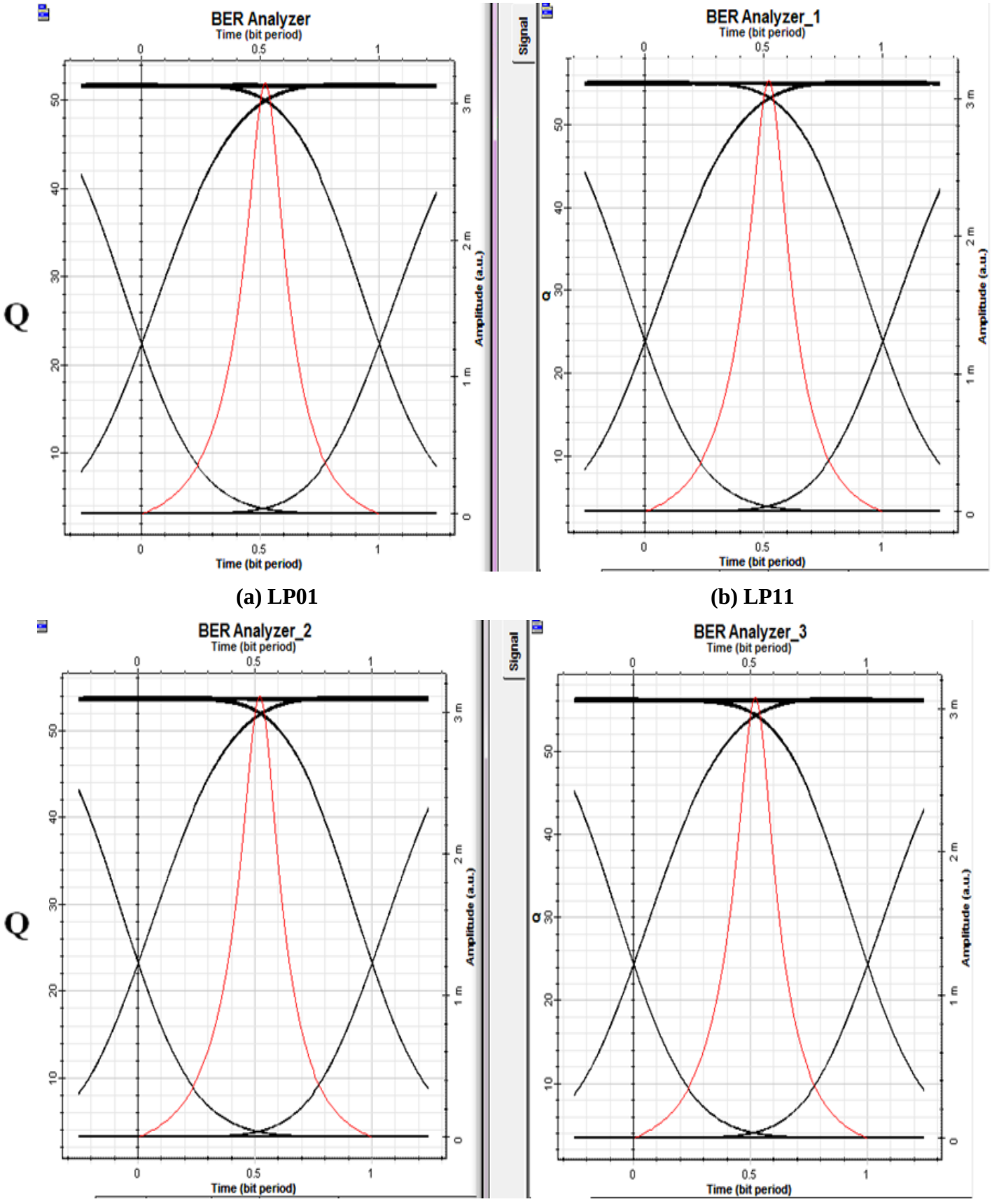

(a) LP01 **(b) LP11**

(c) LP21 (d) LP02

Fig. (4.5): The eye diagram and Quality factor for (a) LP01, (b) LP11, (c) LP21, and (d) LP02 modes with $2*10^9$ bit rate at 10km, 5mW, and 0.8nm channel spacing.

Figure (4.6) displays the Q-factor and eye diagram at $3*10^9$ data rate in modes LP01, LP11, LP21, and LP02. This eye diagram exhibits significant signal degradation. The severely reduced vertical opening indicates a low signal-to-noise ratio and poor distinction between '1' and '0' levels. The narrow horizontal opening points to increased inter-symbol interference (ISI). The much shorter and wider red Q-factor curve indicates a significantly lower Q-factor, directly correlating to a much higher Bit Error Rate (BER). This degradation is commonly observed at higher data rates due to increased dispersion.

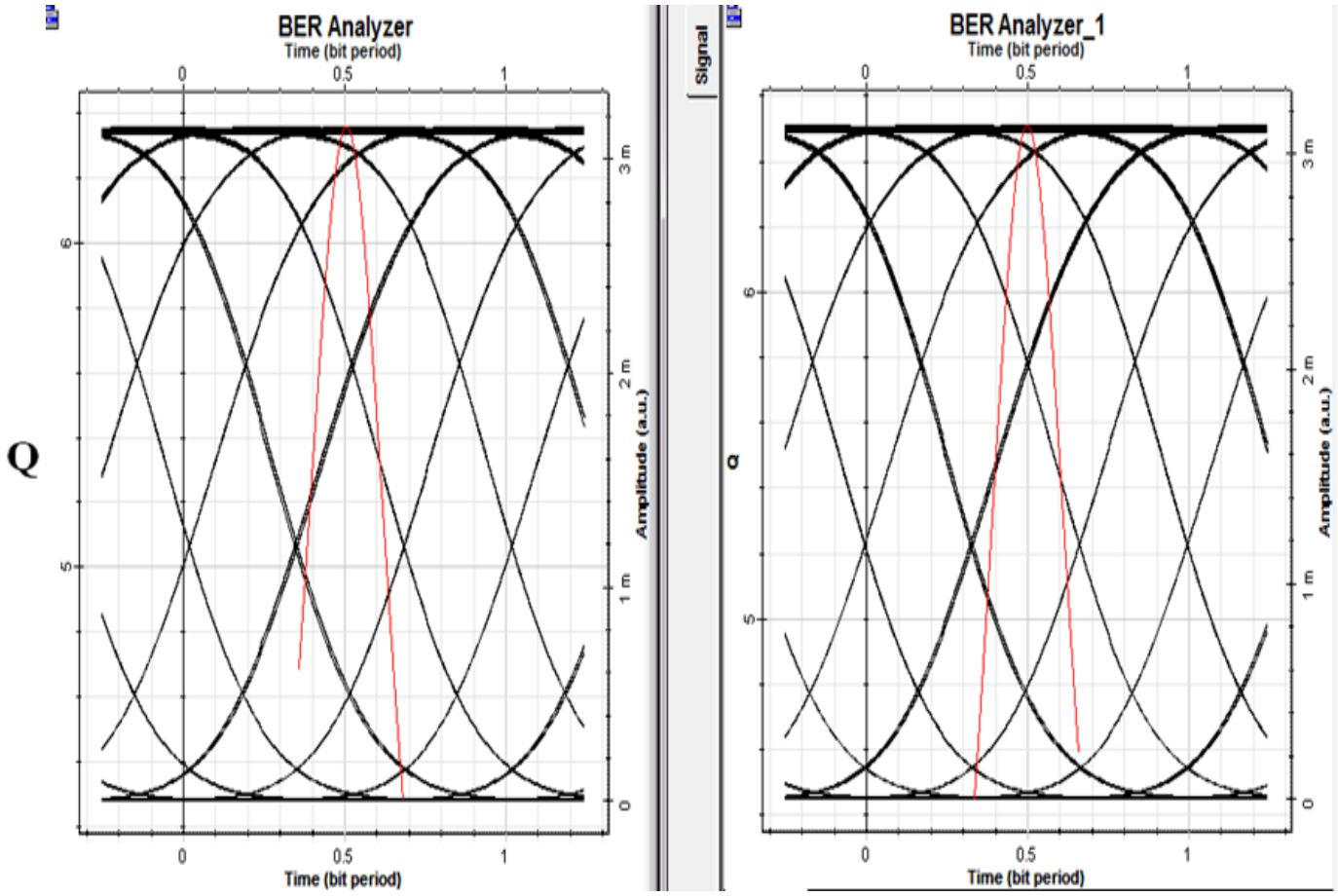

(a) LP01 (b) LP11

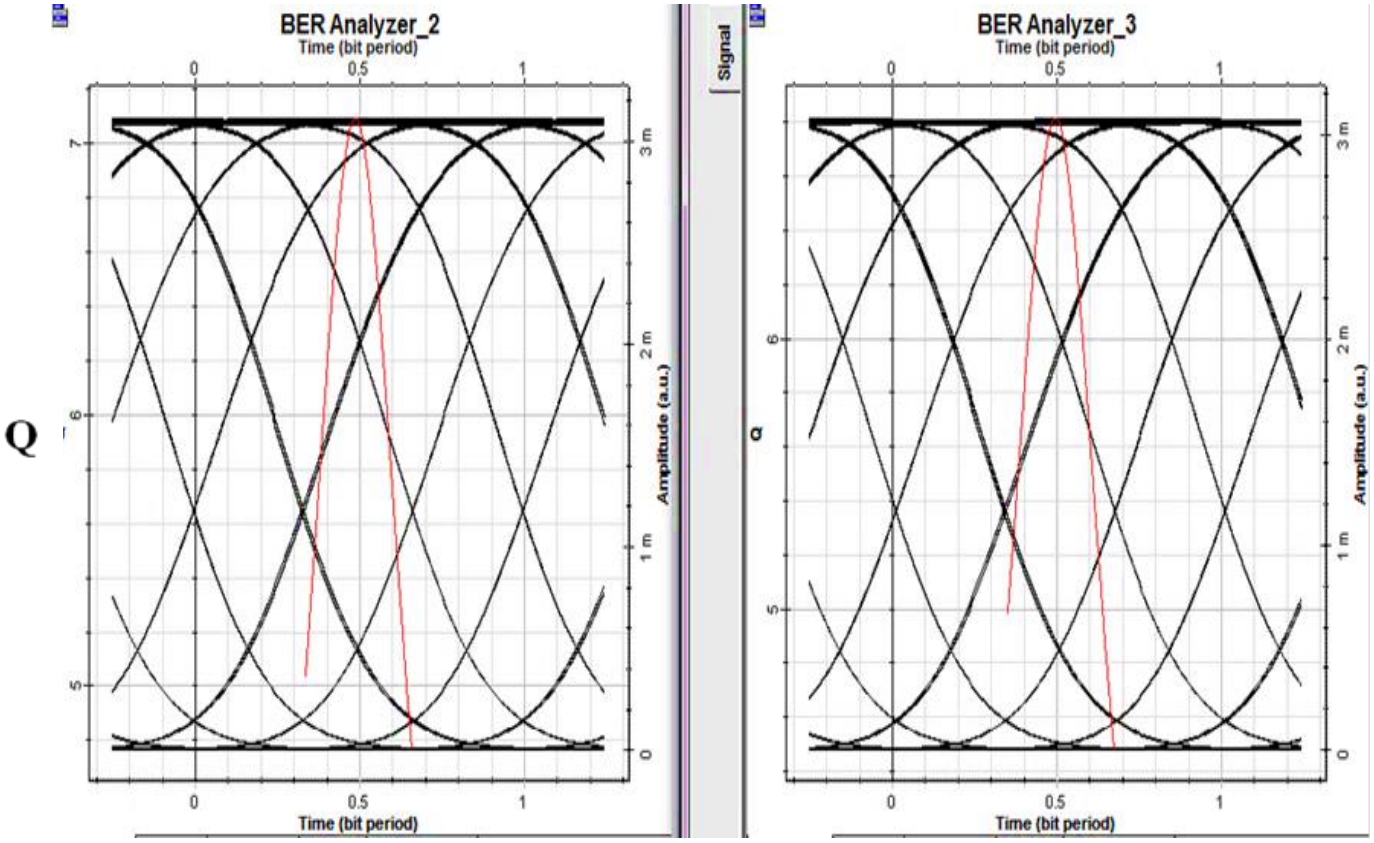

(c) LP21 (d) LP02

Fig. (4.6): The eye diagram and Quality factor for (a) LP01, (b) LP11, (c) LP21, and (d) LP02 modes with $3*10^9$ bit rate at 10km, 5mW, and 0.8nm channel spacing.

Figure (4.7) displays the Q-factor and eye diagram at $3.5*10^9$ data rate in modes LP01, LP11, LP21, and LP02. A noticeable decrease in Q-factor values and a corresponding increase in Bit Error Rate (BER) are observed as the data rate increases. This eye diagram exhibits significant signal degradation. The severely reduced vertical opening indicates a low signal-to-noise ratio and poor distinction between '1' and '0' levels. The narrow horizontal opening points to increased inter-symbol interference (ISI). The much shorter and wider red Q-factor curve indicates a significantly lower Q-factor, directly correlating to a much higher Bit Error Rate (BER). This degradation is commonly observed at higher data rates due to increased dispersion.

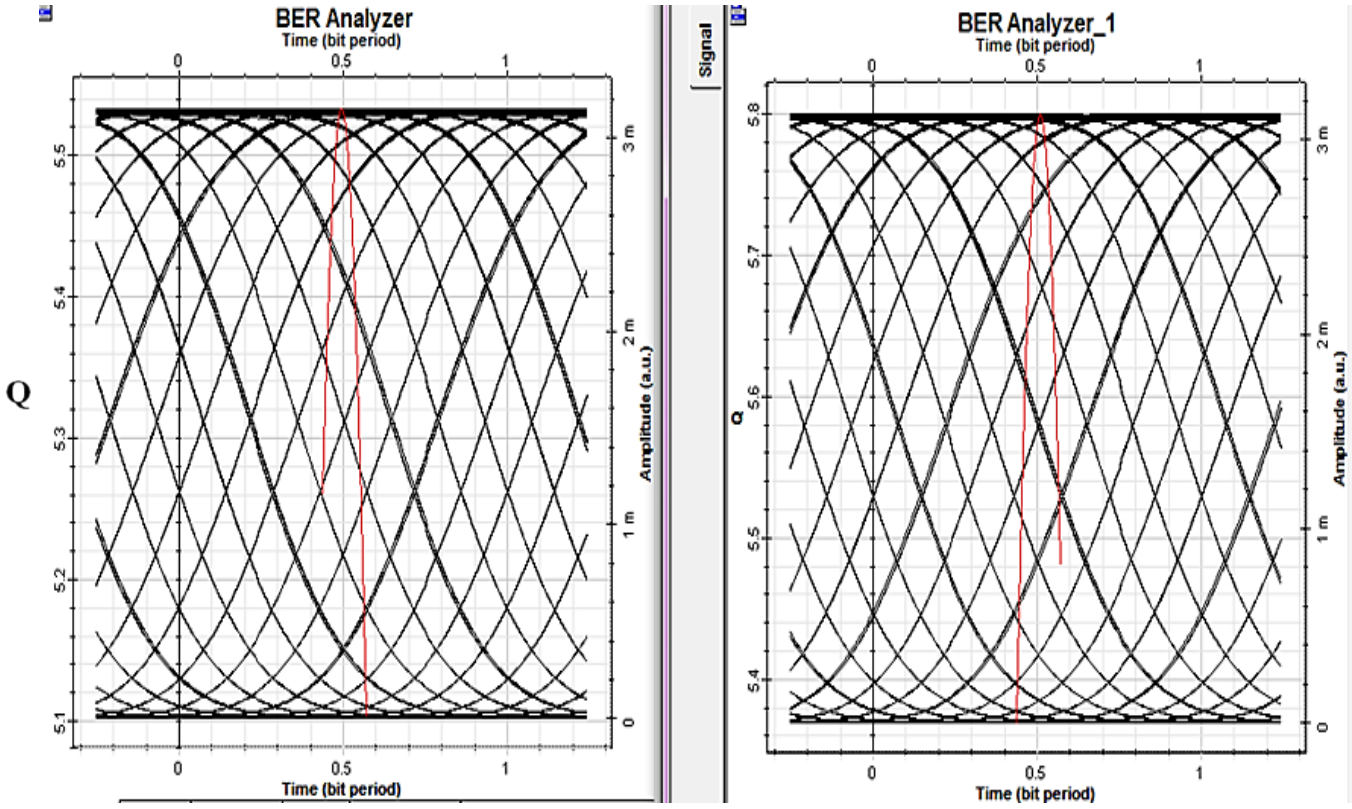

(a) LP01 (b) LP11

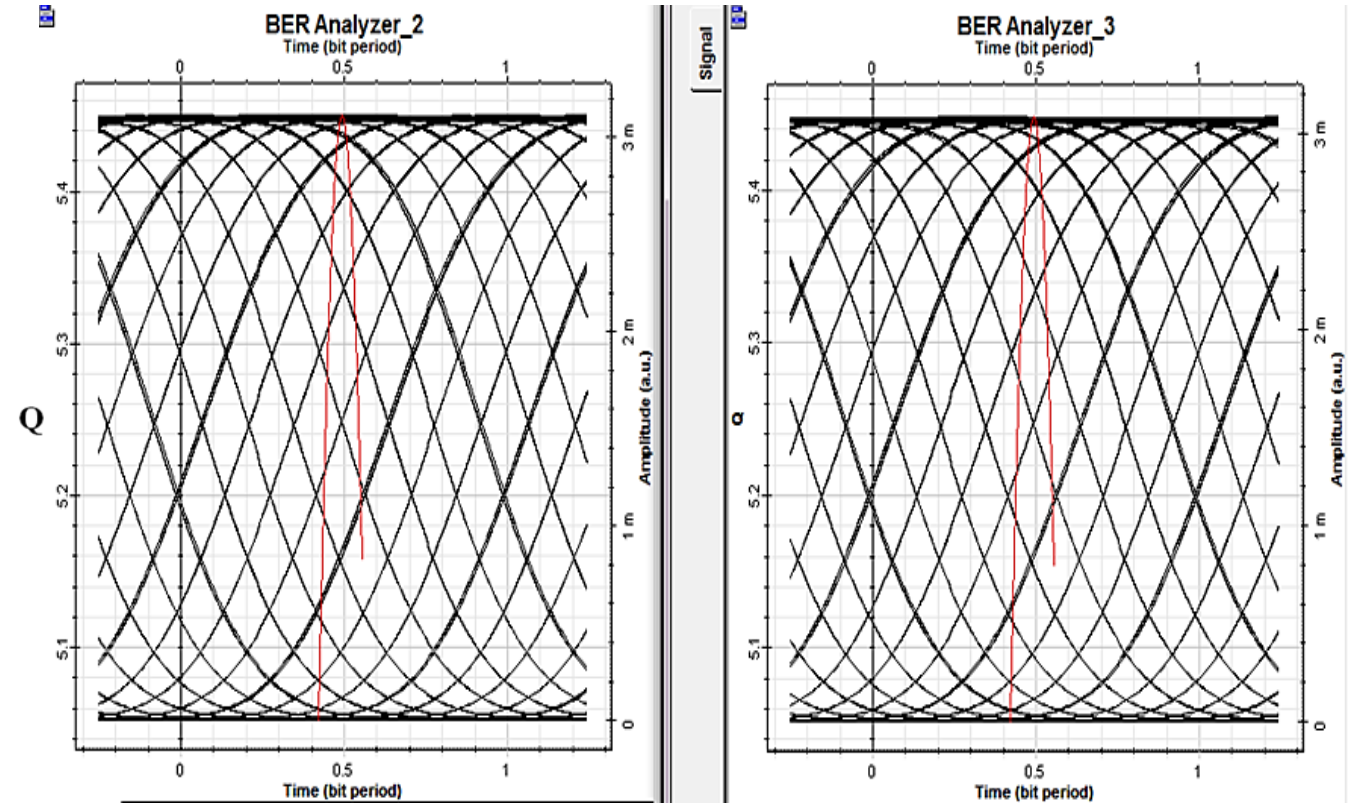

(c) LP21 (d) LP02

Fig. (4.7): The eye diagram and Quality factor for (a) LP01, (b) LP11, (c) LP21, and (d) LP02 modes with $3.5*10^9$ bit rate at 10km, 5mW, and 0.8nm channel spacing.

Table (4-2): Comparison of the receiver performances for various Bit Rate.

Bit Rate (b/s)	Q- Factor	BER
$1*10^9$	59.1721	0
$2*10^9$	56.0781	0
$3*10^9$	6.9578	1.34649e-012
$3.5*10^9$	5.23817	7.29201e-008

Table 4.2 demonstrates that as the bit rate increases, the quality factor (Q-factor) decreases while the Bit Error Rate (BER) increases. This is also evident in Figures 4.4 through 4.7, which show a reduction in both Q-factor and eye height with increasing bit rate. In these graphs, the Q-factor is represented by the red curve. When the data rate increases Increased Inter-Symbol Interference (ISI). At higher data rates, the duration of each bit becomes shorter. Optical fibers, exhibit dispersion (chromatic dispersion and polarization mode dispersion). Dispersion causes different spectral components or polarization modes of the signal to travel at slightly different speeds, leading to pulse broadening. When pulses broaden and overlap with adjacent pulses, it becomes harder for the receiver to distinguish between individual '1's and '0's, contributing to performance degradation. According to Equation (2.14), which models the optical fiber channel, two types of losses are present: linear and nonlinear. It is observed that as the data rate increases, linear losses particularly those caused by dispersion. This leads to further degradation of the signal, which is reflected in a decreasing Q-factor and an increasing BER. Linear losses of the dispersion type can be compensated by loss compensators of the type Dispersion Compensation Fiber (DCF) [65].

4.2.3 Results Of System Design Under Distance Variation

In this case, receiver performance analysis can be seen in running the bit error rate simulation and eye diagram. Figures (4.8), (4.9), (4.10), (4.11), (4.12), show the BER and the eye diagrams, using the same bit rate and power 5mW and space channel 0.8nm with the distance is varied as 10km, 50km, 75km, 100km and 125km respectively, these describe below:

Figure (4.8) displays the Q-factor and eye diagram at 10 km distance in modes LP01, LP11, LP21, and LP02.

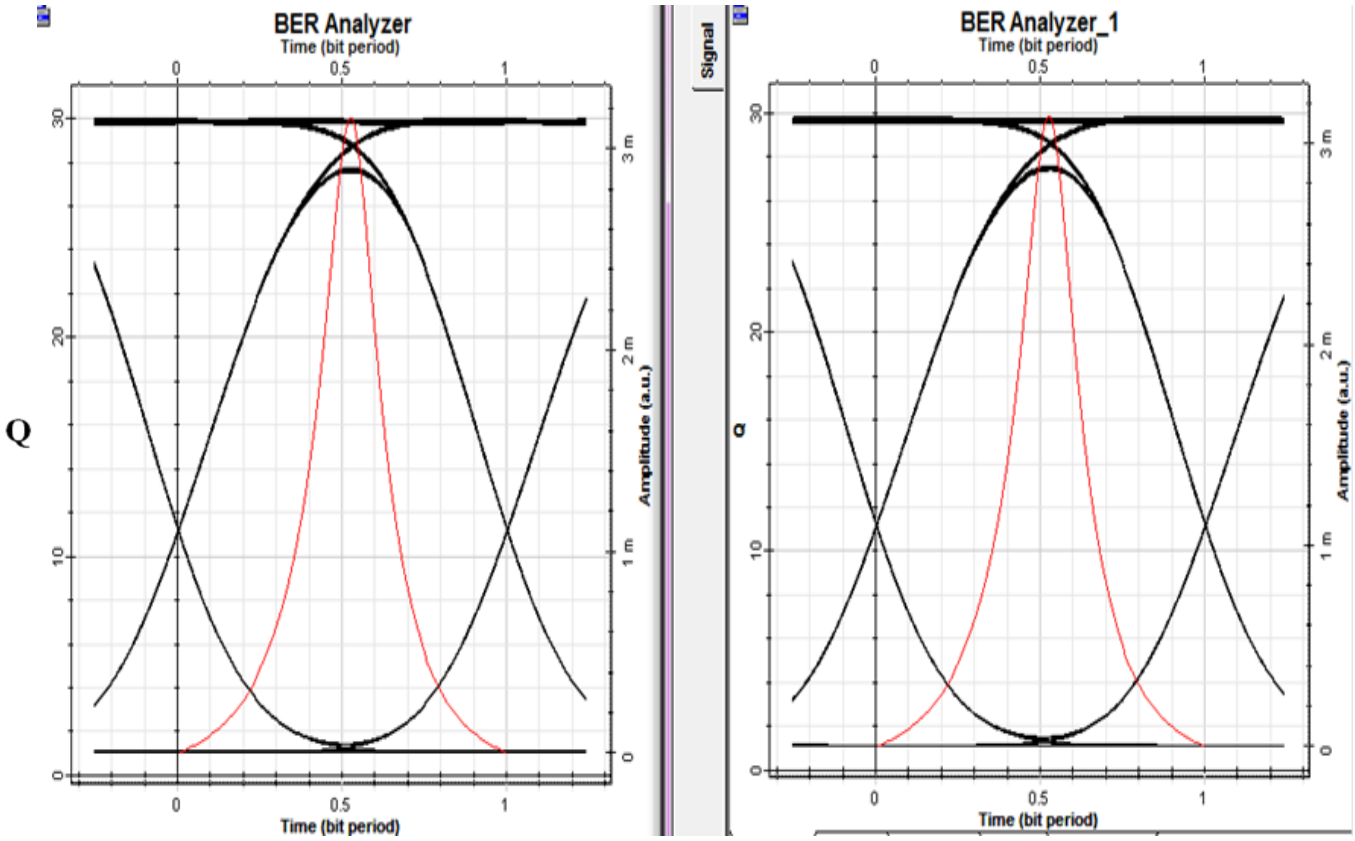

(a) LP01 (b) LP11

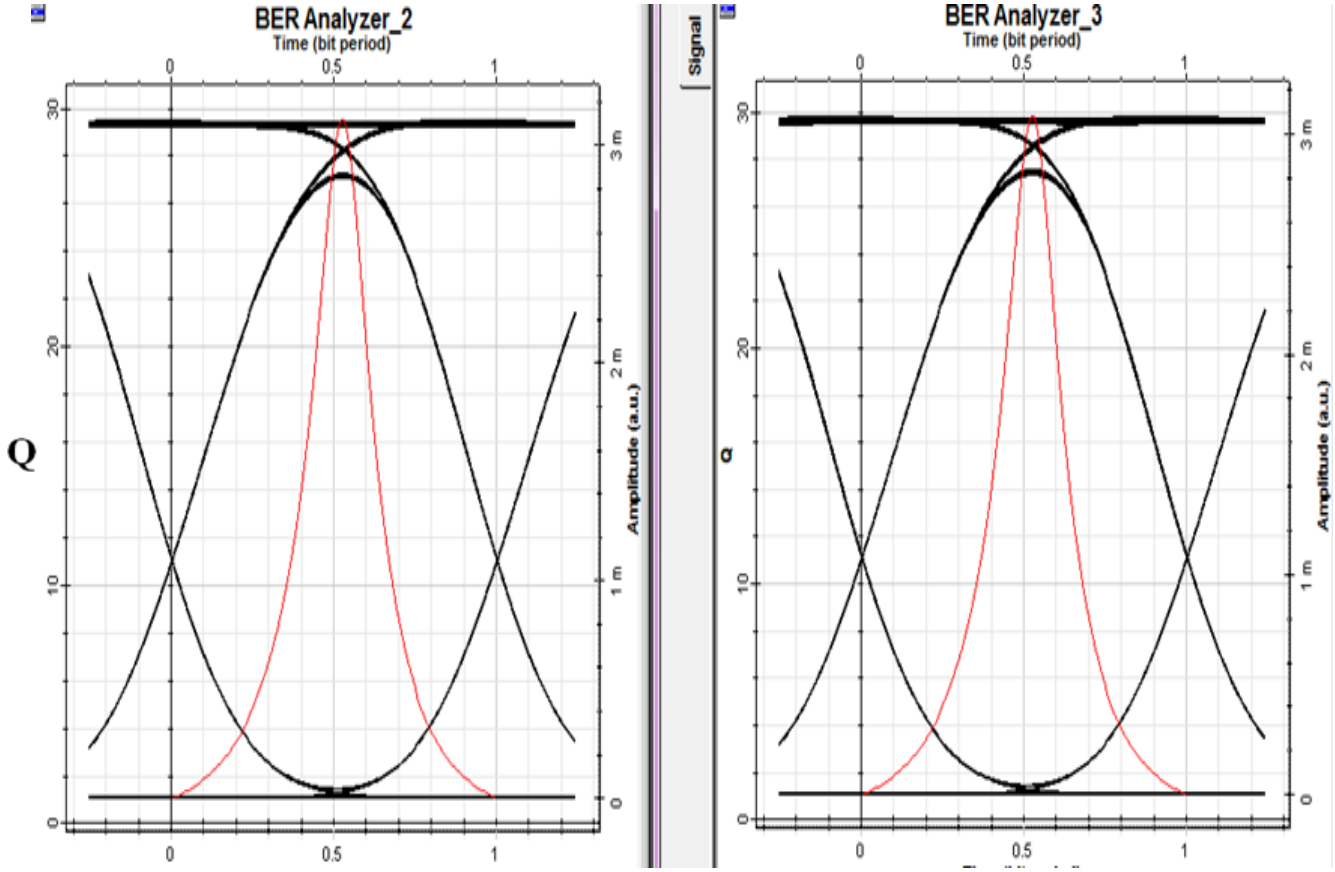

(c)LP21 (d) LP02

Fig. (4.8): The eye diagram and Quality factor for (a) LP01, (b) LP11, (c) LP21, and (d) LP02 modes with 10km distance at 10^9 b/s, 5mW, and 0.8nm channel spacing.

Figure (4.9) displays the Q-factor and eye diagram at a 50 km distance in modes LP01, LP11, LP21, and LP02. This eye diagram shows high signal quality with a clear and open eye, similar to optimal conditions. The Q-factor remains high, signifying a good signal-to-noise ratio and low inter-symbol interference (ISI). This performance ensures a low Bit Error Rate (BER).

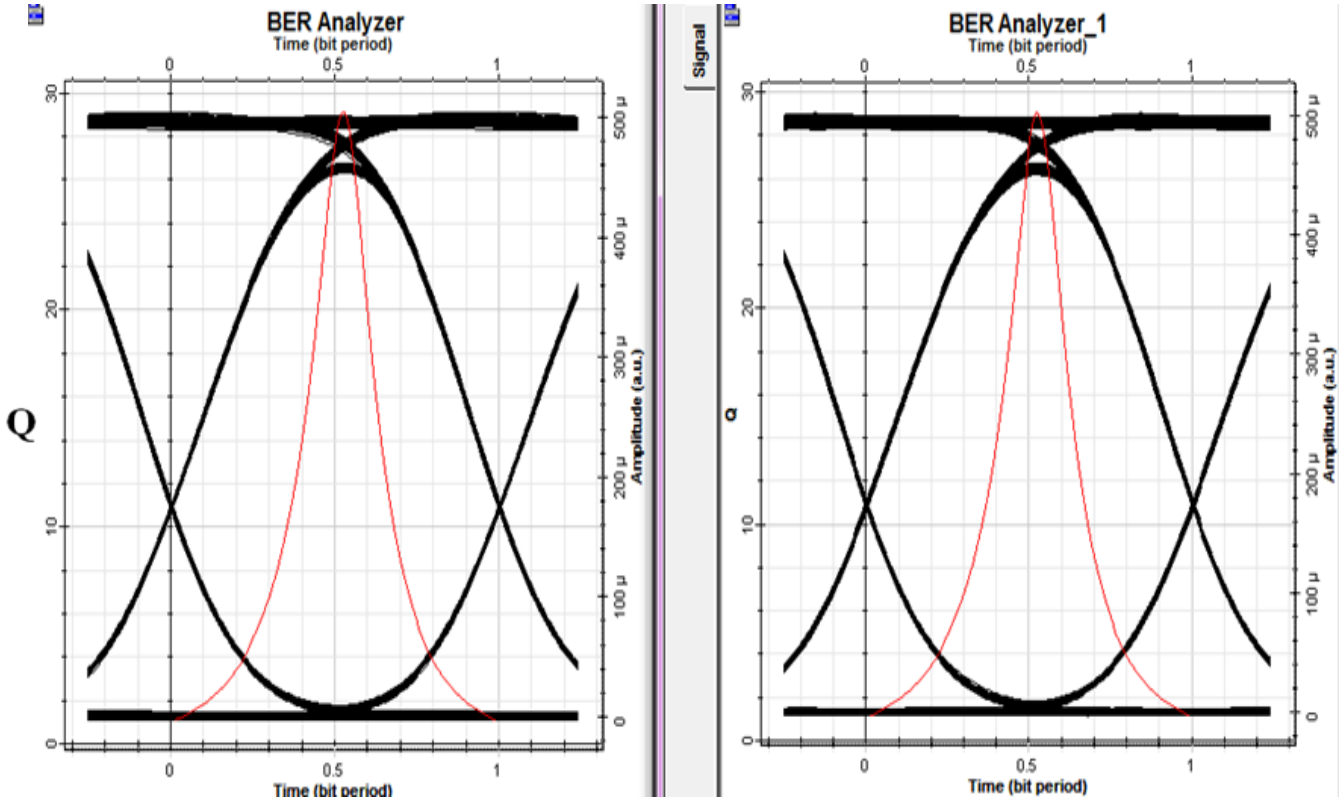

(a) (b)

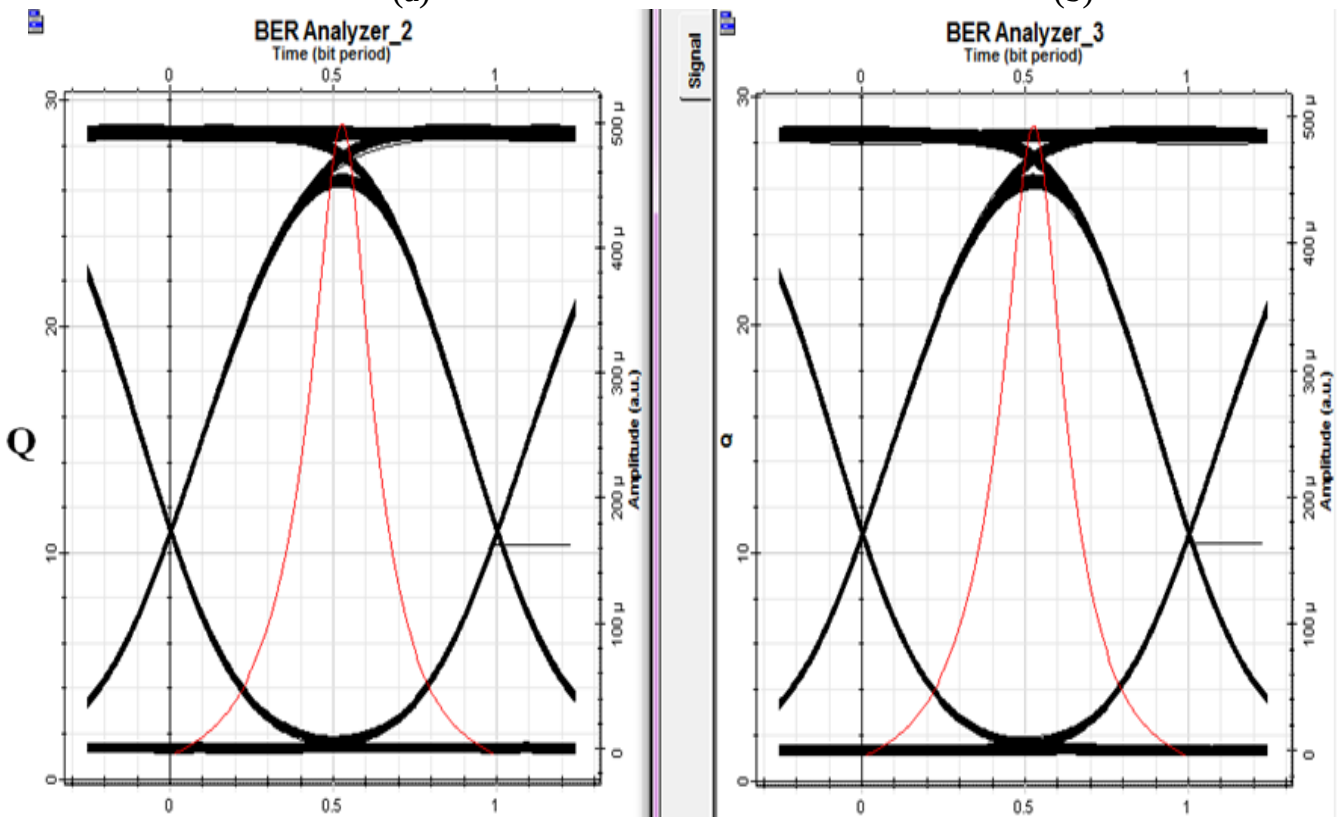

(c) (d)

Fig.(4.9): The eye diagram and Quality factor for (a) LP01, (b) LP11, (c) LP21, and (d) LP02 modes with 50km distance at 10^9 b/s, 5mW, and 0.8nm channel spacing.

Figure (4.10) displays the Q-factor and eye diagram at a 75 km distance in modes LP01, LP11, LP21, and LP02.

This eye diagram indicates good signal quality, characterized by a reasonably open eye and a clearly defined Q-factor. Degradation was observed, likely due to the initial effects of increasing transmission distance, which can introduce slight inter-symbol interference (ISI) or noise. As a result, the Bit Error Rate (BER) remains low but may begin to increase under such conditions.

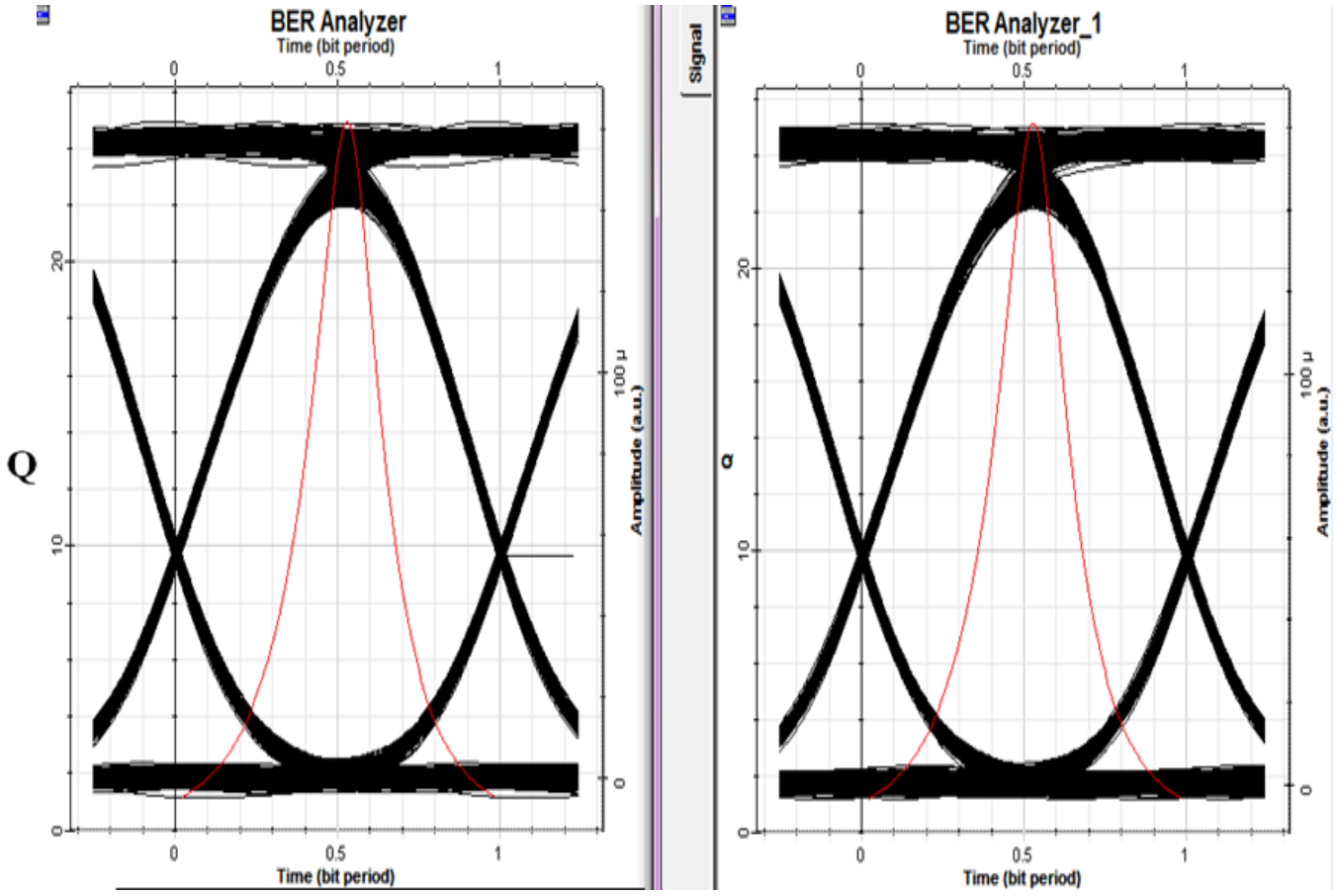

(a) LP01 (b) LP11

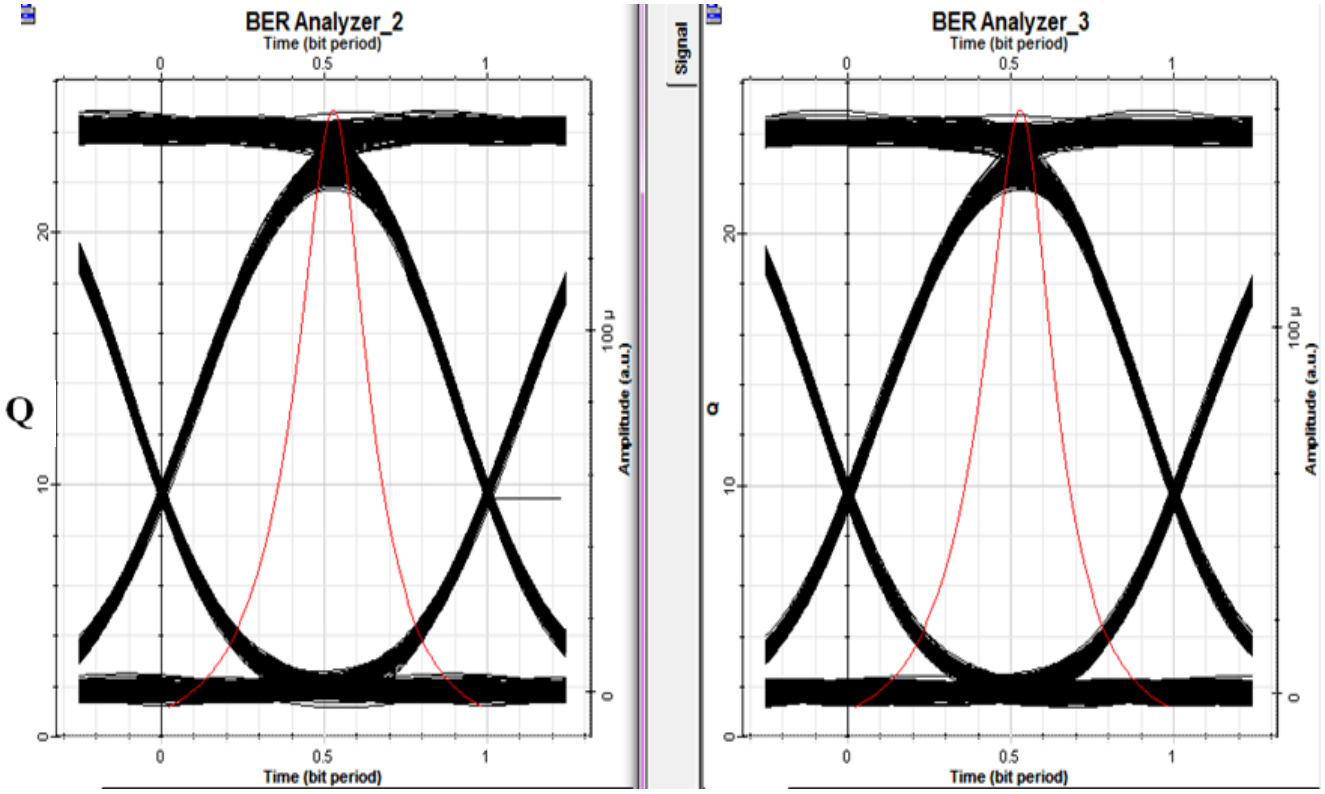

(c) LP21 (d) LP02

Fig(4.10): The eye diagram and Quality factor for (a) LP01, (b) LP11, (c) LP21, and (d) LP02 modes with 75km distance at 10^9 b/s, 5mW, and 0.8nm channel spacing.

Figure (4.11) displays the Q factor and eye diagram at 100 km in modes LP01, LP11, LP21, and LP02. This eye diagram shows noticeable signal degradation. The eye-opening is reduced, and the lines appear thicker due to increased noise and inter-symbol interference (ISI). The Q-factor (red curve) is lower and broader. This indicates that impairments in longer distances are significantly impacting signal quality, resulting in a higher Bit Error Rate (BER). High-quality factors over long distances cannot be achieved without using an optical amplifier.

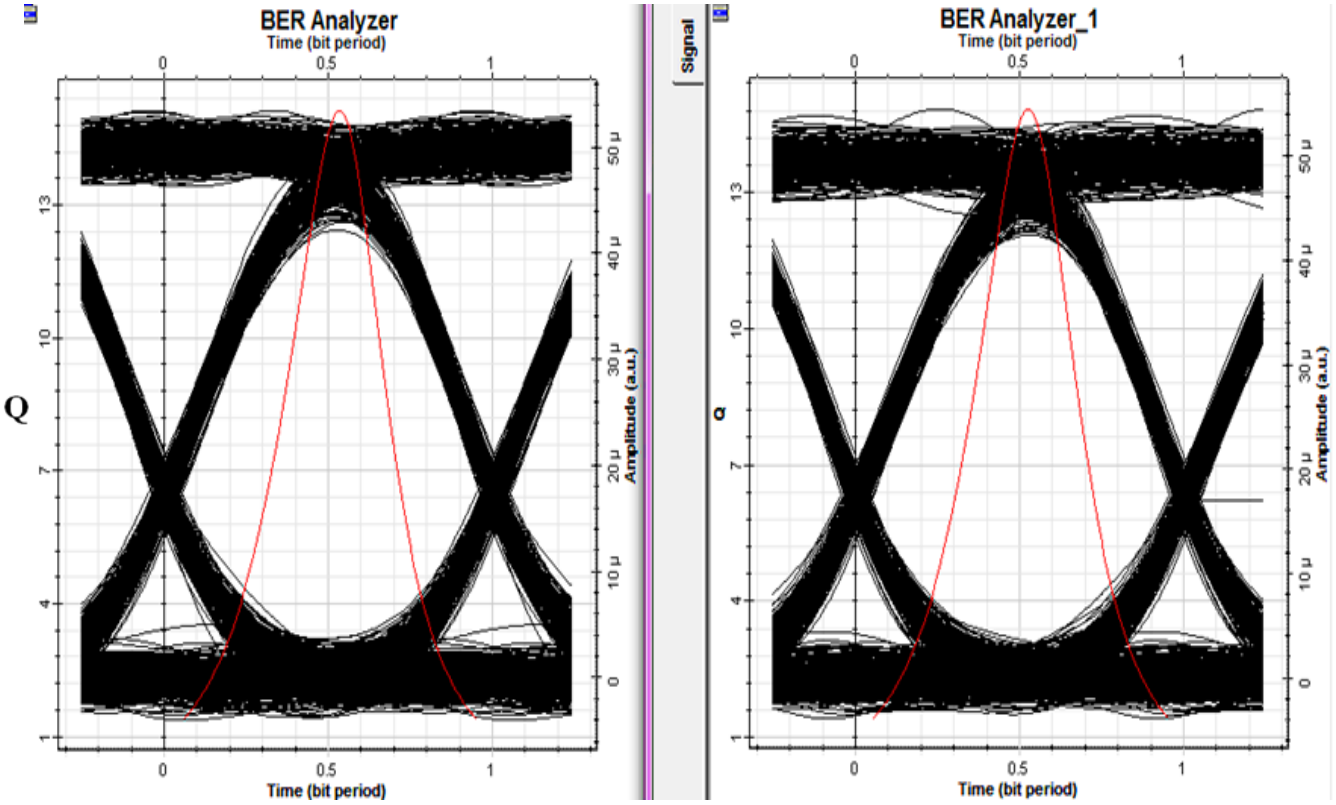

(a) LP01 (b) LP11

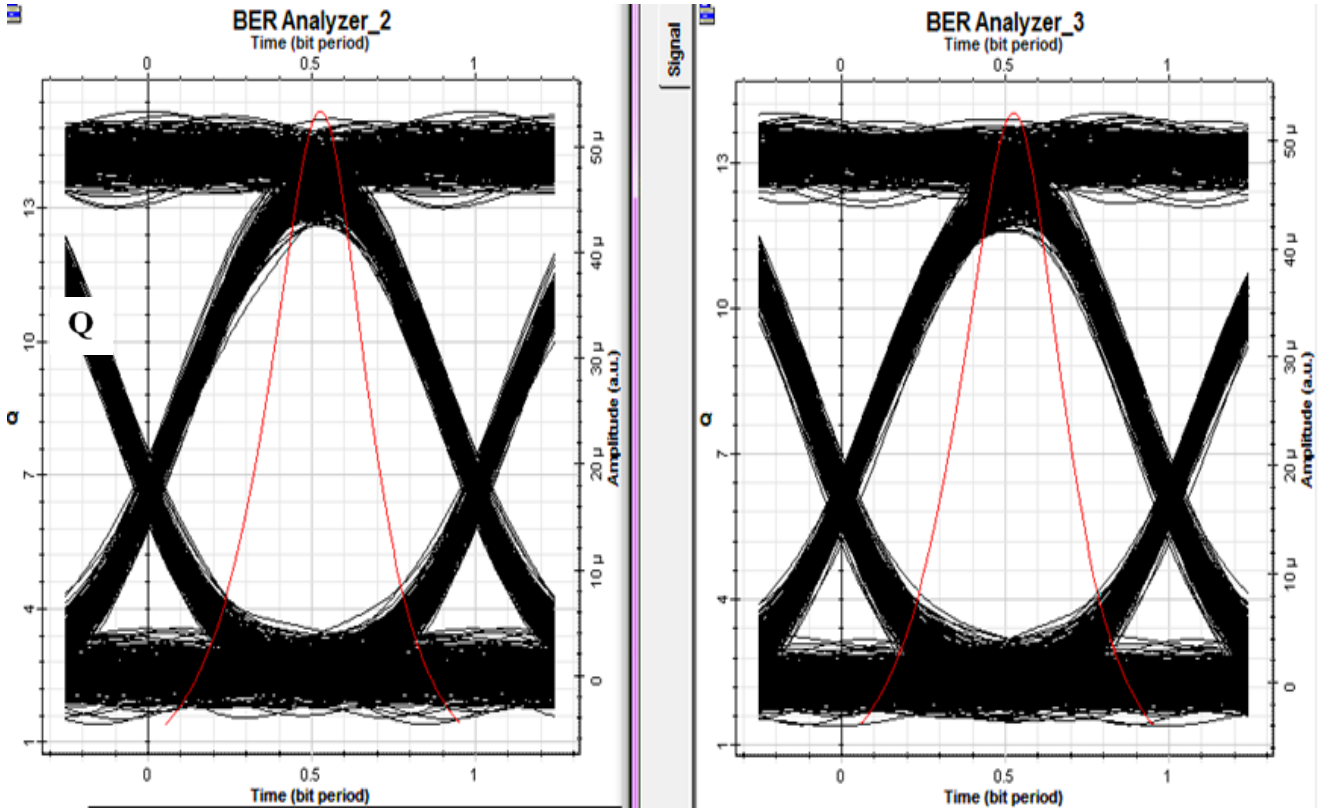

(c) LP21 (d) LP02

Fig(4.11): The eye diagram and Quality factor for (a) LP01, (b) LP11, (c) LP21, and (d) LP02 modes with 100km distance at 10^9 b/s, 5mW, and 0.8nm channel spacing.

Figure (4.12) displays the Q factor and eye diagram at 125 km in modes LP01, LP11, LP21 and LP02. Will notice a significant decrease in Q-factor values as the distance increases. This eye diagram demonstrates severe signal deterioration. The eye is significantly closed and "fuzzy," indicating substantial inter-symbol interference (ISI) and high noise levels. The Q-factor (red curve) is very low and spread out. This level of degradation, often seen at long distances, leads to a very high Bit Error Rate (BER), making reliable data recovery challenging. High-quality factors over long distances cannot be achieved without using an optical amplifier.

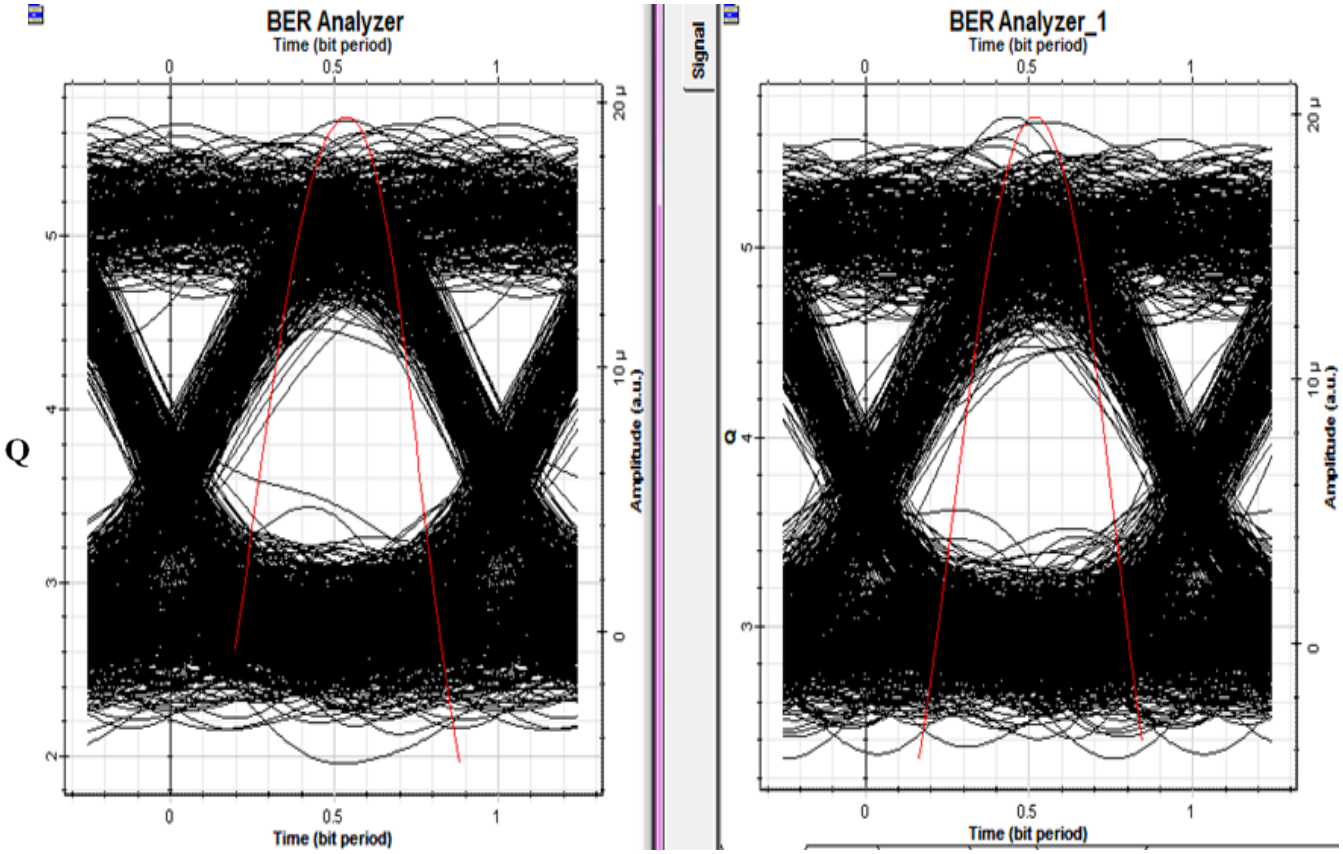

(a) LP01 (b) LP11

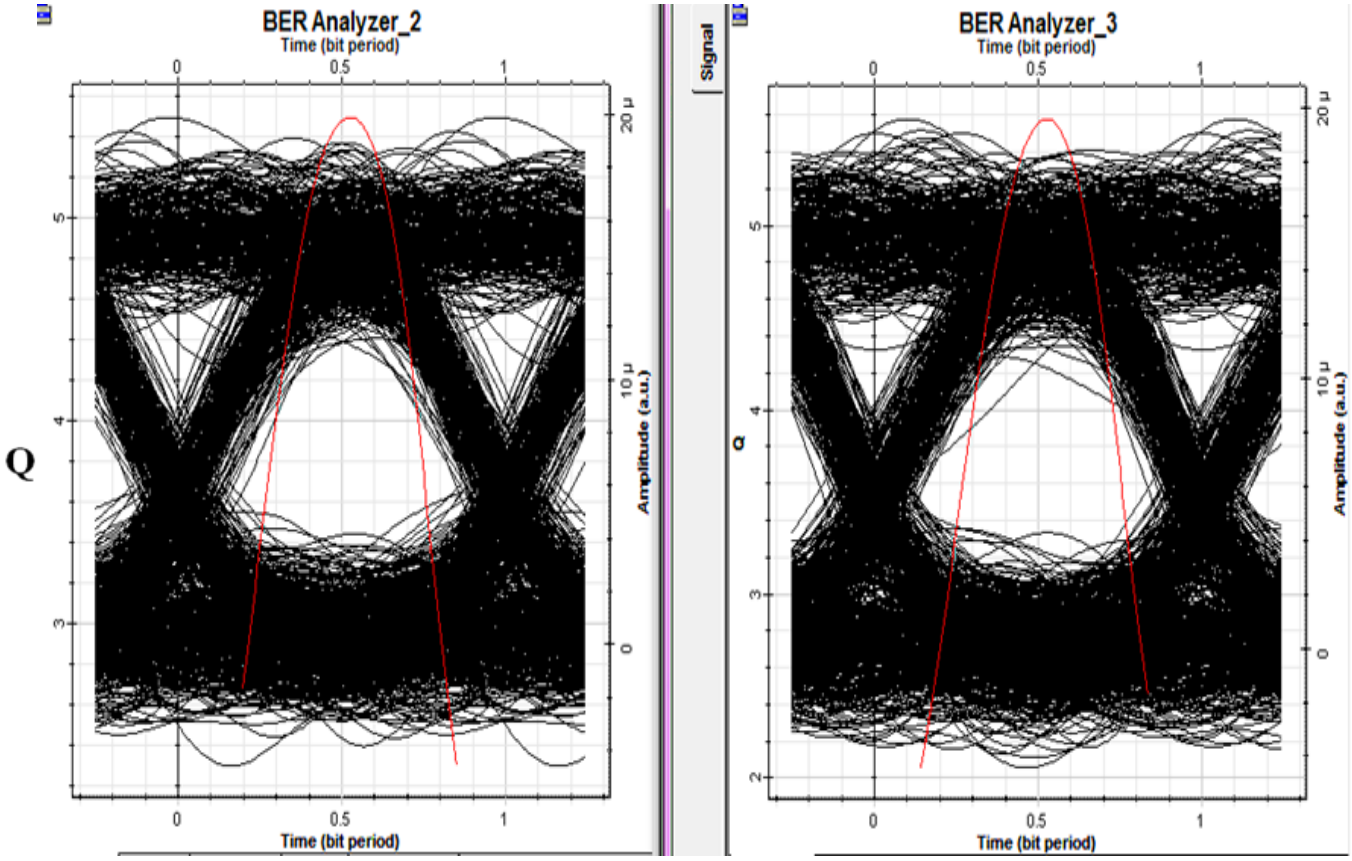

(c) LP21 (d) LP02

Fig.(4.12) : The eye diagram and Quality factor for (a) LP01, (b) LP11, (c) LP21, and (d) LP02 modes with 125km distance at 10^9 b/s, 5mW, and 0.8nm channel spacing.

Table (4-3): Comparison of the receiver performances for different Distance.

Distance (km)	Q- Factor	BER
10	29.975	0
50	28.6626	0
75	24.8377	0
100	14.429	1.65193e-047
125	5.55673	1.37244e-008

Table 4.3 illustrates that as the transmission distance increases, the quality factor (Q-factor) decreases while the Bit Error Rate (BER) rises. A series of eye diagrams (Figures (4.8) to (4.12)) visually demonstrates the impact of increasing optical fiber length on signal integrity. In the illustrations, the Q-factor curve is represented by the red line. Under optimal initial conditions, the eye diagram appears wide open, indicating a high Q-factor, minimal inter-symbol interference (ISI), and a very low BER. However, as the transmission distance increases, cumulative effects such as chromatic dispersion (CD) and polarization mode dispersion (PMD) lead to pulse broadening, increased ISI, and a reduced optical signal-to-noise ratio (OSNR). This degradation is visually evident in the progressive closure of the eye diagram, characterized by diminishing vertical and horizontal openings, blurred signal traces, and a notable decline in Q-factor ultimately resulting in a substantial increase in BER.

Moreover, at practical long-haul distances such as 125 km, nonlinear fiber impairments become significant. Phenomena such as Self-Phase Modulation (SPM), Cross-Phase Modulation (XPM), and Four-Wave Mixing (FWM) contribute to spectral broadening, signal distortion, inter-channel crosstalk, and power depletion. These nonlinear effects further degrade signal quality and increase noise, accelerating eye closure and elevating BER, even in systems where linear impairments have been compensated.

4.2.4 Results Of System Design Under Power Variation

In this case, the results are obtained for the same distance of 10 km and bit rate and space channel 0.8 nm, with the power being varied as 1 mW, 3 mW, 5 mW, and 7 mW, respectively. Receiver performance analysis can be seen in running the bit error rate simulation and eye diagram. Where the results can be seen in Figures (4.13), (4.14), (4.15), and (4.16), these describe below:

Figure (4.13) displays the Q-factor and eye diagram at 1 mW power in modes LP01, LP11, LP21, and LP02.

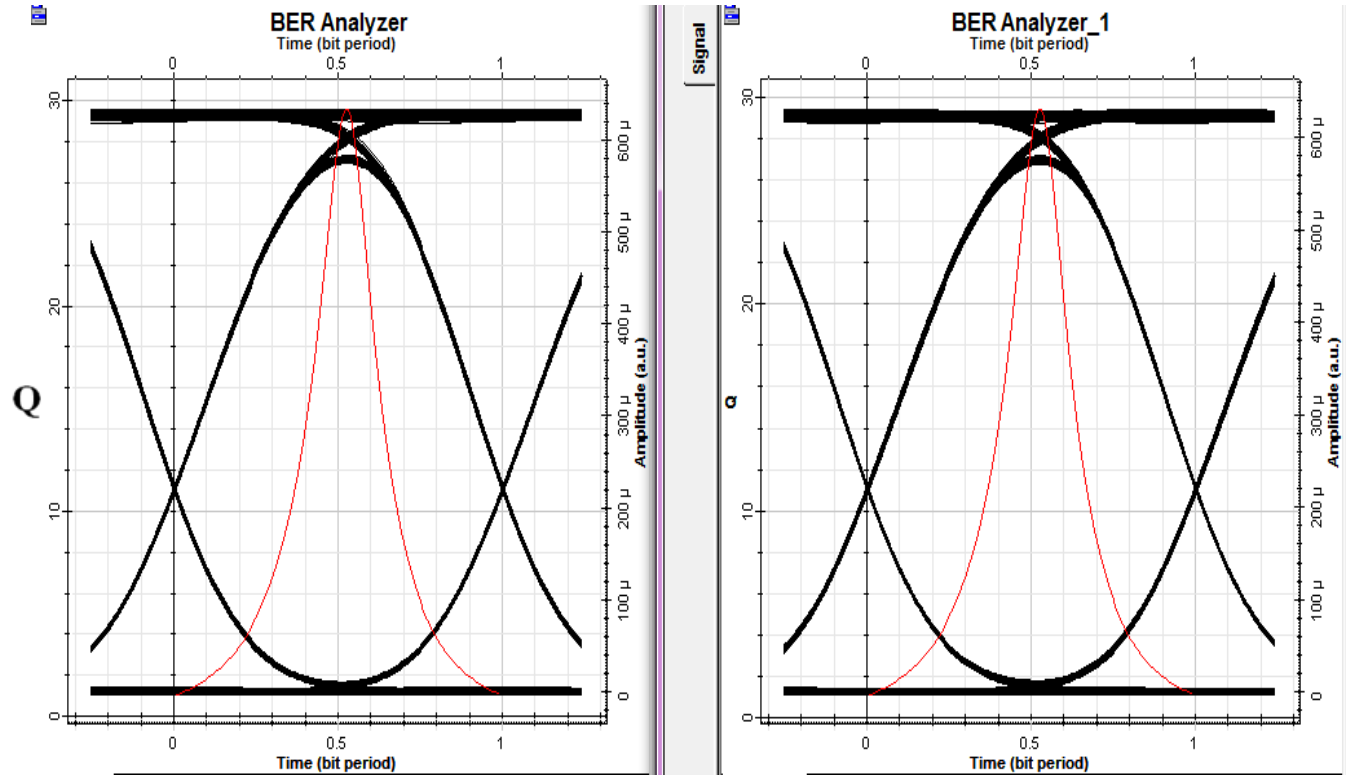

(a) LP01 (b) LP11

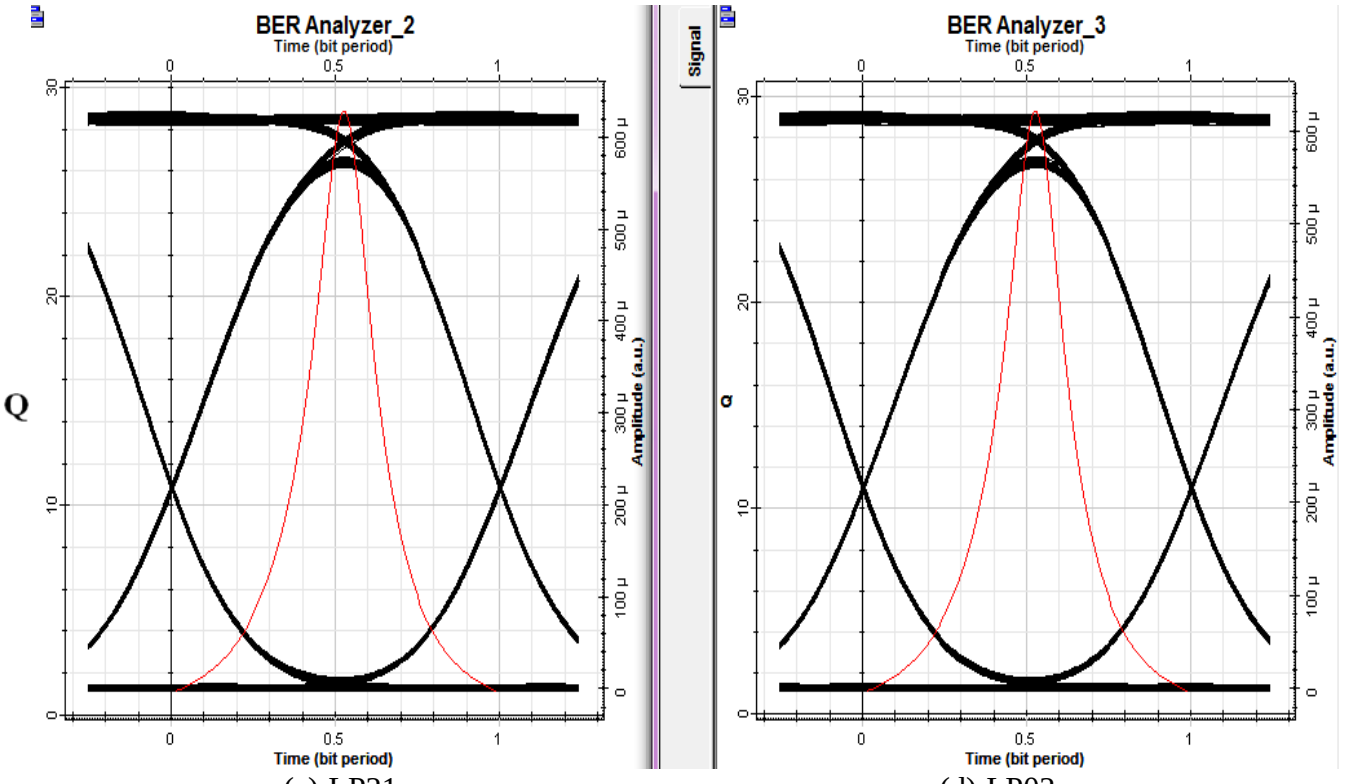

(c) LP21 (d) LP02

Fig.(4.13): The eye diagram and Quality factor for (a) LP01, (b) LP11, (c) LP21, and (d) LP02 modes with 1mW power at 10^9 b/s, 10km, and 0.8nm channel spacing.

Figure (4.14) displays the eye diagram and Q factor at 3mW power in modes LP01, LP11, LP21, and LP02.

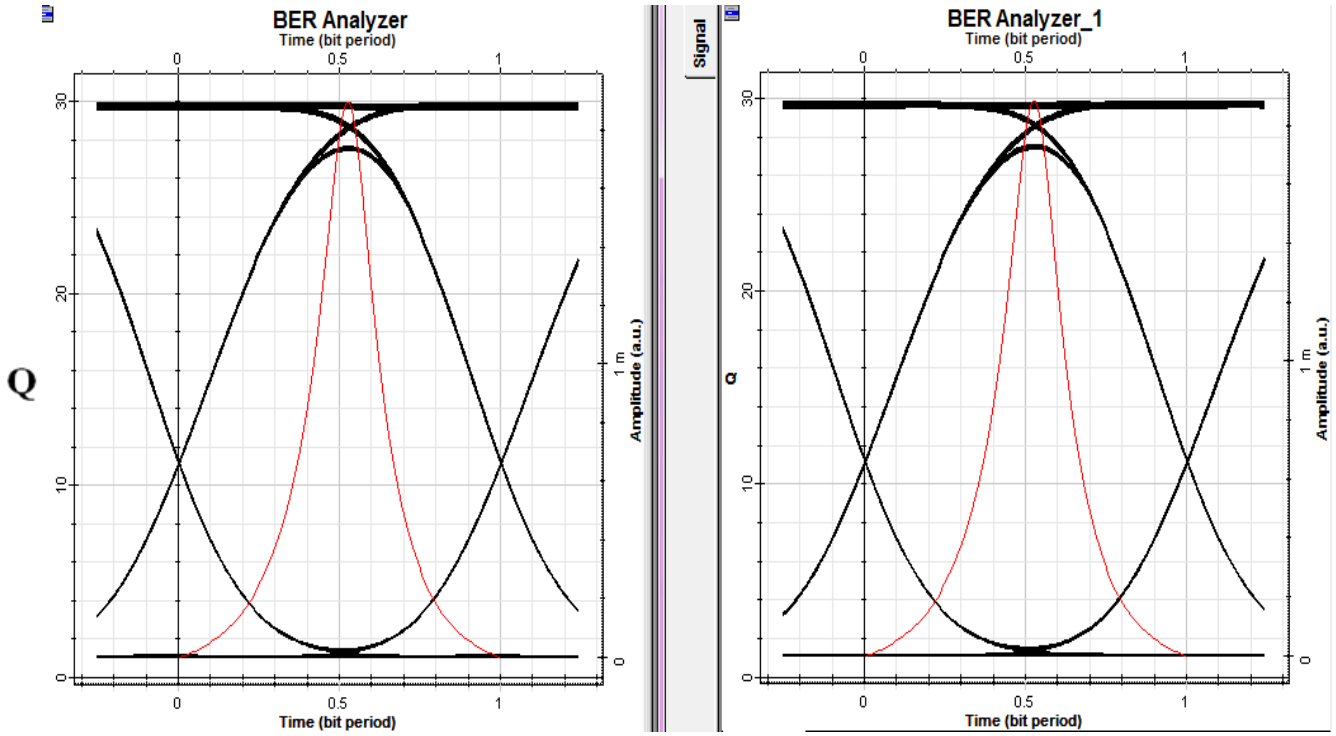

(a) LP01 (b) LP11

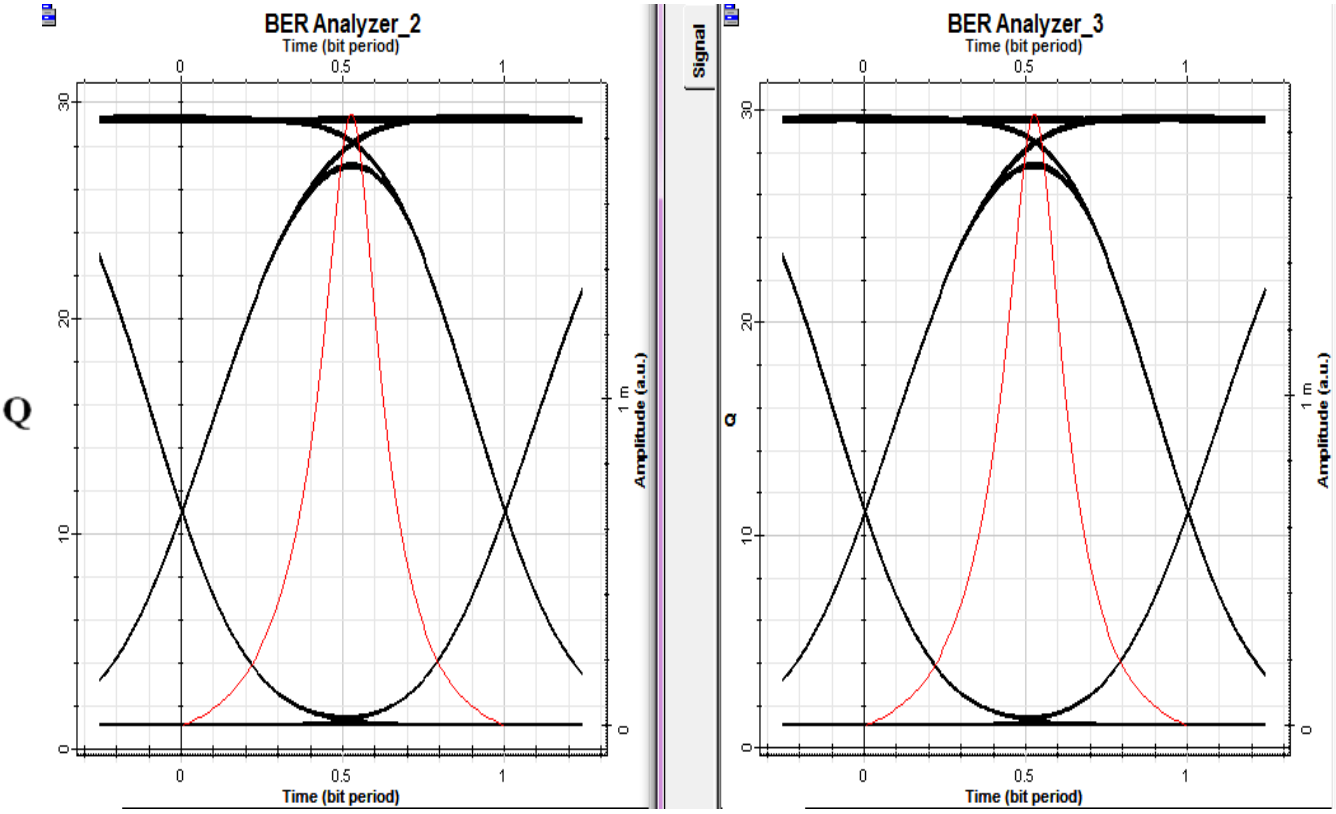

(c) LP21 (d)LP02

Fig.(4.14): The eye diagram and Quality factor for (a) LP01, (b) LP11, (c) LP21, and (d) LP02 modes with 3mW power at 10^9 b/s, 10km, and 0.8nm channel spacing.

These eye diagrams indicate in Fig. (4.14) high signal quality, characterized by a clear and widely open eye pattern. At this power level, the signal strength is significantly improved, which enhances overall system performance by increasing the signal-to-noise ratio (SNR).

Figure (4.15) displays the eye diagram and Q-factor at 5 mW power in modes LP01, LP11, LP21 and LP02. These eye diagrams indicate high signal quality, characterized by a clear and widely open eye pattern. At this power level, the signal strength is significantly improved, which enhances overall system performance by increasing the signal-to-noise ratio (SNR).

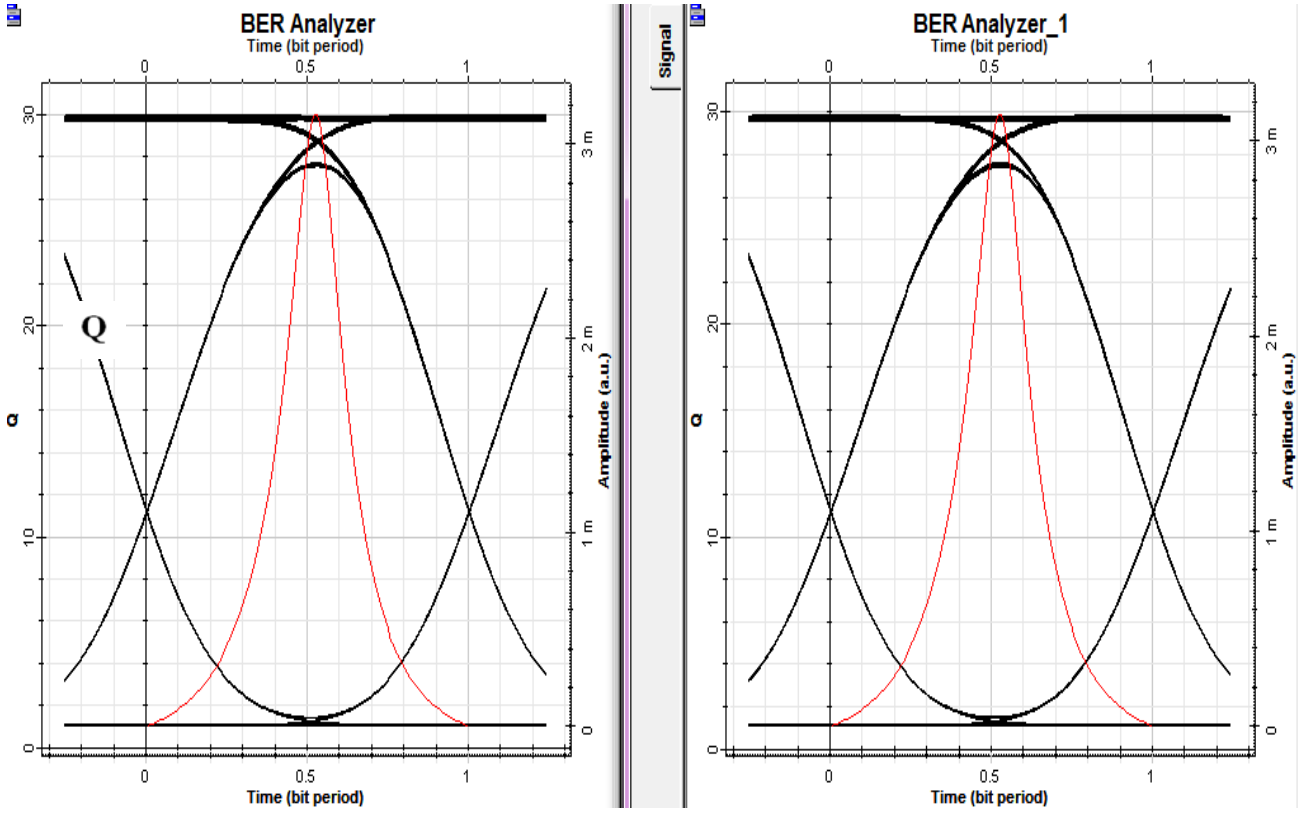

(a) LP01 (b) LP11

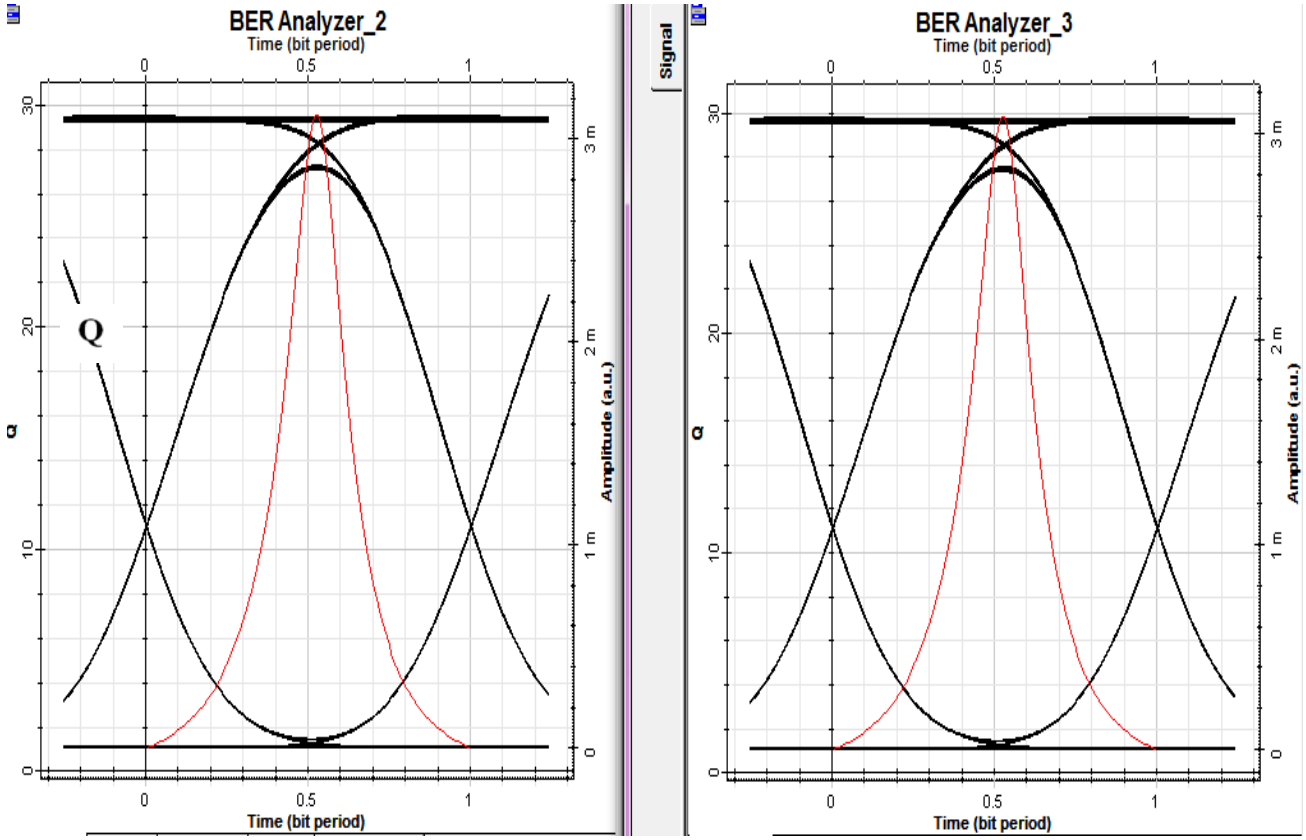

(c) LP21 (d) LP02

Fig.(4.15): The eye diagram and Quality factor for (a) LP01, (b) LP11, (c) LP21, and (d) LP02 modes with 5mW power at 10^9 b/s, 10km, and 0.8nm channel spacing.

Figure (4.14) displays the eye diagram and Q factor at 3mW power in modes LP01, LP11, LP21, and LP02. These eye diagrams indicate high signal quality, characterized by a clear and widely open eye pattern. At this power level, the signal strength is significantly improved, which enhances overall system performance by increasing the signal-to-noise ratio (SNR). As a result, a better distinction between logical '1's and '0's is achieved, contributing to a lower Bit Error Rate (BER).

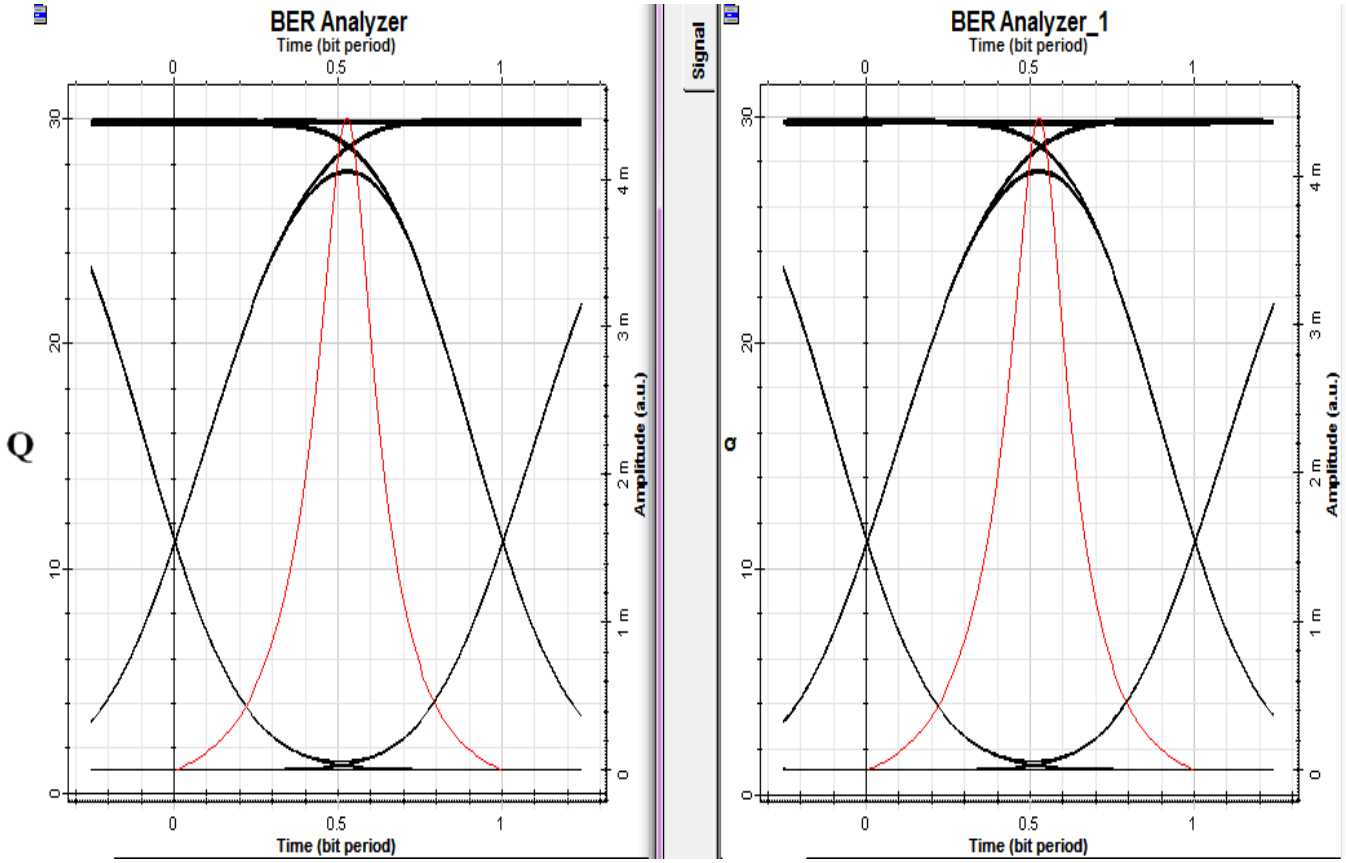

(a) LP01 (b) LP11

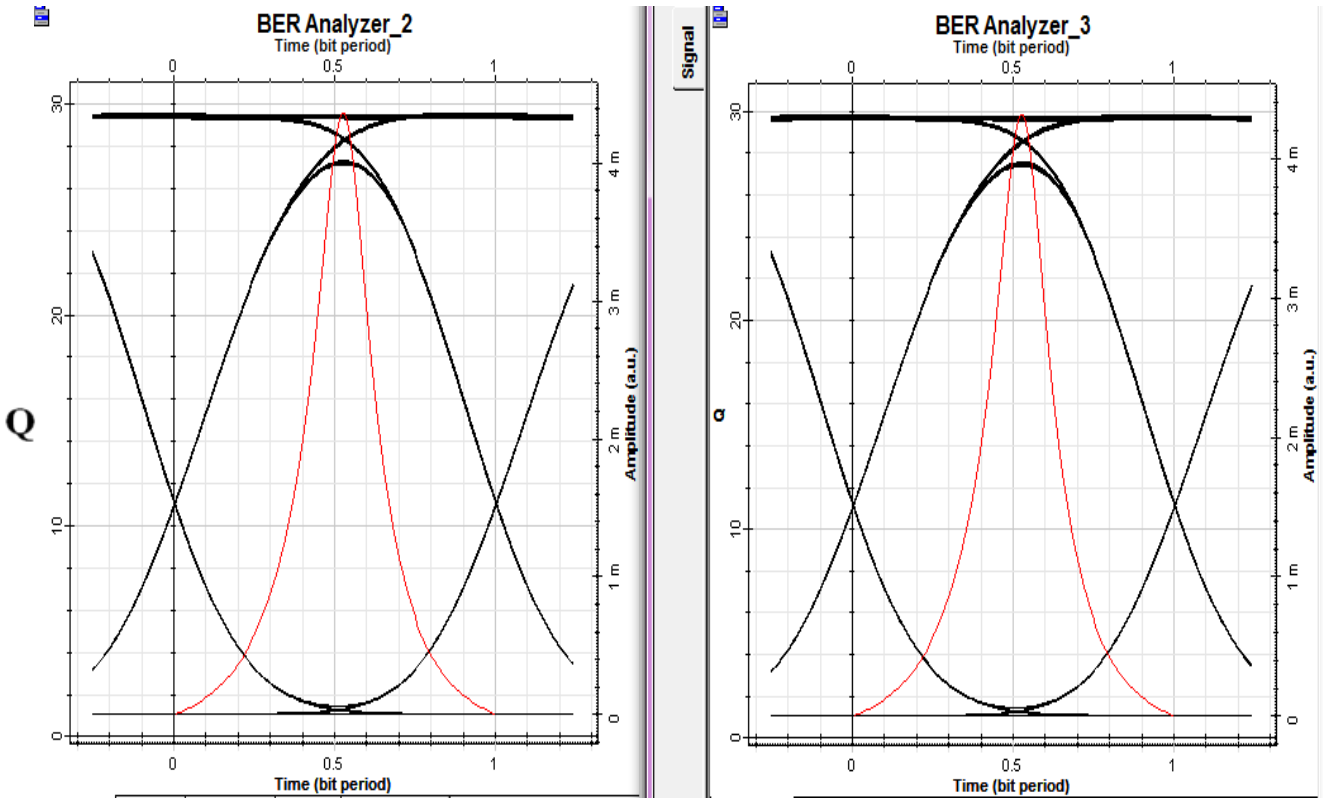

(c) LP21 (d) LP02

Fig.(4.16): The eye diagram and Quality factor for (a) LP01, (b) LP11, (c) LP21, and (d) LP02 modes with 7mW power at 10^9 b/s, 10km, and 0.8nm channel spacing.

Table (4-4): Comparison of the receiver performances for different Power.

Power (mW)	Q- Factor	BER
1	28.8614	1.35211e-183
3	29.468	2.69695e-191
5	29.9022	6.79259e-197
7	30.0548	7.05515e-199

From the Figures (4.13 - 4.16), it is evident that with an increase in power, both the eye height and the quality factor experience a slight rise. Table (4-4) illustrates that when power increases, the quality factor rises and BER drops. The higher the transmitted power, the lower the relative impact of attenuation in the optical fiber, as described by Schuringer's Equation (2.8), where α represents the attenuation coefficient, which depends on the type of optical fiber. The relationship between transmitted and received power is given by:

$$\mathbf{P}_{\text{receiver}} = \mathbf{P}_{\text{transmitter}}\, \boldsymbol{e^{-\alpha L}} \qquad (4.1)$$

According to this equation, the received power decreases exponentially with increasing distance L due to fiber losses. As attenuation (α) increases, the Q-factor decreases, and signal degradation leads to a higher Bit Error Rate (BER). While increasing transmitted power can initially compensate for some loss, excessive power may introduce nonlinear effects. As power increases beyond a certain threshold, nonlinear phenomena such as Self-Phase Modulation (SPM), Cross-Phase Modulation (XPM), and Four-Wave Mixing (FWM) become significant. These effects cause spectral broadening, waveform distortion, and inter-channel interference, all of which degrade signal integrity. As a result, the Bit Error Rate (BER) increases despite

higher power levels, due to the accumulation of nonlinear noise and signal distortion. In practical systems, optical amplifiers are used to compensate for power losses and maintain acceptable signal quality over long distances.

4.2.5 Results Of System Design Under Space channel Variation

In this case, the results are obtained for the same distance of 10 km and bit rate and power of 5 mW, with the channel spacing being varied as 0.4 nm, 0.8 nm, 1.6 nm, and 2 nm, respectively. Receiver performance analysis can be seen in running the bit error rate simulation and eye diagram. Channel spacing refers to the spectral separation between adjacent wavelength channels, typically measured in nanometers (nm). Where the results can be seen in Figures (4.17), (4.18), (4.19), and (4.20), which are described below:

Figure (4.17) displays the eye diagram and Q-factor at 0.4 nm, channel spacing in modes LP01, LP11, LP21, and LP02.

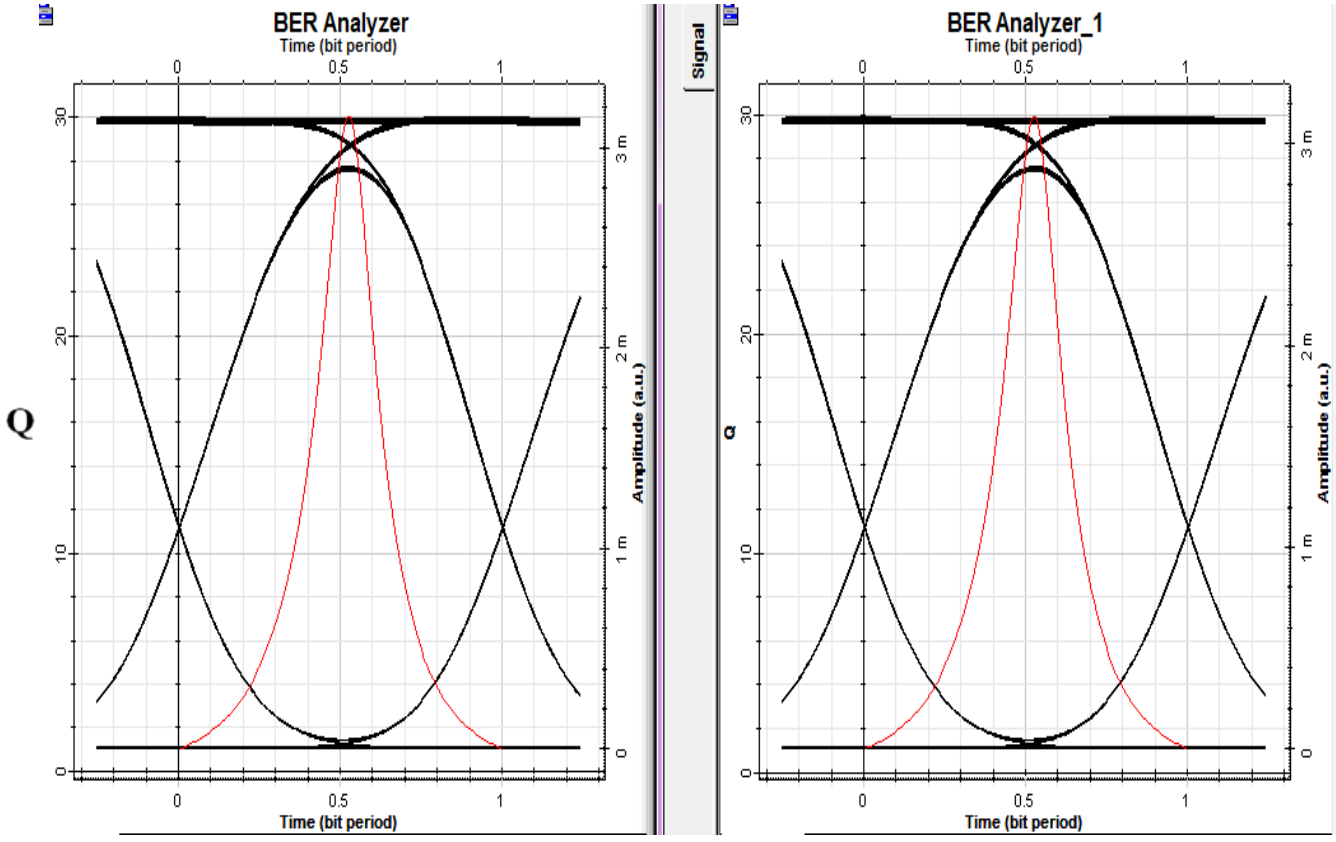

(a) LP01 (b) LP11

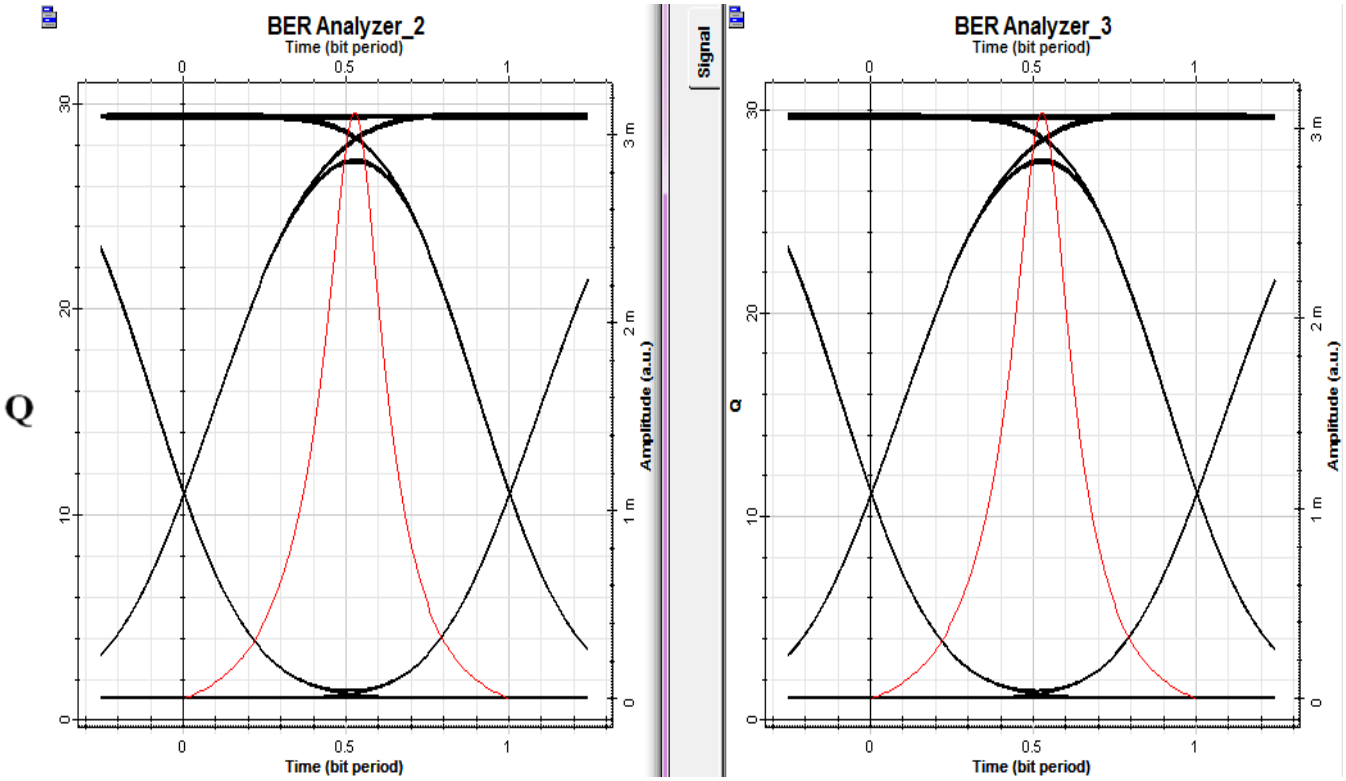

(c) LP21 (d) LP02

Fig.(4.17): The eye diagram and Quality factor for (a) LP01, (b) LP11, (c) LP21, and (d) LP02 modes with 0.4nm channel spacing at 10^9 b/s, 10km, and 5mW power.

In Fig. (4.17), the eye opening is present but shows increased signal overlap, indicating a lower Q-factor and a higher Bit Error Rate (BER). This suggests smaller channel spacing, where inter-channel interference is more likely to occur due to spectral overlap. The smaller the separation between channels, the greater the crosstalk and the more significant the signal degradation.

Figure (4.18) displays the Q-factor and eye diagram at 0.8 nm channel spacing in modes LP01, LP11, LP21 and LP02. The eye diagram shows a wider vertical opening and cleaner eye shape. This indicates a higher Q-factor and lower BER, reflecting better signal integrity.

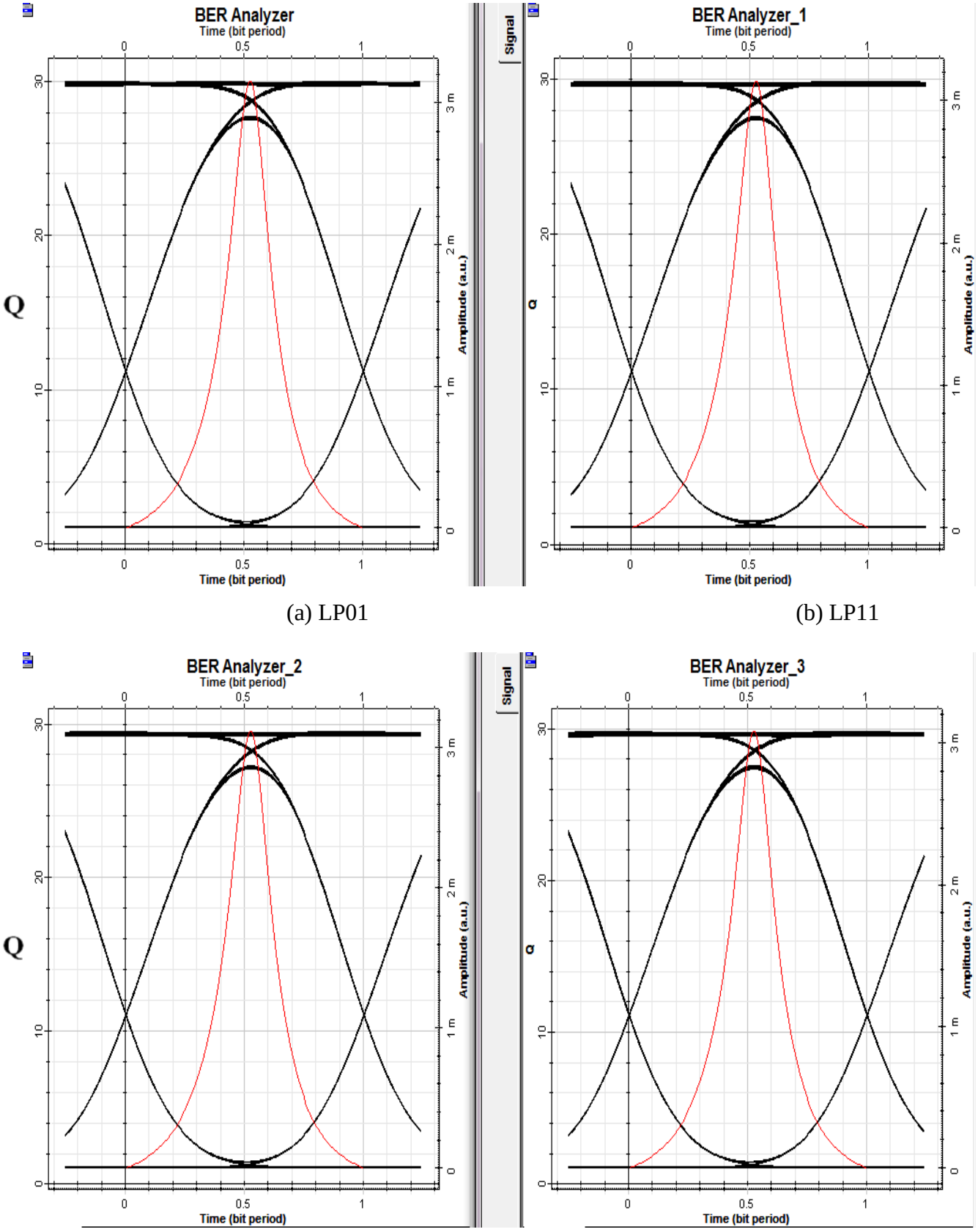

(a) LP01 (b) LP11

(c) LP21 (d) LP02

Fig.(4.18): The eye diagram and Quality factor for (a) LP01, (b) LP11, (c) LP21, and (d) LP02 modes with 0.8nm channel spacing at 10^9 b/s, 10km, and 5mW power.

Figure (4.19) displays the Q-factor and eye diagram at 1.6 nm space channel in modes LP01, LP11, LP21 and LP02. The eye diagram shows a wider vertical opening and cleaner eye shape. This indicates a higher Q-factor and lower BER, reflecting better signal integrity.

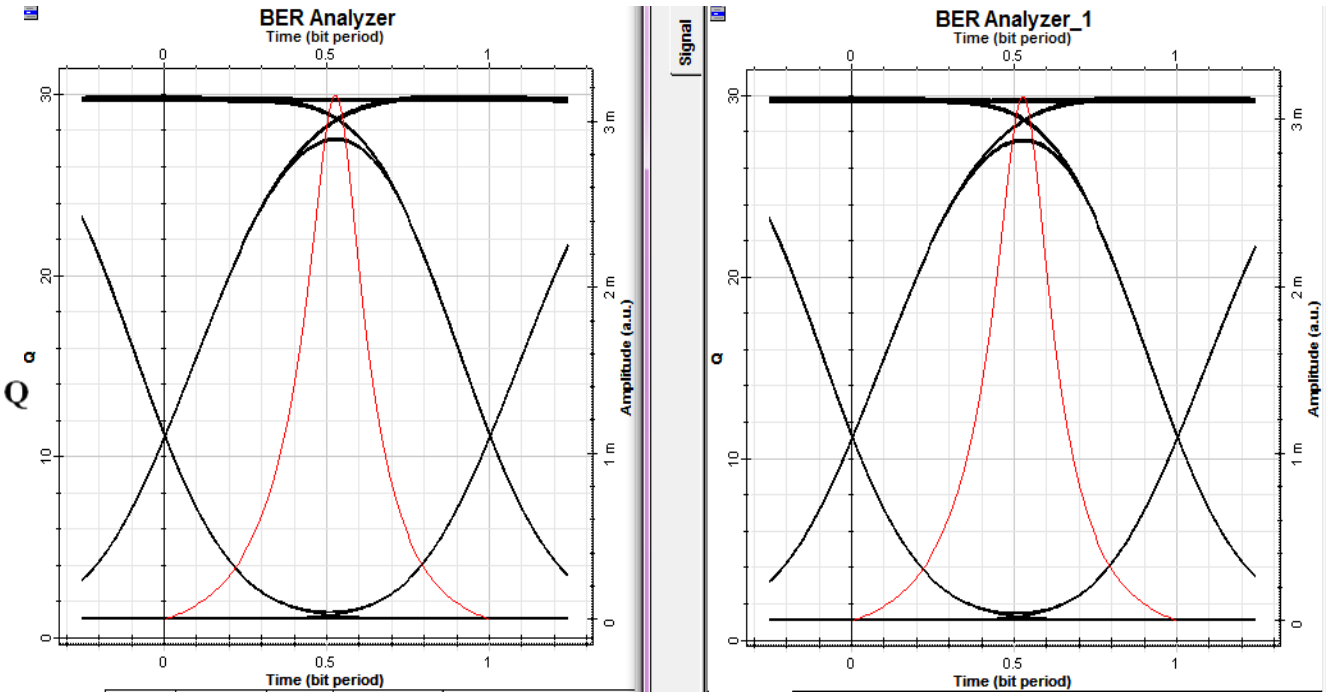

(a) LP01 (b) LP11

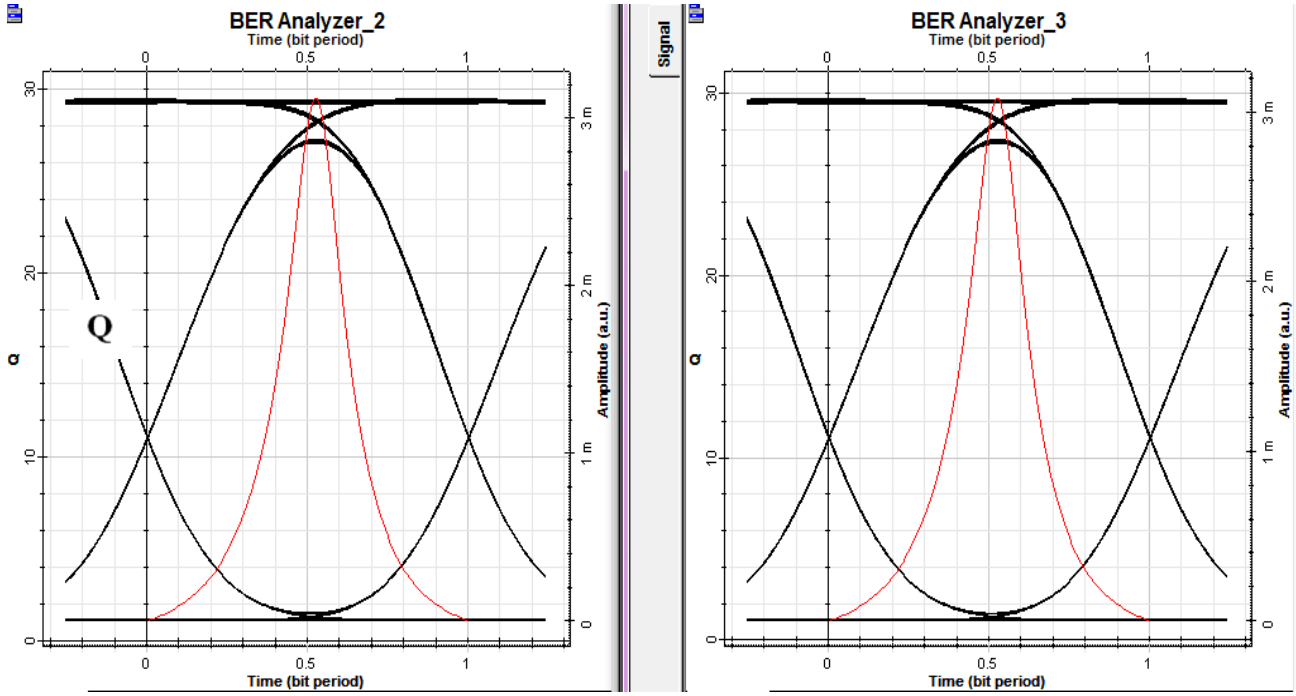

(c) LP21 (d) LP02

Fig. (4.19): The eye diagram and Quality factor for (a) LP01, (b) LP11, (c) LP21, and (d) LP02 modes with 1.6nm channel spacing at 10^9 b/s, 10km, and 5mW power.

Figure (4.20) displays the Q-factor and eye diagram at 2 nm channel spacing in modes LP01, LP11, LP21 and LP02. The eye diagram shows a wider vertical opening and cleaner eye shape. This indicates a higher Q-factor and lower BER, reflecting better signal integrity. This corresponds to a with larger channel spacing, reducing interference and nonlinear effects such as Four-Wave Mixing (FWM) and Cross-Phase Modulation (XPM).

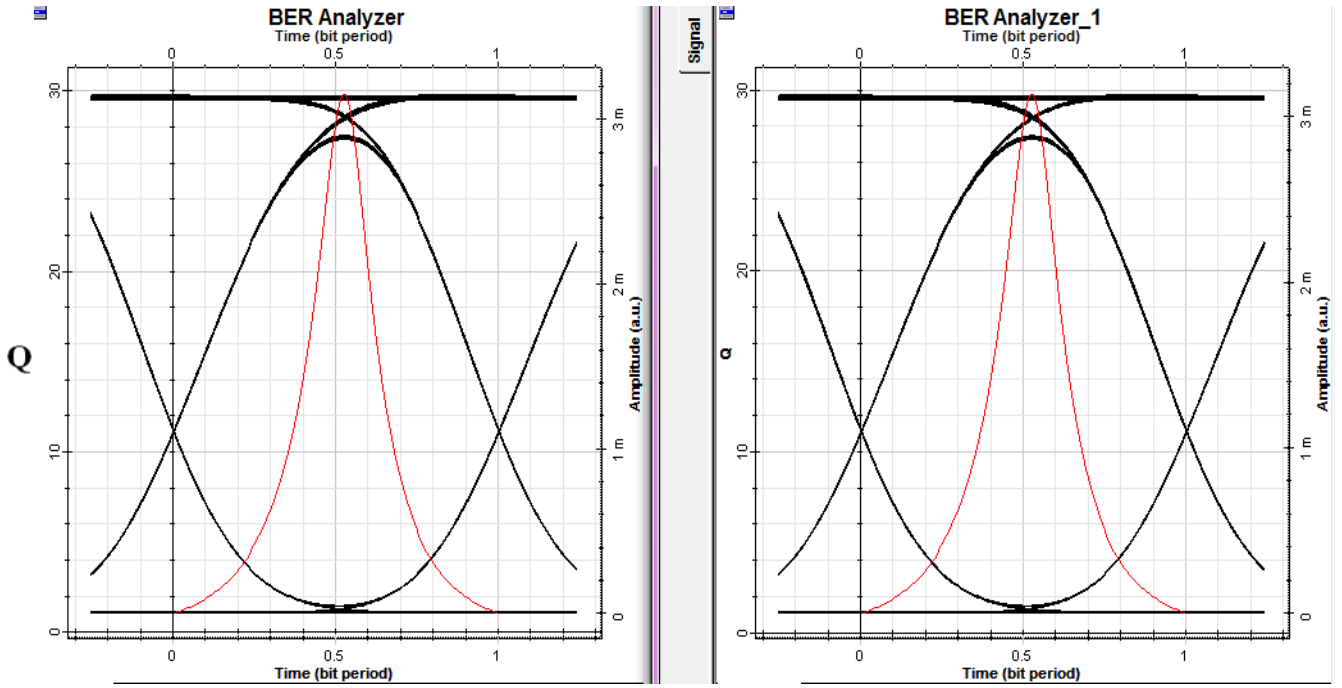

(a) LP01

(b) LP11

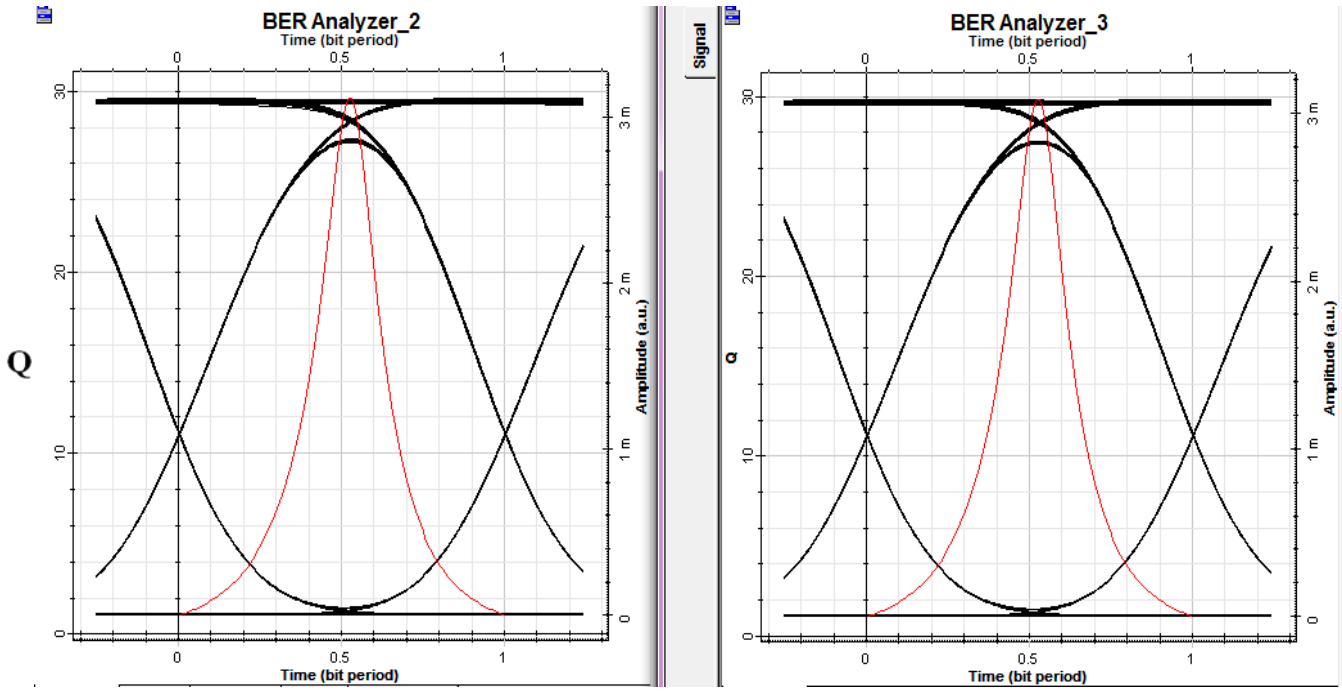

(c) LP21

(d) LP02

Fig.(4.20): The eye diagram and Quality factor for (a) LP01, (b) LP11, (c) LP21, and (d) LP02 modes with 2nm channel spacing at 10^9 b/s, 10km, and 5mW power.

Table (4-5): Comparison of the receiver performances for different Space Channel.

Channel Spacing (nm)	Q- Factor	BER
0.4	29.5531	2.16924e-192
0.8	29.7636	4.18229e-195
1.6	29.9595	1.21076e-197
2	30.0864	2.73567e-199

Table (4-5) illustrates that as the channel spacing increases, the quality factor rises and the Bit Error Rate (BER) decreases. Figures (4.17-4.20) show that this increase in channel spacing results in a slight improvement in both eye height and quality factor, indicating enhanced signal clarity and reduced inter-channel interference. Increasing channel spacing in WDM/SDM systems reduces spectral overlap and minimizes inter-channel interference and nonlinear effects such as Four-Wave Mixing (FWM) and Cross-Phase Modulation (XPM). As the spacing between adjacent channels widens, signal crosstalk is significantly reduced, leading to improved signal clarity and a higher Q-factor. Consequently, the Bit Error Rate (BER) decreases due to enhanced signal separation and reduced distortion. However, while larger channel spacing improves signal integrity, it also reduces spectral efficiency, meaning fewer channels can be transmitted within the same bandwidth. The smaller the channel spacing, the greater the impact of nonlinear losses due to increased inter-channel interactions such as Four-Wave Mixing (FWM) and Cross-Phase Modulation (XPM). These nonlinear impairments can be mitigated using compensation techniques such as Digital Backpropagation (DBP) or Optical Backpropagation, which aim to reverse the nonlinear effects accumulated during signal propagation.

Chapter Five

Conclusion and Future Works

5.1 Conclusions

There are several conclusions that can be drawn. Which is considered according to the following:

- The simulation of a hybrid WDM/SDM system was designed using OptiSystem software. Four modes were utilized to achieve ultra-high data rates, with Non-Return-to-Zero (NRZ) line coding applied to all channels. These systems were discussed and analyzed to explain their performance under four different key parameters: bit rate, transmission distance, power, and channel spacing. The Q-factor, eye diagrams, and Bit Error Rate (BER) were evaluated for each case.
- The best quality factor obtained was 59.1721 at a data rate of 10^9 b/s, a distance of 10 km, 5 mW power, and 0.8 nm channel spacing.
- An increase in bit rate causes pulse broadening, Q-factor reduction, and BER deterioration due to dispersion and Inter-Symbol Interference (ISI).
- An increase in distance leads to cumulative chromatic and modal dispersion, pulse overlap, Q-factor degradation, and higher BER.
- Higher power improves the initial SNR but may introduce nonlinear degradation (SPM, XPM, FWM), which can counterintuitively increase BER.
- Wider channel spacing reduces spectral overlap and nonlinear crosstalk, improving Q-factor and BER at the cost of spectral efficiency.

- SDM modal impairments can be compensated for using Multi-Input Multi-Output (MIMO) DSP.

5.2 Future Work Recommendations

The proposed works for those recommended for optical communication system improvement to enhance the operation of the system are:

- Future work should incorporate the analysis of nonlinear effects and their mitigation using advanced techniques such as optical or digital backpropagation.
- Extending the system model to include more spatial modes and longer transmission distances would allow for a more comprehensive assessment of scalability and real-world applicability.
- One of the promising techniques possible for enhancing system performance is Dense Space Division Multiplexing (DSDM).
- Evaluating the computational complexity and real-time processing capabilities of MIMO-based digital signal processing (DSP) in high-capacity WDM-SDM systems is recommended.

References

[1] L. A. Tapia Martinez, "Investigation on Crosstalk in Multi-core Optical Fibers," Universitat Politècnica de Catalunya, 2015.

[2] E. Awwad, "Emerging space-time coding techniques for optical fiber transmission systems," Télécom ParisTech, 2015. NNT : 2015ENST0004. tel-01230644.

[3] M. Nakazawa, "Giant leaps in optical communcation technologies towards 2030 and beyond," *ECOC, 2010, Plenary Talk*, 2010.

[4] D. Qian, Ming-Fang Huang, E. Ip, Yue-Kai Huang, Y. Shao, J. Hu, and T. Wang., "101.7-Tb/s (370× 294-Gb/s) PDM-128QAM-OFDM transmission over 3× 55-km SSMF using pilot-based phase noise mitigation," in *Optical Fiber Communication Conference*, 2011: Optica Publishing Group, p. PDPB5.

[5] N. Bai, E. Ip, Yue-Kai Huang, E. Mateo, F. Yaman, Ming-Jun Li, S. Bickham, S. Ten, J. Liñares, C. Montero, V. Moreno, X. Prieto, V.Tse, K. Man Chung, A. Pak Tao Lau, Hwa-Yaw Tam, C. Lu, Y. Luo, Gang-Ding Peng, G. Li, and T. Wang, "Mode-division multiplexed transmission with inline few-mode fiber amplifier," Opt. Express 20, 2668-2680 (2012).

[6] L. Gruner-Nielsen, Y. Sun, J. W Nicholson, D. Jakobsen, K. G Jespersen, R. Lingle, B. Palsdottir, "Few mode transmission fiber with low DGD, low mode coupling, and low loss," *Journal of Lightwave Technology*, vol. 30, no. 23, pp. 3693-3698, 2012.

[7] W. Shi, Y. Tian, and A. Gervais, "Scaling capacity of fiber-optic transmission systems via silicon photonics," *Nanophotonics*, vol. 9, no. 16, pp. 4629-4663, 2020.

[8] J. M. Senior and M. Y. Jamro, *Optical fiber communications: principles and practice*. Pearson Education, 2009.

[9] H. Wang, "Two Channel SDM Communication System Simultaneously Operating at 10Gb/s Using C-band Transceivers," 2018.

[10] S. Murshid, B. Grossman, and P. Narakorn, "Spatial domain multiplexing: A new dimension in fiber optic multiplexing," *Optics & Laser Technology*, vol. 40, no. 8, pp. 1030-1036, 2008.

[11] P. Gunasekaran, A. Azhagu Jaisudhan Pazhani, A. Rameshbabu, and B. Kannan, "Role of Wavelength Division Multiplexing in Optical Communication," *Modeling and Optimization of Optical Communication Networks*, pp. 217-234, 2023.

[12] D. Ilcev, "Analyses of code division multiple access (CDMA) schemes for global mobile satellite communications (GMSC)," *TransNav: International Journal on Marine Navigation and Safety of Sea Transportation*, vol. 14, 2020.

[13] C.-W. Pui and E. F. Young, "Lagrangian relaxation-based time-division multiplexing optimization for multi-FPGA systems," *ACM Transactions on Design Automation of Electronic Systems (TODAES)*, vol. 25, no. 2, pp. 1-23, 2020.
[14] X. Tang, Z. Xu, C. Gao, Y. Xiao, L. Liu, X. Zhang, L. Xi, H. Xu, and C. Bai, "Physical layer encryption for coherent PDM system based on polarization perturbations using a digital optical polarization scrambler," *Optics Express*, vol. 31, no. 16, pp. 26791-26806, 2023.
[15] L. Zhang, M. Zheng Chen, W. Tang, J. Yan Dai, L. Miao, X. Yang Zhou, S. Jin, Q. Cheng, T. Jun Cui, "A wireless communication scheme based on space-and frequency-division multiplexing using digital metasurfaces," *Nature electronics*, vol. 4, no. 3, pp. 218-227, 2021.
[16] B. J. Puttnam, G. Rademacher, and R. S. Luís, "Space-division multiplexing for optical fiber communications," *Optica*, vol. 8, no. 9, pp. 1186-1203, 2021.
[17] D. J. Richardson, J. M. Fini, and L. E. Nelson, "Space-division multiplexing in optical fibres," *Nature photonics*, vol. 7, no. 5, pp. 354-362, 2013.
[18] R. Ryf, S. Randel, N. K. Fontaine, M. Montoliu, E. Burrows, S. Corteselli, S. Chandrasekhar, A. H. Gnauck, C. Xie, R.-J. Essiambre, P. J. Winzer, R. Delbue, P. Pupalaikis, A. Sureka, Y. Sun, L. Grüner-Nielsen, R. V. Jensen, and R. Lingle, "32-bit/s/Hz spectral efficiency WDM transmission over 177-km few-mode fiber," in *Optical fiber communication conference*, 2013: Optica Publishing Group, p. PDP5A. 1.
[19] P. J. Winzer, "Spatial multiplexing in fiber optics: The 10x scaling of metro/core capacities," *Bell Labs Technical Journal*, vol. 19, pp. 22-30, 2014.
[20] R. Ryf, H. Chen, N. K. Fontaine, A. M. Velázquez-Benítez, J. Antonio-López, C. Jin, B. Huang, M. Bigot-Astruc, D. Molin, F. Achten, P. Sillard, R. Amezcua-Correa, "10-mode mode-multiplexed transmission over 125-km single-span multimode fiber," in *2015 European Conference on Optical Communication (ECOC)*, 2015: IEEE, pp. 1-3.
[21] B. Li, L. Gan, Z. Feng, S. Fu, P. Ping Shum, W. Tong, and M. Tang, "Experimental demonstration of symmetric WDM-SDM optical access network over multicore fiber," in *Proceedings of the Conference on Lasers and Electro-Optics, San Francisco, CA, USA*, 2016, pp. 13-18.
[22] Y. Tian, J. Li, Z. Wu, Y. Chen, P. Zhu, R. Tang, Q. Mo, Y. He, and Z. Chen, "Wavelength-interleaved MDM-WDM transmission over

weakly-coupled FMF," *Optics Express,* vol. 25, no. 14, pp. 16603-16617, 2017.
[23] Y. Tian, J. Li, Z. Wu, P. Zhu, Y. Chen, Q. Mo, F. Ren, Z. Li, Y. He, and Z. Chen, "IM-DD MDM-WDM transmission over 120-km weakly-coupled FMF enabled by wavelength interleaving," in *Optical Fiber Communication Conference*, 2017: Optica Publishing Group, p. Tu3I. 1.
[24] J. Li, C. Cai, J. Du, S. Jiang, L. Ma, L. Wang, L. Zhu, A. Wang, M. -J. Li, H. Chen, J. Wang, Z. He, "Ultra-low-noise mode-division multiplexed WDM transmission over 100-km FMF based on a second-order few-mode Raman amplifier," *Journal of Lightwave Technology,* vol. 36, no. 16, pp. 3254-3260, 2018.
[25] M. N. Ismael and A. M. Fakhrudeen, "SDM over hybrid FSO link under different weather conditions and FTTH based on electrical equalization," *International Journal of Civil Engineering and Technology (IJCIET),* vol. 10, no. 1, pp. 1396-1406, 2019.
[26] N. M. Mathew, L. Grüner-Nielsen, M. Galili, M. Lillieholm, and K. Rottwitt, "Mdm transmission using air-clad photonic lanterns," *IEEE Photonics Technology Letters,* vol. 32, no. 17, pp. 1049-1052, 2020.
[27] M. Kumari, R. Sharma, and A. Sheetal, "Performance analysis of l ong-reach 40/40 Gbps mode division multiplexing-based hybrid time and wavelength division multiplexing passive optical network/free-space optics using Gamma-Gamma fading model with pointing error under different weather conditions," *Transactions on Emerging Telecommunications Technologies,* vol. 32, no. 3, p. e4214, 2021.
[28] Y. Liang *et al.*, "An all-optical fiber mode converters based on 5-LP mode fiber of weakly coupling and large effective mode area," *Optical Fiber Technology,* vol. 71, p. 102889, 2022.
[29] J. Cui *et al.*, "Low-modal-crosstalk orthogonal combine reception for degenerate modes in IM/DD MDM transmission," *Optics Express,* vol. 31, no. 5, pp. 8586-8594, 2023.
[30] A. Al-Azzawi, *Physical optics: principles and practices*. CRC Press, 2018.
[31] M. Barnoski, *Fundamentals of optical fiber communications*. Elsevier, 2012.
[32] G. Keiser, *Optical fiber communications*. McGraw-Hill New York, 2020.
[33] C. Cox, E. Ackerman, R. Helkey, and G. E. Betts, "Techniques and performance of intensity-modulation direct-detection analog optical links," *IEEE Transactions on Microwave theory and techniques,* vol. 45, no. 8, pp. 1375-1383, 1997.

[34] G. T. Reed, G. Mashanovich, F. Y. Gardes, and D. Thomson, "Silicon optical modulators," *Nature photonics,* vol. 4, no. 8, pp. 518-526, 2010.
[35] C. Xia, "Optical Fibers for Space-Division Multiplexed Transmission and Networking," 2015.
[36] A. A. Alanazi, S. Z. Alamri, S. Shafie, and S. Binti Mohd Puzi, "Solving nonlinear Schrodinger equation using stable implicit finite difference method in single-mode optical fibers," *Mathematical Methods in the Applied Sciences,* vol. 44, no. 17, pp. 12453-12478, 2021.
[37] G. Agrawal, "Nonlinear Fiber Optics," ed: Academic Press, Inc., 2018.
[38] "Theoretical description of transient stimulated Raman scattering in optical fibers," *IEEE Journal of Quantum Electronics,* vol. 25, no. 12, pp. 2665-2673, 1989.
[39] J. M. Dudley, G. Genty, and S. Coen, "Supercontinuum generation in photonic crystal fiber," *Reviews of modern physics,* vol. 78, no. 4, p. 1135, 2006.
[40] G. P. Agrawal, "Nonlinear fiber optics," Elsevier, 0123695163, 2007.
[41] G. P. Agrawal, "Nonlinear fiber optics," in *Nonlinear Science at the Dawn of the 21st Century*: Springer, 2000, pp. 195-211.
[42] G. P. Agrawal, *Fiber-optic communication systems*. John Wiley & Sons, 2012.
[43] D. Felice, "A study of a nonlinear Schrödinger equation for optical fibers," *ArXiv e-prints,* 2016.
[44] A. Mecozzi, C. Antonelli, and M. Shtaif, "Nonlinear propagation in multi-mode fibers in the strong coupling regime," *Optics express,* vol. 20, no. 11, pp. 11673-11678, 2012.
[45] G. P. Agrawal, "Optical communication: its history and recent progress," *Optics in our time,* pp. 177-199, 2016.
[46] K. J. Bogacki, "Design of a 50 GHz Bandwidth DPSK Compatible Monolithically Integrated Optical Receiver," 2007.
[47] J. C. Campbell, "Recent advances in avalanche photodiodes," *Journal of Lightwave Technology,* vol. 34, no. 2, pp. 278-285, 2015.
[48] D. Behera, S. Varshney, S. Srivastava, and S. Tiwari, "Eye Diagram Basics: Reading and applying eye diagrams," *EDN Network,* 2011.
[49] T. F. Hussein, M. Rizk, and M. H. Aly, "A hybrid DCF/FBG scheme for dispersion compensation over a 300 km SMF," *Optical and quantum electronics,* vol. 51, pp. 1-16, 2019.
[50] K. RAJESH, A. Blessie, and S. Krishnan, "Performance Assessment Of Dispersion Compensation Using Fiber Bragg Grating (Fbg) And Dispersion Compensation Fiber (Dcf) Techniques," *Informacije Midem,* vol. 51, no. 4, pp. 215-223, 2021.

[51] A. Sharma, I. Singh, S. Bhattacharya, and S. Sharma, "Performance comparison of DCF and FBG as dispersion compensation techniques at 100 Gbps over 120 km using SMF," in *Nanoelectronics, Circuits and Communication Systems: Proceeding of NCCS 2017*, 2019: Springer, pp. 435-449.
[52] M. Cen, "Study on supervision of wavelength division multiplexing passive optical network systems," ed, 2011.
[53] F. Forghieri, R. W. Tkach, A. R. Chraplyvy, and D. Marcuse, "Reduction of four-wave mixing crosstalk in WDM systems using unequally spaced channels," *IEEE Photonics Technology Letters*, vol. 6, no. 6, pp. 754-756, 1994.
[54] A. Chraplyvy, A. Gnauck, R. Tkach, and R. Derosier, "8* 10 Gb/s transmission through 280 km of dispersion-managed fiber," *IEEE photonics technology letters*, vol. 5, no. 10, pp. 1233-1235, 1993.
[55] P. J. Winzer and R.-J. Essiambre, "Advanced modulation formats for high-capacity optical transport networks," *Journal of Lightwave Technology*, vol. 24, no. 12, pp. 4711-4728, 2006.
[56] M. Secondini, D. Marsella, and E. Forestieri, "Receiver Training for Efficient Nonlinear Equalization and Detection in Optical Communications," in *Signal Processing in Photonic Communications*, 2014: Optica Publishing Group, p. ST2D. 4.
[57] P. J. Winzer and G. J. Foschini, "MIMO capacities and outage probabilities in spatially multiplexed optical transport systems," *Optics express*, vol. 19, no. 17, pp. 16680-16696, 2011.
[58] N. Karelin *et al.*, "Modeling and design framework for SDM transmission systems," in *2015 17th International Conference on Transparent Optical Networks (ICTON)*, 2015: IEEE, pp. 1-4.
[59] T. Mori, T. Sakamoto, M. Wada, T. Yamamoto, and K. Nakajima, "Few-mode fiber technology for mode division multiplexing," *Optical fiber technology*, vol. 35, pp. 37-45, 2017.
[60] L. A. T. Martinez, "Investigation on Crosstalk in Multi-core Optical Fibers," Universitat Politècnica de Catalunya. Escola Tècnica Superior d'Enginyeria …, 2015.
[61] G. Rademacher *et al.*, "93.34 Tbit/s/mode (280 Tbit/s) transmission in a 3-mode graded-index few-mode fiber," in *Optical Fiber Communication Conference*, 2018: Optica Publishing Group, p. W4C. 3.
[62] A. H. Gnauck *et al.*, "WDM Transmission of 603-Gb/s Superchannels over 845 km of 7-Core Fiber with 42.2 b/s/Hz Spectral Efficiency," in *European Conference and Exhibition on Optical Communication*, 2012: Optica Publishing Group, p. Th. 2. C. 2.

[63] R. Ryf, N. K. Fontaine, and R.-J. Essiambre, "Spot-based mode couplers for mode-multiplexed transmission in few-mode fiber," *IEEE Photonics Technology Letters,* vol. 24, no. 21, pp. 1973-1976, 2012.
[64] L. Bigot, G. Le Cocq, and Y. Quiquempois, "Few-mode erbium-doped fiber amplifiers: A review," *Journal of Lightwave Technology,* vol. 33, no. 3, pp. 588-596, 2015.
[65] J. Slim, "Optical signal processing for space division multiplexed systems," Université de Rennes, 2021.
[66] L. Tong, J. Lou, and E. Mazur, "Single-mode guiding properties of subwavelength-diameter silica and silicon wire waveguides," *Optics Express,* vol. 12, no. 6, pp. 1025-1035, 2004.
[67] H. Chen, "Optical devices and subsystems for few-and multi-mode fiber based networks," 2014.
[68] G. Li, N. Bai, N. Zhao, and C. Xia, "Space-division multiplexing: the next frontier in optical communication," *Advances in optics and photonics,* vol. 6, no. 4, pp. 413-487, 2014.
[69] S. Jain, V. Rancaño, T. May-Smith, P. Petropoulos, J. Sahu, and D. Richardson, "Multi-element fiber technology for space-division multiplexing applications," *Optics express,* vol. 22, no. 4, pp. 3787-3796, 2014.
[70] F. Ye, J. Tu, K. Saitoh, and T. Morioka, "Simple analytical expression for crosstalk estimation in homogeneous trench-assisted multi-core fibers," *Optics express,* vol. 22, no. 19, pp. 23007-23018, 2014.
[71] T. Mizuno, H. Takara, K. Shibahara, A. Sano, and Y. Miyamoto, "Dense space division multiplexed transmission over multicore and multimode fiber for long-haul transport systems," *Journal of Lightwave Technology,* vol. 34, no. 6, pp. 1484-1493, 2016.
[72] M. Kumari, N. Sharma, R. Chauhan, K. Joshi and A. Kumar, "Implementation of 16×10Gbps WDM System Incorporating MDM technique," *2024 Asia Pacific Conference on Innovation in Technology (APCIT),* MYSORE, India, 2024, pp. 1-4

الخلاصة

يُعد نظام اتصالات الألياف الضوئية جوهر أنظمة الاتصالات التي تدعم الإنترنت. وقد شهدت الاتصالات الرقمية تطورًا هائلاً على مدار الثلاثين عامًا الماضية بفضل انتشار منصات التواصل الاجتماعي والمواقع الإلكترونية، والتوسع الكبير للإنترنت، إلى جانب التطبيقات التجارية والمالية والعسكرية. ونتيجةً لذلك، برزت الحاجة إلى توفير أنظمة اتصالات رقمية فعّالة ومتعددة الإشارات لنقل البيانات المطلوبة بسرعة وأمان وكفاءة عالية وبأقل معدل خطأ. هناك عدة طرق لزيادة سعة الإرسال، مثل دمج إشارات متعددة مع ناقلات ضوئية على ليف ضوئي واحد بترددات مختلفة، والتعديل باستخدام مستويات مختلفة من السعة، واستخدام ناقلين فرعيين، والاستقطاب. ومع ذلك، هناك بُعد إضافي يمكن الاستفادة منه باستخدام الألياف الضوئية لتعزيز سعة المعلومات، وهو المساحة.

يقدم هذا البحث نماذج محاكاة لأنظمة إرسال بتقسيم الفضاء المتعدد (SDM) التي تستخدم أليافًا قليلة الأنماط (FMF). كما يطبق هذا النظام تقنيات تقسيم الطول الموجي المتعدد (WDM) لتحسين معدلات نقل البيانات. لتلبية متطلبات السعة الفائقة لتقنية SDM، اقتُرح استخدام الألياف قليلة الأوضاع (FMF) كتقنية مثالية لأنظمة معدل البتات الفائق التي تُمكّن من النقل لمسافات طويلة.

في هذه الرسالة، تم تصميم نظام WDM/SDM ومحاكاته وتحليله باستخدام برنامج OptiSystem. استُخدمت أربعة أوضاع للحصول على معدلات بيانات فائقة. تم اختبار النظام المقترح باستخدام أربع حالات مختلفة: معدل بيانات متغير، ومسافة متغيرة، وطاقة متغيرة، وقناة ذات مساحة متغيرة. تم تقييم أداء النظام وتحليله باستخدام معايير مختلفة: مُحلل معدل خطأ البت، وقيمة عامل الجودة، وسعة فتحة مخطط العين.

باستخدام معدل بت متغير، ومسافة 10 كم، وطاقة 5 مللي واط، وتباعد قنوات 0.8 نانومتر، كان أفضل عامل جودة 59.1721 بمعدل بتات 10^9 بت في الثانية. عند مسافة متغيرة، وقوة 5 ميلي واط، وتباعد قنوات 0.8 نانومتر، كان أفضل معامل جودة 29.975 عند 10 كم. وعند قوة متغيرة، وقوة 10 كم، وتباعد قنوات 0.8 نانومتر، كان أفضل معامل جودة 30.0548 عند 7 ميلي واط. وعند تباعد قنوات متغير، وقوة 5 ميلي واط، وتباعد قنوات 10 كم، كان أفضل معامل جودة 30.0864 عند 2 نانومتر.

أثبتت تقنيات SDM أهميتها وقيمتها، إذ تتيح مرونة أكبر للنظام، وقابلية للتوسع، وسعة أكبر، مما يُسهم في تحسين التعامل مع قنوات الاتصال المتعددة والاستخدام الفعال للموارد المتاحة.

جمهورية العـراق

وزارة التعليم العالي والبحث العلمي

جامعــة بابـل

كليـــــة الهندســة

تصميم ومحاكاة نظام اتصالات ضوئية باستخدام تقنيات SDMو WDM لأنظمة الألياف الضوئية ذات الانماط القليلة

رسالة مقدمـــة الى قسم الهندسة الكهربائية / كليـــة الهندســـة / جامعـــــة بابـــل

كجزء من متطلبات نيل درجـــــــة الماجستير في الهندسة /

الهندسة الكهربائية/ الاتصالات

قـــدمت من قبـل

ملاك كاظم صادق عمران

بإشـــراف

الأستاذ الدكتور أبراهيم عبدالله مرداس

1446 هـ ***2025*** م